

Desarrollo de nuevos hidrogeles para aplicaciones biomédicas

Autora: Natalia Pettinelli Obreque

Tesis doctoral UDC / 2020

Directores: Dra. Rebeca Bouza Padín Dr. Luis Barral Losada

Programa Oficial de Doctorado Interuniversitario en Física Aplicada



Agradecimientos

Cuando recién comenzaba la tesis muchos me dijeron que 3 años pasaban volando y yo no lo creía, más aún estando lejos de casa. Ahora, puedo decir que sí, pasaron muy rápido y fue una etapa llena de aprendizaje y desarrollo personal y académico. Es por esto que quiero expresar mi agradecimiento a todas las personas que colaboraron y apoyaron de una u otra forma en la realización de esta tesis.

A mis directores de tesis, Dr. Luis Barral y Dra. Rebeca Bouza, por la oportunidad y confianza para realizar esta tesis y formar parte del Grupo de Polímeros. A Luis, por tu dedicación, consejos y apoyo constante. A Rebeca, por tu apoyo, motivación y siempre entregar buenas vibras. A ambos, muchas gracias por escucharme, animarme y darme la libertad de desarrollar mis ideas y formas de trabajo, lo que permitió mi crecimiento tanto personal como profesional.

A la Dra. Saddys Rodríguez del Centro de Polímeros Avanzados, Chile, por ofrecerme la oportunidad de hacer el doctorado y empujarme a hacerlo. Gracias por tu preocupación.

A la Dra. Francisca Lago y Dra. Sandra Feijóo-Bandín, del Instituto de Investigación Sanitaria de Santiago de Compostela quisiera agradecerles por su orientación, colaboración y conocimientos entregados. Sandra, en especial por tu paciencia y siempre buena disposición.

A todos los miembros del grupo de polímeros, quiero agradecer su ayuda y preocupación. En especial, quisiera agradecer a Ángeles por tu colaboración y buena disposición y a Yousof, por ser un excelente compañero de trabajo, por tu apoyo y contribuciones a este trabajo.

A mis amigas y amigos, muchísimas gracias por estar siempre presentes, por las buenas energías y risas. Mención honrosa a mis amigas de la vida, que hicieron que jamás se notara que un océano nos separaba. A mis compañeros/as que conocí a este lado del charco, muchas gracias porque han hecho de mi estadía, la mejor.

Finalmente, quiero agradecer y dedicar esta tesis a mi querida familia. A mis padres, hermana y hermano, infinitas gracias por el apoyo desde el primer minuto, por animarme a hacerlo y por la confianza. Siempre me acompañaron a lo largo de este recorrido y recargaron de energías en cada reencuentro.

¡Muchas gracias a todos!

Resumen

Los hidrogeles son biomateriales que han recibido una considerable atención como candidatos para un amplio rango de aplicaciones biomédicas. Es por esto, que el diseño de hidrogeles con características óptimas es fundamental para progresar en el área de biomateriales funcionales. El objetivo de esta tesis fue el desarrollo y la caracterización de nuevos hidrogeles basados en biopolímeros para aplicaciones biomédicas como liberación de fármacos, reparación de tejidos y curación de heridas. Para esto, se seleccionaron polímeros sintéticos y naturales para la preparación de hidrogeles interpenetrados y semi-interpenetrados, hidrogeles compuestos incorporando micropartículas e hidrogeles físicos. En primer lugar, se obtuvieron hidrogeles mediante el encapsulamiento de quitosano, pectina o κ -carragenina en hidrogeles a base de metacrilato para mejorar sus propiedades mecánicas y de hinchamiento. En segundo lugar, se preparó un hidrogel compuesto en base a micropartículas de poli(hidroxibutirato-co-hidroxivalerato) cargadas en un hidrogel de κ -carragenina y goma de algarrobo como vehículo de administración dual de fármacos poco solubles en agua. Finalmente, se preparó un hidrogel inyectable que combina iota y kappa carrageninas, goma de algarrobo y gelatina, el cual podría ser útil en la cicatrización de heridas y la reparación de tejidos. Así, la combinación de polímeros de distinto origen y el empleo de diferentes métodos de preparación y tipos de entrecruzamiento permitió obtener hidrogeles con las propiedades adecuadas para un potencial uso en determinadas aplicaciones, como la liberación de fármacos, reparación de tejidos y curación de heridas.

Abstract

Hydrogels are biomaterials that have received increasing attention as candidate for a wide range of biomedical applications. Therefore, the design of hydrogels with optimal characteristics is fundamental to progress in the area of functional biomaterials. The objective of this thesis was the development and characterization of novel biopolymer-based hydrogels for biomedical applications such as drug delivery, tissue repair and wound healing. For this purpose, synthetic and natural polymers were selected for the preparation of interpenetrating and semi-interpenetrating polymer networks, composite hydrogels incorporating microparticles and physical hydrogels. Firstly, hydrogels were obtained by the entrapment of chitosan, pectin or κ -carrageenan within methacrylate- based hydrogels to improve their swelling and the mechanical properties. Secondly, a composite hydrogel based on PHBV microparticles loaded in κ -carrageenan/locust bean gum hydrogel was prepared as a dual delivery carrier of poorly water soluble drugs. Finally, an injectable hydrogel was prepared by combining of iota and kappa carrageenan, locust bean gum and gelatin, which could be useful in wound healing and tissue repair. Thus, the combination of polymers of different origin and the use of distinct preparation methods and crosslinkings led to hydrogels with the suitable properties for potential use in some applications, such as drug delivery, tissue repair and wound healing.

Resumo

Os hidroxelos son biomateriais que recibiron unha considerable atención como candidatos para un amplio rango de aplicacións biomédicas. É por isto, que o deseño de hidroxelos con características óptimas é fundamental para progresar na área de biomateriais funcionais. O obxectivo desta tese foi o desenvolvemento e a caracterización de novos hidroxelos baseados en biopolímeros para aplicacións biomédicas como liberación de fármacos, reparación de tecidos e curación de feridas. Para isto, seleccionáronse polímeros sintéticos e naturais para a preparación de hidroxelos interpenetrados e semi- interpenetrados, hidroxelos compostos incorporando micropartículas e hidroxelos físicos. En primeiro lugar, obtivérónse hidroxelos mediante o encapsulamento de quitosano, pectina ou κ -carragenina en hidroxelos a base de metacrilato para mellorar as súas propiedades mecánicas e de inchamento. En segundo lugar, preparouse un hidroxel composto en base a micropartículas de poli(hidroxibutirato- co- hidroxivalerato) cargadas nun hidroxel de κ -carragenina e goma de algarrobo como vehículo de administración dual de fármacos pouco solubles en auga. Finalmente, preparouse un hidroxel inyectable que combina iota e kappa carrageninas, goma de algarrobo e xelatina, o cal podería ser útil na cicatrización de feridas e a reparación de tecidos. Así, a combinación de polímeros de distinto orixe e o emprego de diferentes métodos de preparación e tipos de entrecruzamento permitiu obter hidroxelos coas propiedades axeitadas para un potencial uso en determinadas aplicacións, como a liberación de fármacos, a reparación de tecidos e a curación de feridas.

Lista de contenidos

Lista de contenidos	1
Lista de figuras	5
Listado de tablas	9
Abreviaturas.....	11
CAPÍTULO 1: Introducción.....	13
1.1. Hidrogeles, una visión general	15
1.2. Clasificación de los hidrogeles	17
1.3. Hidrogeles en aplicaciones biomédicas	22
1.3.1. Hidrogeles basados en polímeros naturales para aplicaciones biomédicas.....	24
1.3.2. Hidrogeles basados en polímeros sintéticos para aplicaciones biomédicas	27
1.4. Referencias.....	29
CAPÍTULO 2: Objetivos y estructura de la tesis	35
2.1. Objetivos de la tesis	37
2.2. Estructura de la tesis	38
CAPÍTULO 3: Materiales y técnicas de caracterización.....	43
3.1. Materiales	45
3.1.1. Quitosano.....	45
3.1.2. Pectina.....	46
3.1.3. Carrageninas	47
3.1.4. Monómeros sintéticos	49
3.1.5. PHBV.....	50
3.1.6. Goma de algarrobo	51
3.1.7. Gelatina	52
3.2. Métodos	53
3.2.1. Microscopía electrónica de barrido	53
3.2.2. Espectroscopía de infrarrojos por transformada de Fourier	54
3.2.3. Espectroscopía de resonancia magnética nuclear	56
3.2.4. Análisis termogravimétrico	58
3.2.5. Propiedades mecánicas.....	58
3.2.5.1. Ensayo de compresión	58
3.2.5.2. Ensayos reológicos	59

3.2.6. Porosimetría.....	60
3.2.7. Espectroscopía ultravioleta-visible	61
3.2.8. Ensayos celulares	62
3.2.8.1. Ensayo de viabilidad celular.....	62
3.2.8.2. Ensayo de nitrito	63
3.2.8.3. Ensayo de herida (In vitro scratch wound assay).....	63
3.3. Referencias.....	65
CAPÍTULO 4: Entrapment of chitosan, pectin or κ -carrageenan within methacrylate based hydrogels: effect on swelling and mechanical properties.	71
4.1. Introduction	73
4.2. Materials and methods	75
4.2.1. Materials	75
4.2.2. Synthesis of the hydrogels	75
4.2.3. Attenuated total reflectance ATR-FTIR spectra	76
4.2.4. ^1H Nuclear magnetic resonance (^1H NMR).....	77
4.2.5. Swelling behavior	77
4.2.6. Field emission scanning electron microscopy.....	77
4.2.7. Thermogravimetric analysis.....	77
4.2.8. Mechanical properties	78
4.2.9. Biocompatibility	78
4.2.9.1. Cell culture	78
4.2.9.2. MTT viability assay	78
4.2.9.3. Nitrite assay.....	79
4.2.9.4. Hydrogel imaging	79
4.2.9.5. Statistical analysis	79
4.3. Results and discussion.....	80
4.3.1. Synthesis of the hydrogels	80
4.3.2. Swelling behavior	82
4.3.3. Field emission scanning electron microscopy.....	84
4.3.4. Thermogravimetric analysis.....	85
4.3.5. Mechanical properties	85
4.3.6. Biocompatibility	87
4.4. Conclusions	89
Supplementary material	90

4.5. References.....	92
CAPÍTULO 5: Poly(hydroxybutyrate-co-hydroxyvalerate) microparticles embedded in κ-carrageenan/locust bean gum hydrogel as a dual drug delivery carrier.....	97
5.1. Introduction	99
5.2. Materials and Methods.....	101
5.2.1. Materials	101
5.2.2. Preparation of PHBV microparticles	102
5.2.3. Preparation of the hydrogels	102
5.2.4. Characterization of the microparticles	104
5.2.4.1. Field emission scanning electron microscopy (FESEM) and particle size analysis	104
5.2.4.2. Zeta potential, surface area and pore size analysis	104
5.2.4.3. Drug loading and entrapment efficiency	104
5.2.5. Characterization of the hydrogels.....	105
5.2.5.1. Swelling behavior	105
5.2.5.2. Morphological properties	105
5.2.5.3. Rheological properties	105
5.2.6. <i>In vitro</i> drug release studies.....	106
5.2.7. Biocompatibility	106
5.2.7.1. Cell culture	106
5.2.7.2. Cell treatment	107
5.2.7.3. MTT viability assay	107
5.2.7.4. Statistical analysis	108
5.3. Results and discussion.....	108
5.3.1. Microparticles characterization	108
5.3.2. Characterization of hydrogels	110
5.3.2.1 Swelling behavior	110
5.3.2.2. Morphologies of the hydrogels	110
5.3.2.3. Rheological behavior.....	111
5.3.3. <i>In vitro</i> drug release studies.....	112
5.3.4. Cytotoxicity assays	116
5.4. Conclusion	117
5.5. References.....	119
CAPÍTULO 6: Carrageenan-based physically crosslinked injectable hydrogel for wound healing and tissue repairing applications.....	125

6.1. Introduction	127
6.2. Materials and methods	129
6.2.1. Materials	129
6.2.2. Preparation of hydrogel	130
6.2.3. Characterization	130
6.2.3.1. Attenuated total reflectance ATR-FTIR spectroscopy.....	130
6.2.3.2. Field emission scanning electron microscopy (FESEM)	130
6.2.3.3. Swelling behavior	131
6.2.3.4. Physiological stability	131
6.2.3.5. Rheological properties	131
6.2.4. Cell assays	132
6.2.4.1. Cell cultures.....	132
6.2.4.2. MTT viability assay	133
6.2.4.3. Cell adhesion	133
6.2.4.4. <i>In vitro</i> scratch wound assay.....	133
6.2.4.5. Statistical analysis	134
6.3. Results and discussion.....	134
6.3.1. Physical interactions and surface morphologies characterization	134
6.3.2. Swelling behavior and physiological stability.....	138
6.3.3. Rheological properties	139
6.3.4. <i>In vitro</i> biological evaluation	140
6.4. Conclusion	144
Supplementary material	146
6.5. References.....	147
CAPÍTULO 7: Conclusiones generales.....	155
ANEXO: Financiamiento	161

Lista de figuras

Capítulo 1

Figura 1.1. Clasificación de los hidrogeles basada en diferentes propiedades.	17
Figura 1.2. Formación y estructura de redes polímericas full y semi interpenetradas [20].	
.....	20
Figura 1.3. Clasificación de los polímeros. PEG: Polyethylene glycol, PLGA: Poly (lactic-co-glycolic acid), PNIPAAm: Poly (N-isopropylacrylamide).....	25

Capítulo 3

Figura 3.1. Estructura química del quitosano.	45
Figura 3.2. Estructura química de la pectina.	46
Figura 3.3. Representación esquemática de unidades repetidas idealizadas de kappa, iota y lambda carrageninas.	48
Figura 3.4. Esquema de la formación del gel de carragenina. La gelificación de las soluciones de carragenina se produce como resultado de la transición conformacional de bobina a hélice y la posterior agregación entre hélices ordenadas. Los cationes son los responsables de la transición final sol-gel del polisacárido [11].	48
Figura 3.5. Estructura química de polietilenglicol metil éter metacrilato (a), 2-dimetilamino etil metacrilato (b).	49
Figura 3.6. Estructura química del PHBV.	50
Figura 3.7. Estructura química del LBG.	51
Figura 3.8. Estructura química básica de la gelatina [33].	52
Figura 3.9. Esquema de un microscopio electrónico de barrido.	54
Figura 3.10. Un sistema de reflectancia total atenuada [38].	56
Figura 3.11. Esquemas de pruebas mecánicas utilizadas para evaluar las propiedades mecánicas del hidrogel. Compresión (a) y reometría de cizalla (b) [40].	60

Capítulo 4

Figure 4.1. FTIR spectra of PEGMEM, DMAEM and SH.	82
Figure 4.2. Water uptake of prepared hydrogels (a) and effect the crosslinker concentration on water uptake of 0.5kC hydrogel (b).	83
Figure 4.3. FESEM images of freeze-dried swollen hydrogels SH,1PC,1CS and 1kC.....	84
Figure 4.4. TGA of swollen hydrogels (a) and TGA curves of lyophilized hydrogels (b).	85

Figure 4.5. MTT assay. Effect of SH, 1PC, 1CS and 1kC hydrogels on J774.A1 macrophages vitality (n = 6) for 24 h. Culture medium with 10% of FBS was used as positive control.	87
Figure 4.6. Nitrite assay. Effect of SH, 1PC, 1CS and 1kC hydrogels on J774.A1 macrophages nitrite production. LPS 250 ng mL ⁻¹ was used as positive control, and culture medium from untreated cells as negative control (n=6).	88
Figure 4.7. Microscopy images of hydrogels surfaces after cell seeding.	88
Figure S. 4.1. FTIR spectra of SH, 1PC, 1CS and 1kC hydrogel.	90
Figure S. 4.2. FTIR spectra of extractables from SH, 1PC, 1CS and 1kC hydrogel.....	90
Figure S. 4.3. ¹ H RMN spectra of extractables from SH, 1PC, 1CS and 1kC hydrogel	91

Capítulo 5

Figure 5.1. Schematic diagram showing the microparticles (a) and composite hydrogel (b) preparation.	103
Figure 5.2. FESEM images of unloaded MPs (a) and KM-MPs (b, c). Fig.5.2c present an enlargement of the central region of the image showing the inner pore structure.	109
Figure 5.3. FESEM images of κCLH (a), κCLH (cross-section) (b), KM-MPs-κCLH (c) and KM-MPs-κCLH (cross-section) (d).	111
Figure 5.4. Rheological measurements of κCLH and KM-MPs- κCLH at 25 °C (a) and 37 °C (b).	112
Figure 5.5. Ketoprofen release from microparticles at 25 °C and 37 °C (a), mupirocin release from microparticles at 25 °C and 37 °C (b), ketoprofen release from κCLH at 25 °C and 37 °C (c), mupirocin release from κCLH at 25 °C and 37 °C (d), ketoprofen release from KM-MPs-κCLH at 25 °C and 37 °C (e), mupirocin release from KM-MPs- κCLH at 25 °C and 37 °C (f).	114
Figure 5.6. MTT assay showing the effect of the treatment for 24 h with unloaded MPs, ketoprofen, mupirocin, κCLH and KM-MPs-κCLH (a) and serial dilutions of the hydrogels extracts (b) on NIH 3T3 fibroblast viability. Solid black line highlights the cytotoxicity threshold. N=6. *p<0.05, **p<0.01.	117

Capítulo 6

Figure 6.1. FTIR spectra of gelatin, κC:LB, lC and CAR:LB:G hydrogel.	136
Figure 6.2. FESEM images of surface of the CAR (a), CAR:LB (c) and CAR:LB:G (e) hydrogels, and cross section surface of the CAR (b), CAR:LB (d) and CAR:LB:G (f) hydrogels.	137
Figure 6.3. Weight loss of CAR, CAR:LB and CAR:LB:G hydrogels in PBS solution over a period of 7 days at physiological temperature (37°C).	139

-
- Figure 6.4.** Rheological measurements of injectable hydrogel CAR:LB:G and control hydrogels CAR and CAR:LB. The elastic (G') and the viscous modulus (G'') of hydrogels (a), shear-thinning characteristics of hydrogels (b) and injectability by hand of CAR:LB:G, the injectable hydrogel was stained with bromophenol blue to enhance visualization (c). 140
- Figure 6.5.** MTT assay showing the effect of the components and the hydrogels on 3T3-L1 fibroblasts for 16 h. Solid black line highlights the cytotoxicity threshold. N=6. * $p < 0.05$. 141
- Figure 6.6.** Fluorescence microscopy images obtained after 48 h to visualize live/dead staining of 3T3-L1 fibroblasts cultured onto glass bottom (cell control) and CAR, CAR:LB and CAR:LB:G hydrogels. The images below show a 3D projection of the hydrogels with viable cells inside. Scale bar represents 250 μm 142
- Figure 6.7.** Number of viable 3T3-L1 fibroblasts cultured on CAR, CAR:LB and CAR:LB:G hydrogels. Viable cells were stained with calcein-AM. Six fluorescence images from each treatment were considered for cell count using ImageJ. ** $p < 0.01$ 142
- Figure 6.8.** Effect of VEGF released from CAR:LB:G hydrogel was evaluated using a scratch wound healing assay after 24 h. Microscope images of the *in vitro* scratches for the different treatments. The scratch was produced by scratching a confluent cell monolayer with a sterile 200 μL pipette tip. Scale bar represents 1 mm. (a). Quantified *in vitro* scratch closure area results for the different treatments after 24 h (b). Positive control: 50 $\mu\text{g ml}^{-1}$ free VEGF; CAR:LB:G control: hydrogel without VEGF; CAR:LB:G + VEGF: hydrogel loaded with 50 $\mu\text{g ml}^{-1}$ VEGF. N=6. ** $p < 0.01$ 144
- Figure S. 6.1.** FTIR spectra of κ -carrageenan (κC) and locust bean gum (LB). 146

Listado de tablas

Capítulo 4

Table 4.1. Preparation of synthetic and composite hydrogels	75
Table 4.2. Mechanical properties of hydrogels	86

Capítulo 5

Table 5.1. The parameters of the different release models in addition to the coefficient of determination R^2_{adj} at 25 °C and 37 °C from fitting into first-order, Higuchi, Korsmeyer-Peppas and Peppas-Sahlin equations for the composite hydrogel.	116
---	-----

Abreviaturas

ATR	reflectancia total atenuada (<i>attenuated total reflectance</i>)
BET	Brunauer-Emmett-Teller
DE	grado de esterificación (<i>degree of esterification</i>)
DMAEM	2-dimetilamino etil metacrilato (<i>2-dimethylamino ethyl methacrylate</i>)
ECM	matriz extracelular (<i>extracellular matrix</i>)
FDA	Administración de Medicamentos y Alimentos (<i>Food and Drug Administration</i>)
FESEM	microscopio electrónico de barrido de emisión de campo (<i>field emission scanning electron microscopy</i>)
FTIR	espectroscopía de infrarrojos por transformada de Fourier (<i>Fourier Transform Infrared Spectroscopy</i>)
HB	hidroxibutirato (<i>hydroxybutyrate</i>)
HM	alto contenido de grupos metoxi (<i>high methoxy</i>)
HUVEC	células endoteliales de la vena de cordón umbilical humano (<i>Human Umbilical Vein Endothelial Cells</i>)
HV	hidroxivalerato (<i>hydroxyvalerate</i>)
IPN	red polimérica interpenetrante (<i>interpenetrating polymeric network</i>)
IR	radiación infrarroja (<i>infrared radiation</i>)
LBG	goma de algarrobo (<i>locust bean gum</i>)
LCST	mínima temperatura crítica de la solución (<i>lower critical solution temperature</i>)
LM	bajo contenido de grupos metoxi (<i>low methoxy</i>)
PEG	polietilenglicol (<i>poly (ethylene glycol)</i>)
PEGMEM	polietilenglicol metil éter metacrilato (<i>polyethylene glycol methyl ether methacrylate</i>)
PHAs	polihidroxialcanoatos (<i>polyhydroxyalcanoates</i>)
PHB	polihidroxibutirato (<i>polyhydroxybutyrate</i>)
PHBV	poli(3-hidroxibutirato-co-3-hidroxivalerato) (<i>poly(3-hydroxybutyrate-co-3-hydroxyvalerate)</i>)
PLGA	ácido poli(láctico-co-glicólico) (<i>poly (lactic-co-glycolic acid)</i>)
RGD	arginina, glicina, ácido aspártico (<i>arginine-glycine-aspartate</i>)
RMN	resonancia magnética nuclear (<i>nuclear magnetic resonance</i>)
SLS	dispersión estática de luz (<i>static light scattering</i>)
TGA	análisis termogravímetrico (<i>thermogravimetric analysis</i>)
UCST	máxima temperatura crítica de solución (<i>upper critical solution temperature</i>)
VEGF	factor de crecimiento endotelial vascular (<i>vascular endothelial growth factor</i>)

CAPÍTULO 1: Introducción

Introducción

Conforme la sociedad va progresando en el ámbito tecnológico, existe un continuo interés en desarrollar y optimizar nuevos materiales que sean capaces de satisfacer nuestras necesidades. En este aspecto, la ciencia de los polímeros ha hecho una importante contribución al desarrollo y diseño de materiales originales en diversos campos de aplicación. Los polímeros han sido empleados en áreas como agricultura [1], tecnología de alimentos [2], farmacéutica [3] y medicina [4], entre otras. En el área biomédica, la necesidad de mejorar la atención al paciente está constantemente presente; por lo tanto, existe una demanda creciente por desarrollar nuevos biomateriales para su uso en la medicina y farmacología. En las últimas décadas, el desarrollo de nuevos biomateriales y su aplicación en medicina ha mejorado notablemente el tratamiento de muchas enfermedades [5]. Un gran desafío en el área de biomateriales es diseñar y sintetizar materiales blandos con propiedades y funciones similares a las de los tejidos humanos blandos. En este sentido, los hidrogeles, una clase de biomaterial blando y con alto contenido de agua, han demostrado gran potencial para su uso en aplicaciones médicas y biológicas.

1.1. Hidrogeles, una visión general

Entre los diferentes biomateriales, los hidrogeles son candidatos prometedores para un amplio rango de aplicaciones biomédicas. Existen varias definiciones para hidrogeles, siendo la más frecuente la dada por Peppas et al.[6], la cual indica que los hidrogeles son redes poliméricas tridimensionales hidrofílicas capaces de absorber grandes cantidades de agua o fluidos biológicos sin perder su estructura. Las redes están compuestas por homopolímeros o copolímeros, y son insolubles debido a la presencia de entrecruzamientos químicos (uniones covalentes) o entrecruzamientos físicos como enredos de cadena o enlaces de asociación [6]. La alta hidrofilicidad de los hidrogeles se debe a la presencia de motivos hidrofílicos tales como grupos carboxilo, amida, amino e hidroxilo distribuidos a lo largo de

la estructura de las cadenas poliméricas, los cuales son capaces de ionizarse en presencia de agua [7]. Estos grupos químicos forman enlaces físicos o químicos entre las redes troncales de los polímeros. Las moléculas de agua penetran en las redes de polímeros, lo que provoca el hinchamiento y da a los hidrogeles su forma original. En estado hinchado, los hidrogeles presentan una consistencia blanda y elástica como los tejidos vivos naturales, lo que se debe a la presencia de una gran cantidad moléculas de agua en la estructura de la red [8].

En comparación con otros tipos de biomateriales, los hidrogeles tienen las ventajas de una mayor biocompatibilidad, biodegradabilidad ajustable, métodos de síntesis adaptables, diversidad de componentes y la capacidad de adaptarse a una forma deseada [9]. Según las distintas aplicaciones, el hidrogel puede ser preparado para responder a diversos estímulos en el cuerpo como el pH, la fuerza iónica y la temperatura. Los hidrogeles que son sensibles al entorno, a menudo se denominan “hidrogeles inteligentes” [10]. Particularmente, los hidrogeles sensibles a la temperatura han recibido una atención considerable en el campo farmacéutico debido a la capacidad de los hidrogeles de hincharse o deshincharse como resultado del cambio de temperatura del fluido circundante [6]. Sus entrecruzamientos están constituidos principalmente por enlaces físicos, puentes de hidrógeno e interacciones hidrofóbicas. El equilibrio entre estas interacciones físicas determina el comportamiento de gelificación termosensible del hidrogel [11]. Se pueden distinguir dos tipos diferentes de materiales sensibles a la temperatura: materiales de temperatura de solución crítica superior (UCST, *upper critical solution temperature*) y materiales de temperatura de solución crítica inferior (LCST, *lower critical solution temperature*). Ambos tipos de sistemas poseen un interesante potencial para aplicaciones biomédicas. Los hidrogeles con una UCST, se contraen al enfriarse debajo del UCST. La gelificación de polímeros como la gelatina y carragenina es inducida a través por la formación reversible y sensible a la temperatura de enlaces intermoleculares de hidrógeno. Mientras que, los hidrogeles con una LCST, se contraen al calentarse por encima de la LCST. Al calentarse, se produce la agregación de los

grupos hidrofóbicos, lo que induce la separación de fases y la formación de hidrogeles. El poli(N-isopropilacrilamida-co-ácido metacrílico), es un ejemplo de este sistema [6,12].

Los hidrogeles tienen numerosas aplicaciones, particularmente en los sectores biomédico y farmacéutico. Su primera aplicación, se remonta a 1960, cuando Wichterle y Lim desarrollaron e investigaron un hidrogel basado en poli(2-hidroxietil metacrilato) como material para lentes de contactos blandos [13]. A partir de ahí, la investigación en el ámbito de los hidrogeles se ha expandido notablemente, particularmente en las últimas dos décadas [11]. Así, el uso de hidrogeles como *films*, *scaffolds* o nanocompositos se ha extendido para satisfacer una amplia gama de aplicaciones en ingeniería de tejido o tisular, liberación controlada de fármacos, vendaje y cicatrización de heridas, entre otras [5].

1.2. Clasificación de los hidrogeles

La clasificación de los hidrogeles depende de sus propiedades físicas, naturaleza de hinchamiento, método de preparación, cargas iónicas, origen, tasa de biodegradación y naturaleza del entrecruzamiento (Fig. 1.1) [14].

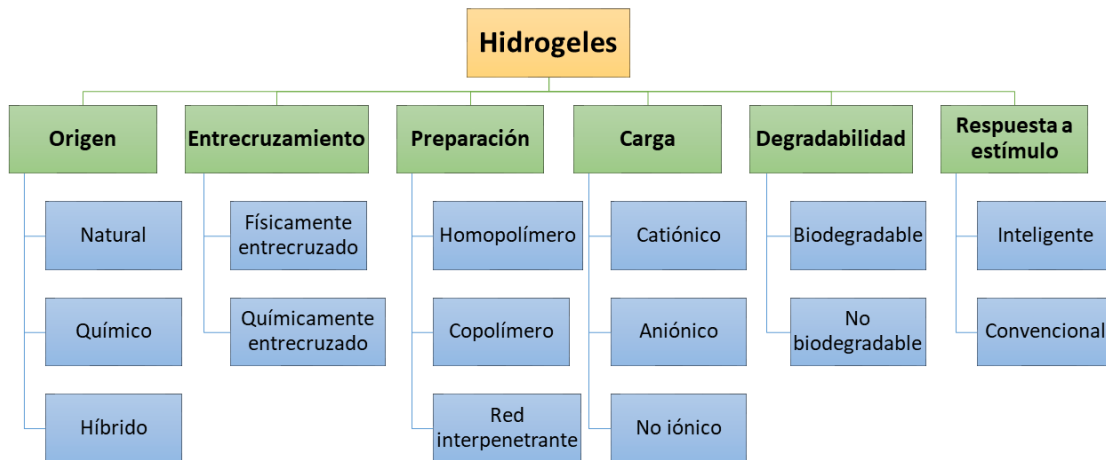


Figura 1.1. Clasificación de los hidrogeles basada en diferentes propiedades.

Algunas de estas clasificaciones son discutidas a continuación:

- Según el origen del hidrogel.

Los hidrogeles pueden ser clasificados en naturales, sintéticos o híbridos según su fuente. Los hidrogeles naturales, son aquellos cuyos polímeros tienen orígenes naturales como polisacáridos y proteínas. Mientras que los hidrogeles sintéticos son preparados utilizando polímeros sintéticos como poli (ácido acrílico), poli (hidroxietil metacrilato) y polietilenglicol, entre otros [15]. Algunas de las ventajas de los polímeros naturales frente a los polímeros sintéticos son: su origen natural, biocompatibilidad, biodegradabilidad, su bajo costo y su capacidad de modificación química [16]. Por otro lado, una ventaja importante de la utilización de polímeros sintéticos es que pueden adaptarse a funciones específicas y, por lo tanto, presentan propiedades controlables, pero una desventaja significativa para su uso es que algunos se degradan en productos desfavorables, por ejemplo, en ácidos. A elevadas concentraciones de estos productos de degradación, la acidez local puede aumentar, lo que provoca respuestas adversas como la inflamación o la encapsulación fibrosa [17]. Así, una estrategia para obtener hidrogeles con propiedades mejoradas es la combinación de polímeros naturales y sintéticos para formar hidrogeles híbridos, lo cual permite desarrollar nuevos biomateriales que muestren propiedades que no se podrían obtener a partir de los polímeros individuales.

- Según el método de preparación.

El método de preparación lleva a la formación de hidrogeles homopoliméricos, copoliméricos o interpenetrados. Los hidrogeles homopoliméricos se caracterizan por una red polimérica derivada de una sola especie de monómero, la cual es una unidad estructural básica que comprende cualquier red de polímeros. Los hidrogeles copoliméricos están formados por dos o más especies diferentes de monómeros con

al menos un componente hidrófilo, dispuestos en una configuración aleatoria, en bloque o alterna a lo largo de la cadena de la red de polímeros [18].

Por último, una red polimérica interpenetrada (IPN, *interpenetrating polymeric network*) consiste en dos (o más) redes, al menos una de las cuales se sintetiza y/o reticula en presencia inmediata de la otra, sin que existan vínculos covalentes entre ellas, y que no pueden separarse a menos que se rompan los enlaces químicos [19].

Las IPN pueden formarse ya sea en presencia de un entrecruzador para producir un full IPN o en su ausencia para obtener una semi-IPN, como se muestra en la Fig. 1.2 [20]. En una semi-IPN, uno o más polímeros son entrecruzados y uno o más polímeros son lineales o ramificados. Según estas definiciones, la semi-IPN difiere de la IPN porque las macromoléculas lineales o ramificadas sólo se dispersan en la red polimérica, sin formar otra red interpenetrada [21].

Las IPNs han sido desarrolladas con el objetivo de mejorar al menos una propiedad de las redes constituyentes. Los hidrogeles IPN tienen un gran impacto en el campo biomédico, principalmente en los sistemas de liberación de medicamentos. La cinética de deshinchamiento/hinchamiento y la carga/liberación de fármacos han sido mejoradas principalmente por la preparación de hidrogeles semi-IPN [22]. La combinación de polímeros debe producir efectivamente un sistema polimérico multicomponente, con un nuevo perfil. Polímeros naturales como polisacáridos y proteínas, y polímeros sintéticos hidrofílicos han sido usados para la formación de hidrogeles IPN [23].

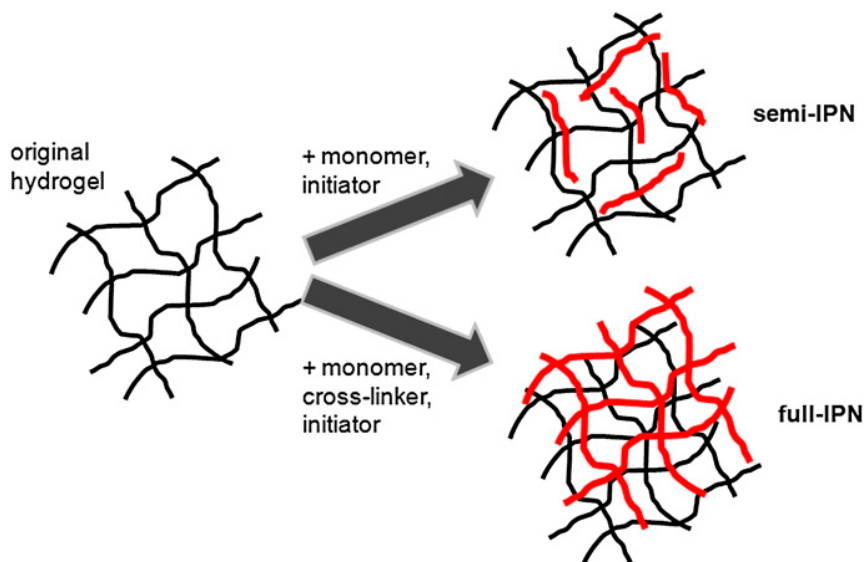


Figura 1.2. Formación y estructura de redes polímericas full y semi interpenetradas [20].

- Según el tipo de entrecruzamiento.

Los hidrogeles pueden dividirse en dos categorías en función de la naturaleza química o física de las uniones de los enlaces entrecruzados. Los hidrogeles físicos están formados por interacciones físicas tales como fuerzas de Van der Waals, interacciones hidrofóbicas, puentes de hidrógeno o agregación de cadenas. Los enlaces del hidrogel físico son reversibles debido a cambios conformacionales. Para las preparaciones de hidrogeles físicamente entrecruzados, se han aplicado varias técnicas como: ciclos repetitivos de congelación-descongelación que conlleva a la formación de microcristales en la estructura debido a la congelación y descongelación; formación de complejos polielectrolitos donde se forman enlaces entre los sitios cargados a lo largo de las columnas vertebrales de los polímeros; interacciones iónicas para gelificar una solución de un polielectrolito con iones de carga opuesta; y vía puentes de hidrógeno [8,24].

Por otro lado, en los hidrogeles químicos, enlaces covalentes están presentes entre las distintas cadenas poliméricas, por lo tanto, son permanentes e irreversibles [14].

Para las preparaciones de hidrogeles químicamente entrecruzados, se han aplicado

diversos métodos como: el uso de agentes entrecruzantes como glutaraldehído; reacciones entre grupos funcionales activados de las cadenas poliméricas como la reacción amina/ácido carboxílico; injertos químicos o por radiación que consisten en la polimerización de un monómero en la cadena lineal principal de un polímero preformado; y polimerización por radicales libres, que es uno de los métodos más usados para la preparación de hidrogeles [8,24]. La polimerización por radicales libres involucra los pasos de iniciación, propagación, transferencia en cadena y terminación. En el paso de iniciación se puede utilizar una amplia variedad de iniciadores térmicos, ultravioletas y redox para la generación de radicales. Estos radicales reaccionan con los monómeros convirtiéndolos en formas activas que reaccionan con más monómeros y así sucesivamente en la etapa de propagación. Los radicales de cadena larga resultantes experimentan una terminación ya sea por transferencia en cadena o por combinación de radicales formando matrices poliméricas [7].

Con un entrecruzamiento químico se obtiene un hidrogel con una resistencia mecánica relativamente alta y dependiendo de los enlaces pueden producirse tiempos de degradación relativamente prolongados. Aun así, existe un interés en aumento para los hidrogeles físicos por su relativa facilidad de producción y la ventaja de no usar agentes entrecruzantes durante su síntesis, los cuales no solo pueden afectar la integridad de las sustancias atrapadas (células o proteínas) sino que también pueden ser tóxicos y deben ser extraídos antes de que el hidrogel sea aplicado [24].

Evidentemente, los hidrogeles poseen características únicas que les permiten exhibir significativas propiedades que pueden ser aprovechadas en el área biomédica. Se deben identificar los requisitos que necesita el biomaterial para su utilización y de acuerdo con esto,

seleccionar, por ejemplo, la combinación de materiales, el método de preparación y el tipo de entrecruzamiento para desarrollar biomateriales con propiedades físicas, químicas y biológicas controladas.

1.3. Hidrogeles en aplicaciones biomédicas

Los hidrogeles son biomateriales ideales en diversas aplicaciones biomédicas. Su uso en sistemas de liberación de fármacos, encapsulación celular, lentes de contacto, apósticos para heridas, reemplazo de tejidos blandos, medicina regenerativa, ingeniería de tejidos y como biosensores podría representar un gran avance para la ciencia biomédica [25]. Debido a las propiedades de los hidrogeles, como su alto contenido de agua y su consistencia blanda y elástica, se espera que sean potenciales alternativas para los tejidos naturales.

Según las diferentes aplicaciones, el hidrogel puede prepararse para responder a diversos estímulos del cuerpo, como el pH, la fuerza iónica y la temperatura [26]. Estos hidrogeles inteligentes, son polímeros altamente versátiles y adaptables que pueden percibir cambios en el entorno y responder induciendo cambios estructurales (aumentando o disminuyendo su grado de hinchamiento) sin necesidad de una fuerza externa. Este fenómeno de "cambio de volumen" es especialmente útil en las aplicaciones de administración de agentes bioactivos como proteínas o fármacos, ya que la liberación del agente puede desencadenarse a partir de estos cambios ambientales. La capacidad de los hidrogeles para hincharse como resultado de factores ambientales externos depende en gran medida de tres fuerzas: la interacción de los polímeros y los disolventes, la elasticidad de los polímeros y la fuerza osmótica de los iones [27]. El grado de entrecruzamiento es uno de los factores más importantes que afectan al hinchamiento de los hidrogeles. El entrecruzamiento dificulta la movilidad de las cadenas de polímeros, por lo que se reduce el grado de hinchamiento [6].

Además del comportamiento de hinchamiento, las propiedades mecánicas de los hidrogeles son muy importantes para aplicaciones farmacéuticas. El vehículo de liberación debe mantener su integridad durante la vida útil de su aplicación, a menos que el vehículo sea diseñado como un sistema biodegradable. Cambios en el grado de entrecruzamiento permiten modificar las propiedades mecánicas. De este modo, un aumento del grado de entrecruzamiento conduce a hidrogeles más fuertes, pero a su vez genera estructuras más quebradizas. Por lo tanto, es importante encontrar el grado óptimo de entrecruzamiento para lograr un hidrogel relativamente fuerte y a la vez elástico [6]. Asimismo, para la liberación de agentes bioactivos, la estructura porosa de los hidrogeles puede proporcionar una matriz para la carga del fármaco y protegerlo de un ambiente hostil al mismo tiempo. La porosidad puede ser controlada variando la densidad de entrecruzamiento de la matriz de hidrogel [28].

En relación al uso de hidrogeles para la reparación de tejido, es necesario que el hidrogel sea capaz de soportar fuerzas mecánicas específicas de aplicación prolongada, que permita la adhesión celular, la migración, así como lograr una estructura que se ajuste con el sitio de reparación. Además, el hidrogel ideal debe permitir la difusión de nutrientes y productos; y liberar y retener células y factores bioquímicos [29]. Para cumplir con estos requerimientos se ha potenciado el desarrollo de hidrogeles compuestos, es decir, hidrogeles que se forman a partir de mezclas de distintos componentes con diferentes propiedades químicas, físicas y biológicas. Pueden ser considerados como materiales compuestos de la misma manera que los tejidos humanos actúan como compuestos naturales debido a su composición variable [30].

Otra área en que los hidrogeles se aplican eficientemente es en el vendaje de las heridas. Los apó�itos a base de hidrogel son uno de los materiales más prometedores en el cuidado de las heridas, ya que cumplen importantes requisitos en materia de apóśitos, tales como:

mantener la herida húmeda mientras se absorbe un exudado extenso, recubrimiento libre de adhesión del tejido sensible subyacente, reducción del dolor mediante el enfriamiento y un potencial de intervención activa en el proceso de curación de la herida. También, los hidrogeles actúan como una barrera frente a agresiones externas como microorganismos, cuerpos extraños o tejido dañado [31]. En la búsqueda de nuevas estrategias para el tratamiento de heridas agudas y crónicas, se han diseñado apósticos de hidrogel con liberación controlada de fármacos que se dirigen a estructuras esenciales para el proceso de curación de las heridas [32]. La clase más reciente de apósticos de hidrogel bioactivo que se han desarrollado se basa en una cicatrización estimulada por factores de crecimiento, citoquinas o células. Dentro de estas últimas, se incluyen los fibroblastos, queratinocitos y células madre de diversos orígenes [33,34].

Por otro lado, los hidrogeles inyectables, preparados con polímeros naturales, sintéticos o híbridos, se han convertido en una prometedora solución para la liberación eficiente de factores angiogénicos o de células madre y progenitoras para la reparación *in situ* de tejidos, regeneración y neovascularización [35]. Su aplicación es mínimamente invasiva y pueden utilizarse para la entrega y liberación sostenida de agentes bioactivos en el sitio de inyección [36].

1.3.1. Hidrogeles basados en polímeros naturales para aplicaciones biomédicas

El uso de polímeros naturales o biopolímeros en la fabricación de hidrogeles depende de la finalidad del material. Los polímeros naturales se caracterizan ser modificables, de baja toxicidad y susceptibles de degradación por enzimas humanas o por hidrólisis, así como renovables y sostenibles, lo que da lugar a un uso más amplio, especialmente en campos

como las ciencias biomédicas [37]. Los dos principales tipos de polímeros naturales son los polímeros basados en proteínas y polisacáridos (Fig. 1.3).

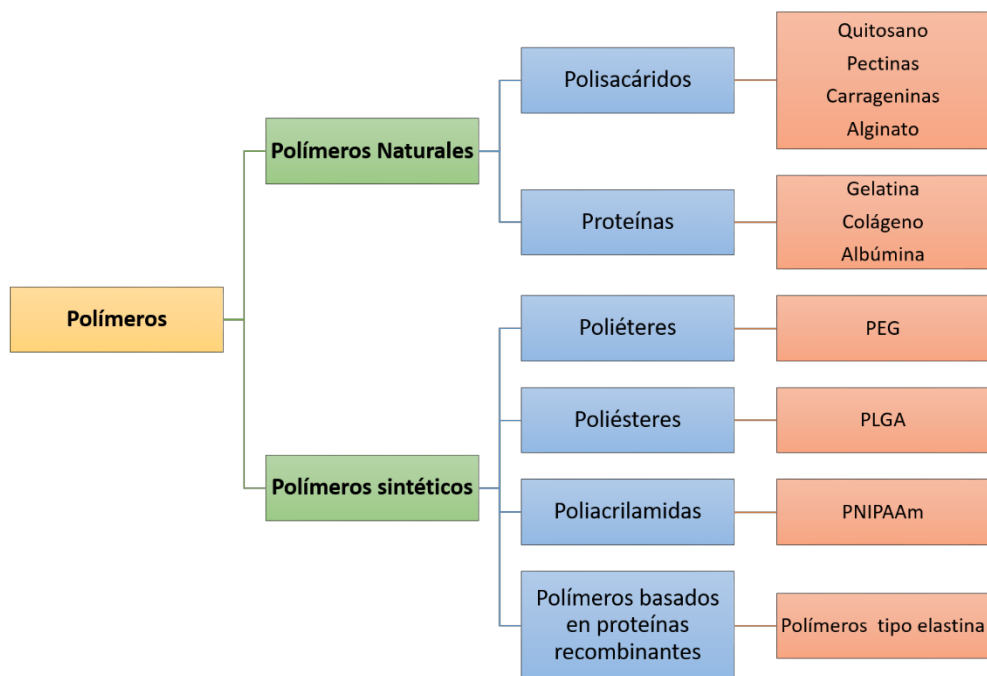


Figura 1.3. Clasificación de los polímeros. PEG: Polyethylene glycol, PLGA: Poly (lactic-co-glycolic acid), PNIPAAm: Poly (N-isopropylacrylamide).

Entre ellos, polisacáridos como el quitosano, pectina y carragenina se han utilizado ampliamente en ámbitos biomédico y farmacéutico, algunos de los cuales se señalan a continuación.

El quitosano, un polisacárido catiónico, es conocido como un material biológico para promover el proceso de curación de los tejidos conectivos blandos y duros. Además de ser biocompatible y no tóxico para los tejidos vivos, posee una actividad antibacteriana [38]. Otra propiedad muy importante del quitosano, dada su naturaleza catiónica, es su capacidad para interactuar con moléculas estructurales como glicosaminoglicanos y glicoproteínas presentes en la matriz extracelular, o incluso con otros biopolímeros aniónicos [39]. Sin embargo, ofrece propiedades mecánicas bajas, por lo tanto, para mejorarlas, se hace énfasis en el desarrollo de hidrogeles híbridos basados en mezclas de quitosano y polímeros naturales o sintéticos, redes de polímeros interpenetradas, así como hidrogeles compuestos

preparados mediante la incorporación de nanopartículas [40]. Los hidrogeles en base a quitosano tienen potencial uso en liberación de fármacos, ingeniería de tejidos y curación de heridas [41].

La pectina, un heteropolisacárido complejo de naturaleza aniónica, ha sido combinada con quitosano formando complejos polielectrolíticos como vehículos de administración de fármacos [42]. También ha sido mezclada con otros polímeros naturales como almidón para la liberación de fármacos, con colágeno para regeneración de hueso y con polímeros sintéticos como polidextrosa y óxido de polietileno para su uso en liberación de fármacos y como dispositivo electroquímico, respectivamente [43].

La carragenina, es una clase de polisacáridos sulfatados, que actualmente es un candidato prometedor en la ingeniería de tejidos y la medicina regenerativa, ya que se asemeja a los glicosaminoglicanos nativos. Su uso en el campo farmacéutico se ha incrementado rápidamente en la última década. La carragenina no sólo se emplea para el suministro de pequeñas fármacos y proteínas, sino también para la regeneración de tejidos mediante el transporte de biomacromoléculas terapéuticas y células [44]. Los hidrogeles de carragenina se forman generalmente a través de gelación termorreversible, entrecruzamiento iónico, así como la modificación de la estructura de la carragenina con fracciones de metacrilato mediante fotoentrecruzamiento [45]. El comportamiento tixotrópico de la carragenina la hace apropiada para formar matrices inyectables para el transporte de células y la inclusión de otras macromoléculas. Los hidrogeles de carragenina presentan altos índices de hinchamiento y presentan una baja estabilidad en condiciones fisiológicas. Para superar estos inconvenientes, se han desarrollado estrategias como la combinación con otros biopolímeros, la adición de fotoentrecruzadores y la formación de complejos polielectrolitos [46].

1.3.2. Hidrogeles basados en polímeros sintéticos para aplicaciones biomédicas

Los polímeros sintéticos son, por su naturaleza química, mecánicamente más fuertes comparados con los polímeros naturales. Esta mejorada resistencia mecánica proporciona una excelente durabilidad del biomaterial al reducir la tasa de su degradación. Los hidrogeles sintéticos para uso biomédico por lo general incorporan polímeros como la poliacrilamida y sus derivados; alcohol polivinílico o polietilenglicol (PEG), entre otros [15].

PEG es uno de los polímeros más estudiados para la administración eficiente de proteínas y péptidos terapéuticos. Es conocido por ser no inmunogénico, no tóxico, no antigénico, altamente soluble en agua y está aprobado por la FDA [16]. Hidrogeles basados en sus derivados, como metacrilato de polietilenglicol, dimetacrilato de polietilenglicol y diacrilato de polietilenglicol también son aplicados ampliamente en aplicaciones biomédicas [47].

Los hidrogeles de poliacrilamida se sintetizan generalmente a partir de monómeros de acrilamida. Según la aplicación, sus propiedades pueden alterarse ajustando las condiciones de síntesis, mediante la copolimerización con otros monómeros o mediante la modificación química de los hidrogeles sintetizados. Los hidrogeles de poliacrilamida suelen tener una red reticulada estructurada y se suelen emplear como polímeros que responden a estímulos, en particular a la temperatura y al pH [15].

Considerando lo anteriormente expuesto, a pesar de la considerable investigación y desarrollo acerca de biomateriales para aplicaciones médicas en los últimos años, aún quedan desafíos por superar para encontrar los polímeros ideales para la liberación de fármacos, regeneración de tejidos y curación de heridas, entre otras aplicaciones. El diseño y la síntesis de nuevas matrices poliméricas como los hidrogeles, que proporcionen biocompatibilidad, biodegradabilidad y capacidades adaptables es esencial para progresar en el campo de los biomateriales funcionales. Las estrategias recientes se han centrado en

el desarrollo de hidrogeles compuestos o híbridos a partir de polímeros naturales o sintéticos, para obtener las propiedades requeridas para su correspondiente aplicación.

1.4. Referencias

- [1] S. Behera, P.A. Mahanwar, Superabsorbent polymers in agriculture and other applications: a review, *Polym. Technol. Mater.* 59 (2020) 341–356. doi:10.1080/25740881.2019.1647239.
- [2] A. Nešić, G. Cabrera-Barjas, S. Dimitrijević-Branković, S. Davidović, N. Radovanović, C. Delattre, Prospect of polysaccharide-based materials as advanced food packaging, *Molecules*. 25 (2020). doi:10.3390/molecules25010135.
- [3] S. Saghzadeh, C. Rinoldi, M. Schot, S. Saheb, F. Shari, E. Jalilian, K. Nuutila, G. Giatsidis, P. Mostafalu, H. Derakhshandeh, K. Yue, W. Swieszkowski, A. Memic, A. Tamayol, A. Khademhosseini, Drug delivery systems and materials for wound healing applications, *Adv. Drug Deliv. Rev.* 127 (2018) 138–166. doi:10.1016/j.addr.2018.04.008.
- [4] R. Choudhary, M. Saraswat, S.K. Venkatraman, A Fundamental Approach Toward Polymers and Polymer Composites: Current Trends for Biomedical Applications, in: *Polym. Nanocomposites Biomed. Eng.*, 2019: pp. 1–28. doi:10.1007/978-3-030-04741-2_1.
- [5] N.A. Peppas, J.Z. Hilt, A. Khademhosseini, R. Langer, Hydrogels in biology and medicine : from molecular principles to bionanotechnology, *Adv. Mater.* 18 (2006) 1345–1360. doi:10.1002/adma.200501612.
- [6] N.A. Peppas, P. Bures, W. Leobandung, H. Ichikawa, Hydrogels in pharmaceutical formulations, *Eur. J. Pharm. Biopharm.* 50 (2000) 27–46. doi:10.1016/S0939-6411(00)00090-4.
- [7] I.M. El-Sherbiny, M.H. Yacoub, Hydrogel scaffolds for tissue engineering: Progress and challenges, *Glob. Cardiol. Sci. Pract.* 38 (2013) 1–27. doi:10.5339/gcsp.2013.38.
- [8] S. Khan, A. Ullah, K. Ullah, N.U. Rehman, Insight into hydrogels, *Des. Monomers Polym.* 19 (2016) 456–478. doi:10.1080/15685551.2016.1169380.
- [9] B. V Slaughter, S.S. Khurshid, O.Z. Fisher, A. Khademhosseini, N.A. Peppas, Hydrogels in Regenerative Medicine, *Adv. Mater.* 21 (2009) 3307–3329. doi:10.1016/B978-0-323-22805-3.00012-8.
- [10] N.N. Ferreira, L.M.B. Ferreira, V.M.O. Cardoso, F.I. Boni, A.L.R. Souza, M.P.D. Gremião, Recent advances in smart hydrogels for biomedical applications: From self-assembly to functional approaches, *Eur. Polym. J.* 99 (2018) 117–133.

- doi:10.1016/j.eurpolymj.2017.12.004.
- [11] S.J. Buwalda, K.W.M. Boere, P.J. Dijkstra, J. Feijen, T. Vermonden, W.E. Hennink, Hydrogels in a historical perspective: From simple networks to smart materials, *J. Control. Release.* 190 (2014) 254–273. doi:10.1016/j.jconrel.2014.03.052.
 - [12] S. Van Vlierberghe, P. Dubrule, E. Schacht, Biopolymer-based hydrogels as scaffolds for tissue engineering applications: A review, *Biomacromolecules.* 12 (2011) 1387–1408. doi:10.1021/bm200083n.
 - [13] O. Wichterle, D. Lím, Hydrophilic Gels for Biological Use, *Nature.* 185 (1960) 117–118. doi:<https://doi.org/10.1038/185117a0>.
 - [14] F. Ullah, M.B.H. Othman, F. Javed, Z. Ahmad, H.M. Akil, Classification, processing and application of hydrogels: A review, *Mater. Sci. Eng. C.* 57 (2015) 414–433. doi:10.1016/j.msec.2015.07.053.
 - [15] D.A. Gyles, L.D. Castro, J.O.. Silva Jr, R.M. Ribeiro-Costa, A review of the designs and prominent biomedical advances of natural and synthetic hydrogel formulations, *Eur. Polym. J.* 88 (2017) 373–392. doi:10.1016/j.eurpolymj.2017.01.027.
 - [16] M.S. Hamid Akash, K. Rehman, S. Chen, Natural and synthetic polymers as drug carriers for delivery of therapeutic proteins, *Polym. Rev.* 55 (2015) 371–406. doi:10.1080/15583724.2014.995806.
 - [17] O. Robles-Vazquez, I. Orozco-Avila, J.C. Sánchez-Díaz, E. Hernandez, An Overview of Mechanical Tests for Polymeric Biomaterial Scaffolds Used in Tissue Engineering, *J. Res. Updat. Polym. Sci.* 4 (2015) 168–178.
 - [18] E.M. Ahmed, Hydrogel: Preparation, characterization, and applications: A review, *J. Adv. Res.* 6 (2015) 105–121. doi:10.1016/j.jare.2013.07.006.
 - [19] L.H. Sperling, V. Mishra, The current status of interpenetrating polymer networks, *Polym. Adv. Technol.* 7 (1996) 197–208. doi:10.1002/(SICI)1099-1581(199604)7:4<197::AID-PAT514>3.0.CO;2-4.
 - [20] T.R. Hoare, D.S. Kohane, Hydrogels in drug delivery: Progress and challenges, *Polymer (Guildf).* 49 (2008) 1993–2007. doi:10.1016/j.polymer.2008.01.027.
 - [21] N. Zoratto, P. Matricardi, Semi-IPNs and IPN-based hydrogels, in: *Polym. Gels*, Elsevier Ltd, 2018: pp. 91–124. doi:10.1016/b978-0-08-102179-8.00004-1.
 - [22] E.S. Dragan, Design and applications of interpenetrating polymer network hydrogels . A review, *Chem. Eng. J.* 243 (2014) 572–590. doi:10.1016/j.cej.2014.01.065.
 - [23] E.S. Dragan, Advances in interpenetrating polymer network hydrogels and their

- applications, 86 (2014) 1707–1721. doi:10.1515/pac-2014-0713.
- [24] K. Varaprasad, G.M. Raghavendra, T. Jayaramudu, M.M. Yallapu, R. Sadiku, A mini review on hydrogels classification and recent developments in miscellaneous applications, *Mater. Sci. Eng. C*. 79 (2017) 958–971. doi:10.1016/j.msec.2017.05.096.
- [25] L.R. Feksa, E.A. Troian, C.D. Muller, F. Viegas, A.B. Machado, V.C. Rech, Hydrogels for biomedical applications, in: *Nanostructures Eng. Cells, Tissues Organs From Des. to Appl.*, 2018: pp. 403–438. doi:10.1016/B978-0-12-813665-2.00011-9.
- [26] Q. Chai, Y. Jiao, X. Yu, Hydrogels for biomedical applications: Their characteristics and the mechanisms behind them, *Gels.* 3 (2017) 6. doi:10.3390/gels3010006.
- [27] A. Parodi, I. Yazdi, M. Evangelopoulos, N.T. Furman, Smart Hydrogels, in: *Encycl. Nanotechnol.*, 2015: pp. 1–13. doi:10.1007/978-94-007-6178-0.
- [28] J. Li, D.J. Mooney, Designing hydrogels for controlled drug delivery, *Nat. Rev. Mater.* 1 (2016) 16071. doi:10.1038/natrevmats.2016.71.
- [29] D.P. Pacheco, L. Zorzetto, P. Petrini, Soft tissue application of biocomposites, in: *Biomed. Compos.*, Second Edi, Elsevier Ltd., 2017: pp. 59–82. doi:10.1016/b978-0-08-100752-5.00004-4.
- [30] C. Sheffield, K. Meyers, E. Johnson, R. Rajachar, Application of Composite Hydrogels to Control Physical Properties in Tissue Engineering and Regenerative Medicine, *Gels.* 4 (2018) 51. doi:10.3390/gels4020051.
- [31] J. Koehler, F.P. Brandl, A.M. Goepferich, Hydrogel wound dressings for bioactive treatment of acute and chronic wounds, *Eur. Polym. J.* 100 (2018) 1–11. doi:10.1016/j.eurpolymj.2017.12.046.
- [32] L. Elviri, A. Bianchera, C. Bergonzi, R. Bettini, Controlled local drug delivery strategies from chitosan hydrogels for wound healing, *Expert Opin. Drug Deliv.* 14 (2017) 897–908. doi:10.1080/17425247.2017.1247803.
- [33] N. Kalai Selvan, T.S. Shanmugarajan, V.N.V.A. Uppuluri, Hydrogel based scaffolding polymeric biomaterials: Approaches towards skin tissue regeneration, *J. Drug Deliv. Sci. Technol.* 55 (2020). doi:10.1016/j.jddst.2019.101456.
- [34] A.P. Veith, K. Henderson, A. Spencer, A.D. Sligar, A.B. Baker, Therapeutic strategies for enhancing angiogenesis in wound healing, *Adv. Drug Deliv. Rev.* 146 (2019) 97–125. doi:10.1016/j.addr.2018.09.010.
- [35] A. Pal, B.L. Vernon, M. Nikkhah, Therapeutic neovascularization promoted by injectable hydrogels, *Bioact. Mater.* 3 (2018) 389–400.

- doi:10.1016/j.bioactmat.2018.05.002.
- [36] H.F. Darge, A.T. Andrgie, H.C. Tsai, J.Y. Lai, Polysaccharide and polypeptide based injectable thermo-sensitive hydrogels for local biomedical applications, *Int. J. Biol. Macromol.* 133 (2019) 545–563. doi:10.1016/j.ijbiomac.2019.04.131.
- [37] L.F. Santos, I.J. Correia, A.S. Silva, J.F. Mano, Biomaterials for drug delivery patches, *Eur. J. Pharm. Sci.* 118 (2018) 49–66. doi:10.1016/j.ejps.2018.03.020.
- [38] A. Oryan, S. Sahviev, Effectiveness of chitosan scaffold in skin, bone and cartilage healing, *Int. J. Biol. Macromol.* 104 (2017) 1003–1011. doi:10.1016/j.ijbiomac.2017.06.124.
- [39] J. Nilsen-Nygaard, S.P. Strand, K.M. Vårum, K.I. Draget, C.T. Nordgård, Chitosan: Gels and interfacial properties, *Polymers (Basel)*. 7 (2015) 552–579. doi:10.3390/polym7030552.
- [40] L. Racine, I. Texier, R. Auzély-Velty, Chitosan-based hydrogels: Recent design concepts to tailor properties and functions, *Polym. Int.* 66 (2017) 981–998. doi:10.1002/pi.5331.
- [41] T. Wu, Y. Li, D.S. Lee, Chitosan-based composite hydrogels for biomedical applications, *Macromol. Res.* (2017) 1–9. doi:10.1007/s13233-017-5066-0.
- [42] L. Neufeld, H. Bianco-Peled, Pectin–chitosan physical hydrogels as potential drug delivery vehicles, *Int. J. Biol. Macromol.* 101 (2017) 852–861. doi:10.1016/j.ijbiomac.2017.03.167.
- [43] A. Noreen, Z. i. H. Nazli, J. Akram, I. Rasul, A. Mansha, N. Yaqoob, R. Iqbal, S. Tabasum, M. Zuber, K.M. Zia, Pectins functionalized biomaterials; a new viable approach for biomedical applications: A review, *Int. J. Biol. Macromol.* 101 (2017) 254–272. doi:10.1016/j.ijbiomac.2017.03.029.
- [44] L. Li, R. Ni, Y. Shao, S. Mao, Carrageenan and its applications in drug delivery, *Carbohydr. Polym.* 103 (2014) 1–11. doi:10.1016/j.carbpol.2013.12.008.
- [45] R. Yegappan, V. Selvaprithiviraj, S. Amirthalingam, R. Jayakumar, Carrageenan based hydrogels for drug delivery , tissue engineering and wound healing, *Carbohydr. Polym.* 198 (2018) 385–400. doi:10.1016/j.carbpol.2018.06.086.
- [46] D. Diekjürgen, D.W. Grainger, Polysaccharide matrices used in 3D *in vitro* cell culture systems, *Biomaterials.* 141 (2017) 96–115. doi:10.1016/j.biomaterials.2017.06.020.
- [47] I. Gibas, H. Janik, Review: Synthetic polymer hydrogels for biomedical application, *Chem Chem Technol.* 4 (2010) 297–304.

CAPÍTULO 2: Objetivos y estructura de la tesis

2.1. Objetivos de la tesis

El objetivo general de este trabajo de tesis fue el desarrollo y la caracterización de nuevos hidrogeles basados en biopolímeros para aplicaciones médicas. Esta tesis doctoral se ha centrado en las aplicaciones de liberación de fármacos, reparación de tejidos y curación de heridas.

Para esto, se seleccionaron polímeros sintéticos y naturales para la preparación y caracterización de hidrogeles híbridos o compuestos, con el fin de encontrar los biomateriales con las mejores propiedades de acuerdo a la aplicación deseada. A partir de los antecedentes bibliográficos y los ensayos que se realizaron en el laboratorio, diversas estrategias fueron adoptadas para obtener los hidrogeles. Dentro de ellas se encuentran la combinación de diferentes polímeros, cambio en diseño de hidrogel según el origen de los polímeros y su entrecruzamiento, variación en las concentraciones de polímeros, incorporación de micropartículas y pruebas preliminares de liberación de moléculas. Estas consideraciones llevaron al diseño de hidrogeles interpenetrados y semi-interpenetrados, hidrogeles compuestos incorporando micropartículas e hidrogeles físicos híbridos.

A continuación, se detallan los objetivos específicos del trabajo que fueron desarrollados en este trabajo de tesis:

1. Desarrollar un nuevo hidrogel biocompatible mediante la combinación de polímeros de origen natural y sintético que presente propiedades mecánicas y de hinchamiento mejores que las obtenidas con los polímeros individuales con potencial para aplicaciones de ingeniería de tejidos y liberación de fármacos.
2. Preparar un nuevo hidrogel compuesto a través de la incorporación de micropartículas dentro del hidrogel para la administración simultánea de dos fármacos hidrofóbicos. Adicionalmente, demostrar que un hidrogel compuesto

permite obtener una liberación de fármacos más prolongada que la obtenida con las micropartículas o con el hidrogel por separado.

3. Obtener un nuevo hidrogel inyectable usando una mezcla de polímeros naturales físicamente entrecruzados con la capacidad de liberar moléculas y permitir la adhesión y migración celular para la curación de heridas y reparación de tejidos.

Los hidrogeles preparados fueron ampliamente evaluados y caracterizados en diferentes aspectos tales como propiedades morfológicas y mecánicas, comportamiento de hinchamiento, identificación de los grupos funcionales y ensayos celulares *in vitro*.

En consecuencia, los objetivos que se propusieron alcanzar en este trabajo doctoral son de gran interés para el desarrollo de nuevos biomateriales funcionales con potenciales aplicaciones médicas.

2.2. Estructura de la tesis

El presente trabajo fue dividido en siete capítulos principales, cuyo resumen de contenidos se presenta a continuación:

- Capítulo 1: Introducción

Este capítulo da una visión general de los hidrogeles, su clasificación y su estado actual con respecto a su uso en distintas aplicaciones biomédicas.

- Capítulo 2: Objetivos y estructura de la tesis

En este capítulo se indican el objetivo general y los objetivos específicos de la tesis, además de señalar la estructura de los contenidos de la tesis.

- Capítulo 3: Materiales y técnicas de caracterización

En este capítulo se explican los principales materiales y técnicas de caracterización utilizados en esta tesis.

- Capítulo 4: Entrapment of chitosan, pectin or κ -carrageenan within methacrylate based hydrogels: Effect on swelling and mechanical properties.

Este capítulo describe la obtención de nuevos hidrogeles compuestos mediante la incorporación de quitosano, pectina o κ -carragenina dentro de hidrogeles a base de metacrilato para mejorar las propiedades mecánicas y de hinchamiento con potenciales aplicaciones en ingeniería de tejido o liberación de fármacos. Este capítulo corresponde al desarrollo del objetivo específico 1.

- Capítulo 5: Poly(hydroxybutyrate-co-hydroxyvalerate) microparticles embedded in κ -carrageenan/locust bean gum hydrogel as a dual drug delivery carrier.

Este capítulo explica la preparación y caracterización de un nuevo hidrogel compuesto como vehículo de administración dual de fármacos. Se prepararon micropartículas de poli(hidroxibutirato-co-hidroxivalerato) para encapsular simultáneamente dos fármacos hidrofóbicos. Estas micropartículas fueron embebidas en un hidrogel físicamente reticulado de κ -carragenina y goma de algarrobo. Se evaluó la cinética de liberación de los fármacos. Este capítulo corresponde al objetivo específico 2.

- Capítulo 6: Novel carrageenan-based physically crosslinked injectable hydrogel for wound healing applications and tissue repairing.

En este capítulo se presenta un nuevo hidrogel inyectable entrecruzado físicamente compuesto de kappa y iota carragenina, goma de algarrobo y gelatina para aplicaciones en reparación de tejidos y curación de heridas. Este capítulo corresponde al objetivo específico 3.

- Capítulo 7: Conclusiones generales

En este capítulo se resumen las conclusiones de cada uno de los capítulos y se presentan las conclusiones generales.

Cada capítulo, que está relacionado con los objetivos específicos, fue escrito de manera independiente en formato de publicación. Cada uno de estos capítulos está dividido en una introducción, una sección de materiales y métodos, una sección de resultados y discusión y una sección de conclusiones. Las referencias fueron presentadas por separado para el capítulo 1 de introducción y para cada capítulo individual posterior.

CAPÍTULO 3: Materiales y técnicas de caracterización

3.1. Materiales

3.1.1. Quitosano

El quitosano es un polisacárido que se obtiene por desacetilación alcalina de la quitina, la cual es el componente principal del exoesqueleto de crustáceos. Es el segundo polisacárido más abundante en la naturaleza después de la celulosa [1]. Está formado por unidades de D-glucosamina y N-acetil-D-glucosamina, unidas por enlaces glucosídicos β -1,4 (Fig. 3.1). La relación entre estas dos unidades se considera como el grado de desacetilación. Cuando el grado de desacetilación alcanza alrededor del 50%, se vuelve soluble en medios acuosos ácidos. Cuando el quitosano se disuelve en un medio ácido, los grupos amino se protonan (pK_a alrededor de 6.5) y el polímero se vuelve catiónico, permitiéndole interactuar con diversos tipos de moléculas [2]. La solubilidad del quitosano no solo depende del grado de desacetilación sino también de la distribución de los grupos acetilos a lo largo de la cadena principal, además del peso molecular [3]. La presencia de grupos amino primario hace del quitosano un polímero atractivo para la modificación química mediante la unión covalente de varios grupos químicos. Además, puede formar complejos con un gran número de diferentes poli-aniones, como el ADN, alginatos, pectinas, glucosaminoglicanos, gelatina, así como polímeros sintéticos [4].

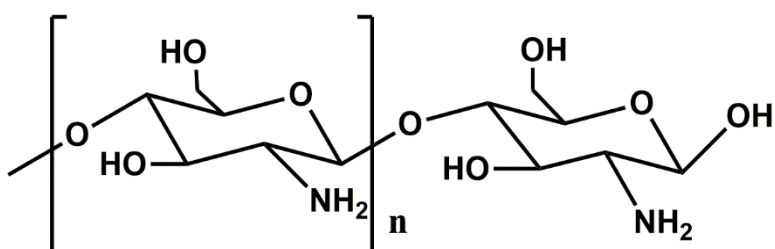


Figura 3.1. Estructura química del quitosano.

3.1.2. Pectina

La pectina es un heteropolisacárido complejo y el componente más abundante y multifuncional de la pared celular de todas las plantas terrestres. Comercialmente, las pectinas se extraen principalmente de la cáscara de los cítricos y del orujo de manzana, ambos son subproductos de las unidades de fabricación de jugos. Está compuesta básicamente por una cadena lineal de residuos de ácido α -(1,4)-D-galacturónico cuyos grupos carboxílicos se encuentran parcialmente metoxilados y una variedad de azúcares neutros como la arabinosa, la galactosa, la ramnosa y cantidades menores de otros azúcares [5] (Fig. 3.2). Las pectinas se clasifican en función de su grado de esterificación (DE). El grado de esterificación es el número de grupos metoxilo que sustituyen a la fracción de ácido carboxílico (-COOH) en los residuos de ácido galacturónico [6]. Las pectinas de alto contenido de metoxilo (HM), con DE > 50%, requieren una concentración relativamente alta de sólidos solubles y un pH bajo para la formación del gel. Las pectinas de bajo contenido de metoxilo (LM), con DE < 50%, forman geles rígidos por la acción del calcio o de cationes multivalentes, que entrecruzan las cadenas de ácido galacturónico [7].

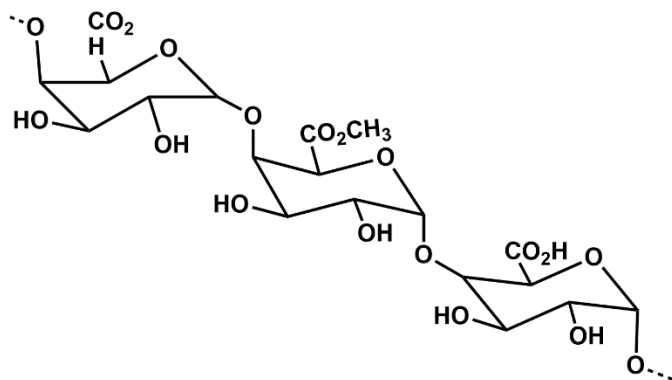


Figura 3.2. Estructura química de la pectina.

3.1.3. Carrageninas

Las carrageninas son polisacáridos lineales sulfatados extraídos de ciertas algas rojas de la clase *Rhodophyceae*. Están formadas por unidades alternas de D-galactosa y 3,6-anhidro-galactosa unidas por enlaces glucosídicos α -1,3 y β -1,4. La reactividad química de las carrageninas se debe principalmente a sus grupos sulfato, que son fuertemente aniónicos, siendo comparables al sulfato inorgánico [8]. Las tres carrageninas comerciales más importantes son: Iota (ι), Kappa (κ) y Lambda (λ) carragenina, cada subtipo es extraído de distintas fuentes de algas. Las principales diferencias que influyen en las propiedades del tipo carragenina son el número y la posición de los grupos éster sulfato, así como el contenido de 3,6-anhidrogalactosa. Se ha informado que niveles más altos de éster sulfato resultan en una temperatura de solubilidad menor y una disminución de la fuerza de gel [9]. Los dímeros de κ , ι y λ -carragenina tienen uno, dos y tres grupos de éster de sulfato, respectivamente, lo que da como resultado un contenido de sulfato calculado correspondiente del 20%, 33% y 41% (p/p) (Fig. 3.3). Por lo general, κ -carragenina comercial contiene un 22% (p/p) de sulfato, ι -carragenina un 32% (p/p) y λ -carragenina un 38% (p/p), aunque pueden producirse grandes variaciones debido a las diferencias entre las especies o partidas de algas marinas. Entre las carrageninas comerciales, la κ - y ι - son carrageninas gelificantes, mientras que la λ -carragenina se caracteriza sólo como un agente espesante. Las kappa y iota-carrageninas forman una red de dobles hélices tridimensionales, resultado del entrecruzamiento de las cadenas螺旋ales adyacentes que contienen grupos de sulfatos orientados hacia su parte externa. En la λ -carragenina, los grupos sulfato en la posición 2 están orientados hacia la parte interna, evitando así este entrecruzamiento [10]. La gelificación de κ y ι -carrageninas es inducida térmicamente, donde a elevadas temperaturas ambas cadenas existen en bobinas aleatorias y al enfriarse las cadenas se reorientan a una conformación más ordenada que consiste en hélices, las cuales posteriormente se agregan en hélices ordenadas en presencia de cationes [9] (Fig. 3.4). La

presencia de un catión adecuado, habitualmente potasio o calcio, es un requisito imprescindible para que se produzca la gelificación [10].

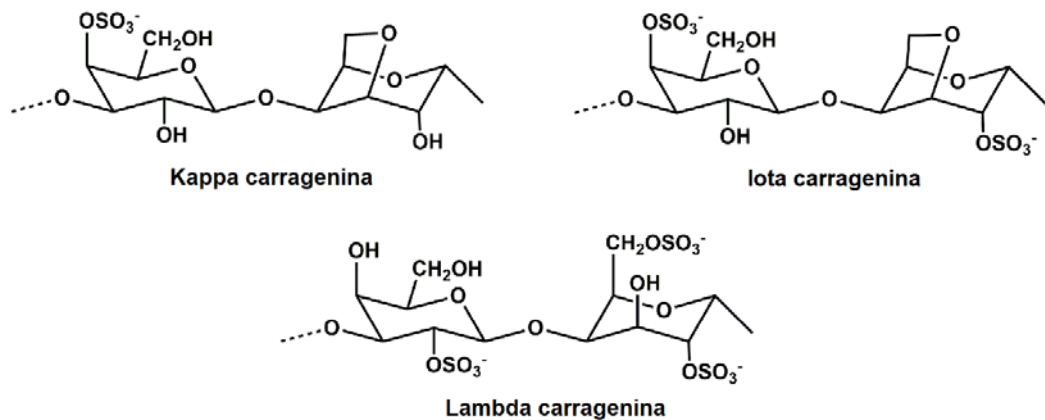


Figura 3.3. Representación esquemática de unidades repetidas idealizadas de kappa, iota y lambda carrageninas.

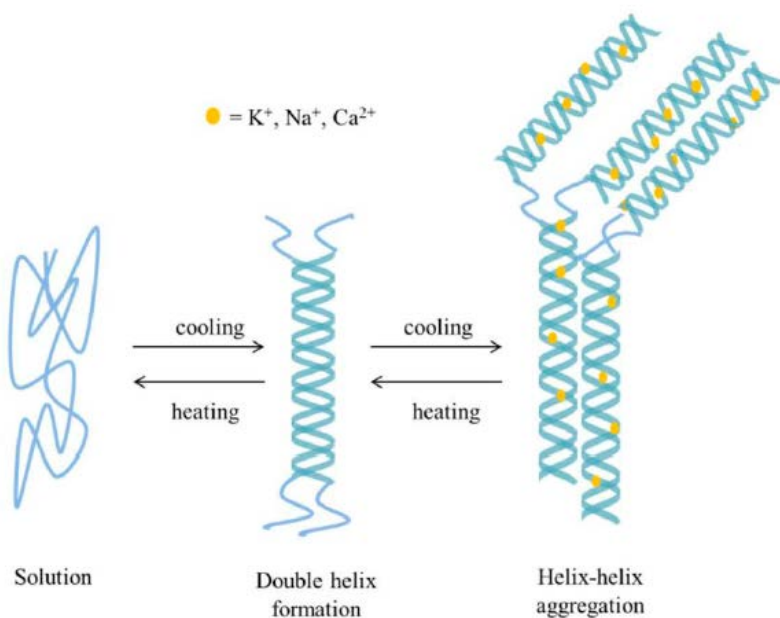


Figura 3.4. Esquema de la formación del gel de carragenina. La gelificación de las soluciones de carragenina se produce como resultado de la transición conformacional de bobina a hélice y la posterior agregación entre hélices ordenadas. Los cationes son los responsables de la transición final sol-gel del polisacárido [11].

3.1.4. Monómeros sintéticos

El poli(etilenglicol) (PEG), es uno de los polímeros sintéticos más ampliamente usados en biomedicina. Los hidrogeles basados en sus derivados como el polietilenglicol metacrilato, el polietilenglicol dimetacrilato y el polietilenglicol diacrilato, también se aplican extensamente [12]. Las propiedades del PEG, incluyendo su biocompatibilidad, no inmunogenicidad y resistencia a la adsorción de proteínas, fueron los factores que influyeron en su aprobación por parte de la Administración de Medicamentos y Alimentos (FDA, *Food and Drug Administration*) para su uso en diversas aplicaciones biomédicas [13].

En este trabajo se utilizó polietilenglicol metil éter metacrilato (PEGMEM) (Fig. 3.5a), anteriormente utilizado en la preparación de hidrogeles para aplicaciones médicas [14,15]. El PEGMEM es una clase de monómeros polimerizables, que forman fácilmente homopolímeros o copolímeros. Al mismo tiempo, tiene la misma estructura y cristalinidad que el PEG [16].

Otro monómero sintético utilizado en este trabajo fue 2-dimetilamino etil metacrilato (DMAEM) (Fig. 3.5b), también utilizado previamente en el desarrollo de hidrogeles para aplicaciones médicas [17,18]. El poli(2-dimetilamino)etil metacrilato es un polímero hidrófilo, biocompatible, biodegradable, no citotóxico, sensible al pH y a la temperatura, con grupos funcionales de aminas terciarias [18].

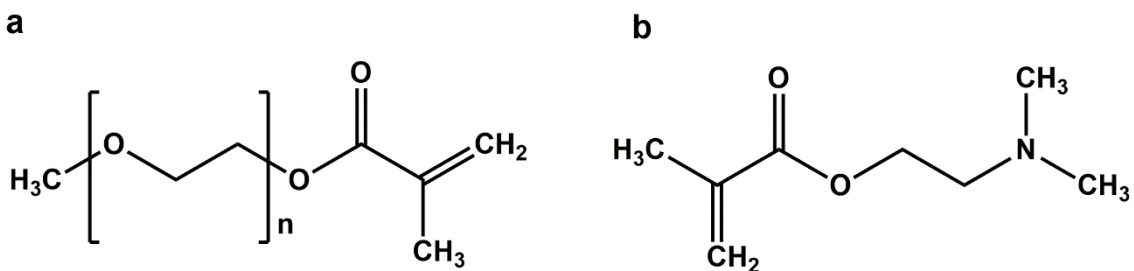


Figura 3.5. Estructura química de PEGMEM (a) y DMAEM (b).

3.1.5. PHBV

El poli(3-hidroxibutirato-co-3-hidroxivalerato) (PHBV) es un poliéster alifático obtenido a través de la copolimerización de polihidroxibutirato (PHB) e hidroxivalerato, los cuales pertenecen a una clase de polímeros naturales llamados poli (ácidos hidroxialcanoatos) (PHAs) (Fig. 3.6). PHB es un polímero rígido y altamente cristalino con una tasa de degradación lenta, mientras que el PHBV tiene una temperatura de transición vítrea y de fusión más baja y como consecuencia es más flexible y más fácil de procesar que el PHB [19]. Dependiendo del porcentaje de unidades de hidroxibutirato (HB) e hidroxivalerato (HV), se puede obtener una amplia variedad de propiedades y procesabilidad. Se ha señalado que un incremento en los bloques de HB da como resultado una temperatura de transición vítrea y punto de fusión más alta. Mientras que un aumento en los bloques de HV conducen a una mayor ductilidad y una menor cristalinidad [20]. El PHBV muestra propiedades fisicoquímicas casi idénticas al ácido poliláctico-co-glicólico (PLGA). En comparación con la PLGA, el PHBV tiene un menor coste de producción y muestra un mayor rendimiento de la producción. Además, otra ventaja del PHBV es que puede ser producido por microorganismos en condiciones de crecimiento desfavorables como el estrés físico o nutricional [21]. Debido a estas ventajas, el PHBV se ha convertido en un candidato prometedor en el campo del desarrollo de nuevos sistemas de administración de medicamentos [22–24]. Micropartículas de PHAs han sido desarrolladas por diferentes métodos de microencapsulación que se basan en técnicas de evaporación de solventes, emulsificación-difusión, entre otras [25].

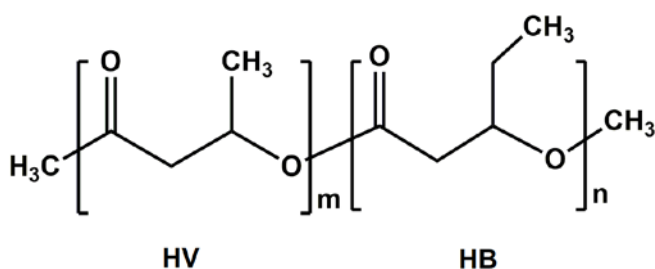


Figura 3.6. Estructura química del PHBV.

3.1.6. Goma de algarrobo

La goma de algarrobo (*Locust bean gum*, LBG) es un polisacárido neutro compuesto de unidades de manosa y galactosa y, por lo tanto, pertenece a la categoría de los galactomananos. Se obtiene del endospermo de las semillas presentes en los granos de *Ceratonia siliqua* (algarrobo), (familia *Leguminosae*). La estructura general consiste en una cadena lineal de D-manoasas unidas por enlace β (1,4) que presenta ramificaciones de D-galactosa, unidas a la cadena principal mediante enlaces α (1-6) (Fig. 3.7). Las unidades de manosa y galactosa están presentes en la proporción 4:1 [26]. La distribución de los residuos de D-galactosa o cadenas laterales a lo largo de la cadena principal de manosa puede ser aleatoria, en bloque y ordenada. Se considera que la molécula de galactomanano exhibe una estructura extendida en forma de cinta en el estado sólido y una conformación en forma de bobina semi-flexible en solución. LBG es parcialmente soluble en agua fría y necesita ser calentada para alcanzar la máxima solubilidad. LBG no forma gel en condiciones normales, pero se puede obtener un gel débil con un procedimiento de congelación-descongelación. LBG forma un gel en presencia de una gran cantidad de azúcar [27]. Puede interactuar sinéricamente con otros biopolímeros como la carragenina y el xantano para formar geles más elásticos y fuertes [28]. LBG se utiliza con frecuencia para aumentar la estabilidad mecánica del hidrogel de kappa carragenina, debido a su capacidad de interactuar con los grupos de sulfato de la carragenina a través de los enlaces de hidrógeno [29]. LBG se utiliza en aplicaciones biofarmacéuticas con varias funciones distintas, que van desde el excipiente de liberación controlada hasta tabletas de desintegración [30].

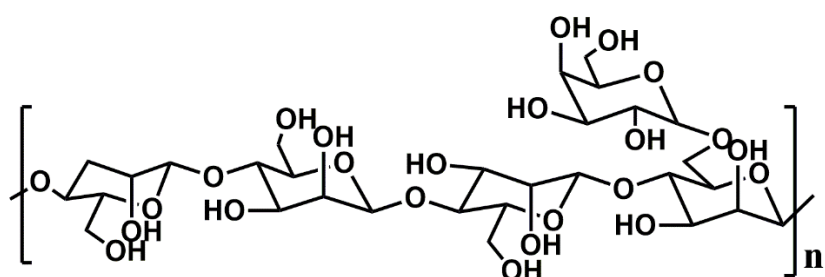


Figura 3.7. Estructura química del LBG.

3.1.7. Gelatina

La gelatina es una proteína de una sola hebra extraída del colágeno que es el principal componente de la matriz extracelular (ECM) [31]. Se produce por hidrólisis parcial de colágeno extraído de la piel, los huesos y los tejidos conectivos de los animales, por lo cual está ampliamente disponible, es degradable y muestra una excelente biocompatibilidad *in vivo* [32].

La gelatina es una mezcla heterogénea de polipéptidos de una o varias cadenas, que contiene entre 300 y 4000 aminoácidos (Fig. 3.8). Se obtiene comercialmente mediante la ruptura ácida o básica de los enlaces covalentes intermoleculares e intramoleculares que estabilizan el colágeno porcino o bovino. Según el proceso utilizado para su fabricación, la gelatina puede ser de tipo A o tipo B. La gelatina de tipo A se obtiene por tratamiento ácido del colágeno y tiene un punto isoeléctrico (*pI*) entre 7.0 y 9.0. La gelatina de tipo B, se obtiene por hidrólisis alcalina de colágeno y tiene un *pI* entre 4.8 y 5.0 [33]. La gelatina forma un gel termorreversible y transparente por debajo de la temperatura de transición sol-gel (aprox. 40 °C) por la formación de hélices triples [34]. Este biopolímero ha demostrado ser un candidato ideal para aplicaciones relacionadas con la ECM, estructuras de soporte y el trasplante de células. Sin embargo, tiene propiedades mecánicas deficientes y requiere de entrecruzamiento, el cual puede ser físico, químico o enzimático para ser funcional como una ECM [13]. Además, la gelatina muestra propiedades de interacción celular debido a la presencia de tripéptidos de arginina, glicina y ácido aspártico (RGD) en su estructura [31].

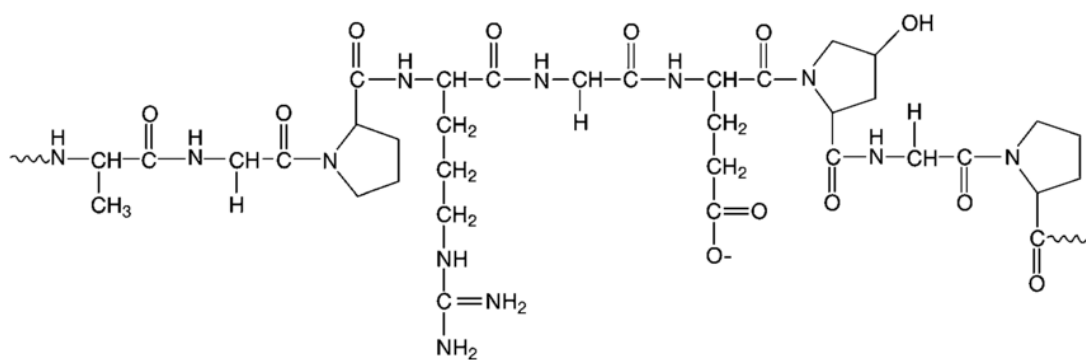


Figura 3.8. Estructura química básica de la gelatina [33].

3.2. Métodos

3.2.1. Microscopía electrónica de barrido

El microscopio electrónico de barrido permite obtener imágenes de alta resolución de materiales minerales, metálicos y orgánicos. La luz es sustituida por un haz de electrones, las lentes por electroimanes y las muestras no conductoras se vuelven conductoras al metalizar su superficie con metales específicos como el oro, la plata, el platino y el iridio. El material para observar queda cubierto con átomos conductores. Esta capa de átomos conductores no forma una carga negativa cuando el haz de electrones de alta energía incide sobre la muestra. Interactúa con la nube de electrones de la muestra y emite electrones de baja energía. Un detector de electrones secundarios cargados atrae inmediatamente todos los electrones de baja energía hacia el interior del tubo. Cada captura corresponde a un píxel en la imagen de la superficie del objeto.

La computadora transforma la señal, píxel a píxel, del barrido de una superficie en la correspondiente imagen visible en un tubo de rayos catódicos. Los puntos elevados de la muestra aparecen blancos en la pantalla, los puntos bajos aparecen oscuros. Los puntos inclinados hacia el detector se ven un poco más brillantes y los inclinados en la dirección opuesta, algo más atenuados. La Fig. 3.9 muestra un esquema de un microscopio electrónico de barrido.

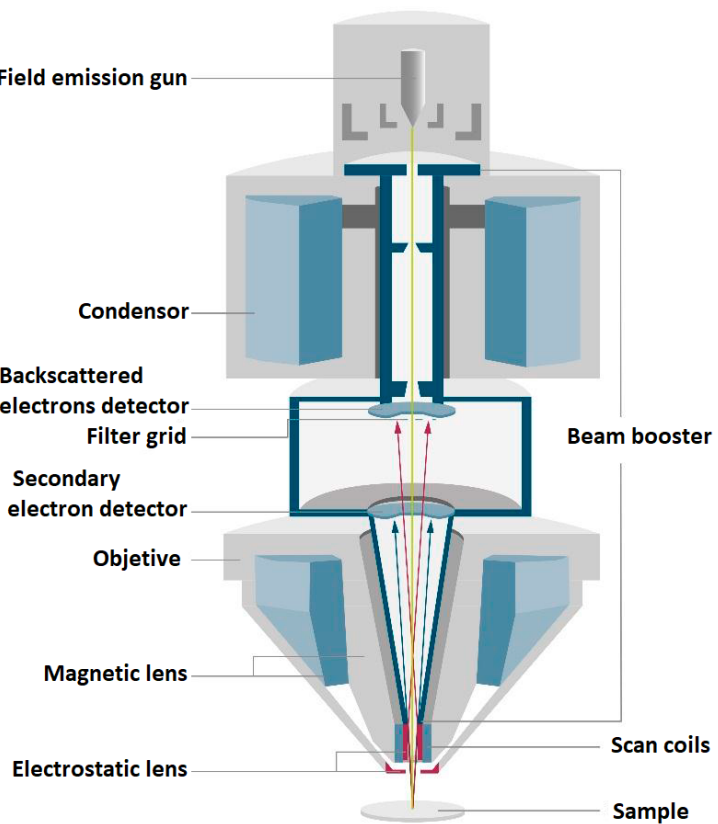


Figura 3.9. Esquema de un microscopio electrónico de barrido.

3.2.2. Espectroscopía de infrarrojos por transformada de Fourier

La espectroscopía de infrarrojos por transformada de Fourier (FTIR) es una técnica analítica rápida y ampliamente usada para la caracterización de biomateriales. El FTIR es un método basado en la interacción de la radiación infrarroja (IR) y en las vibraciones naturales de los enlaces químicos que conectan los átomos que componen el material [35]. Los grupos funcionales pueden asociarse con bandas características de absorción de infrarrojos, que corresponden a las vibraciones fundamentales de los grupos funcionales [36]. En algunas moléculas durante la vibración hay un cambio del momento del dipolo eléctrico. En este caso, hablamos de sustancias activas IR y la absorción de la radiación corresponde a un cambio del momento del dipolo. Para las sustancias inactivas IR el momento del dipolo eléctrico es cero,

independientemente de la duración del enlace en la molécula (IR-activo: enlaces polares, moléculas asimétricas. IR inactivo: enlace no polar, molécula simétrica) [37]. En la región del infrarrojo medio ($4000\text{-}400\text{ cm}^{-1}$) que es la más estudiada para caracterizar materiales, se observan dos tipos principales de vibraciones: vibraciones a lo largo de los enlaces químicos, denominadas vibraciones de estiramiento (*stretching*) (ν), que implican cambios en la longitud de los enlaces; y vibraciones que involucran cambios en los ángulos de enlace, y en particular vibraciones de deformación (δ -en plano, π -fuera de plano) [36]. El IR cercano y el lejano (denominados NIR y FIR, respectivamente) no se estudian con frecuencia, ya que en estas regiones sólo se producen vibraciones secundarias, que producen espectros difíciles de analizar [35]. Usualmente, hay cuatro regiones según el tipo de enlace, que pueden ser analizadas de los espectros FTIR. El enlace simple (O-H, C-H y N-H) es detectable en la región del espectro entre $2500\text{-}4000\text{ cm}^{-1}$. El triple y el doble enlace son detectables en la región entre $2000\text{-}2500\text{ cm}^{-1}$ y $1500\text{-}2000\text{ cm}^{-1}$, respectivamente. Además, la vibración de la molécula en su conjunto da lugar a un complejo patrón de vibraciones en la región entre $650\text{-}1500\text{ cm}^{-1}$ que es característico de la molécula en su totalidad y que, por lo tanto, puede utilizarse para la identificación [38]. Generalmente, un espectro FTIR es una representación gráfica de la transmitancia, en porcentaje (T%) o la absorción, en unidades (A) frente a la frecuencia IR en términos de número de onda (cm^{-1}). En un espectro IR las bandas de absorción se caracterizan por un número de onda en el que se produce la absorción (correspondiente a los enlaces químicos) y la intensidad de absorción (proporcional a la cantidad de sustancia de la muestra) [37].

Existen cuatro técnicas de manipulación de muestras que incluyen la transmisión, la reflectancia total atenuada, la reflectancia difusa y reflectancia especular. La reflectancia total atenuada (ATR) es una técnica útil para observar directamente muestras en estado sólido o líquido, sin preparación adicional. En la espectroscopia ATR-FTIR, el accesorio ATR se utiliza para medir los cambios que se producen en un rayo IR reflejado internamente cuando el rayo entra en contacto con una muestra. En principio, un haz de IR se dirige a un cristal ópticamente denso con un alto

índice de refracción (como el diamante, el seleniuro de zinc (ZnSe) y el germanio) con un cierto ángulo, como se muestra en la Fig. 3.10. El haz de IR entra en contacto con el cristal de ATR y produce múltiples reflectancias internas, que más tarde crean una onda evanescente que se extiende más allá de la superficie del cristal. La muestra en contacto con la onda evanescente absorberá la energía de la onda y, en consecuencia, la onda evanescente será atenuada. El haz atenuado se reflejará de nuevo en el cristal y luego saldrá por el extremo opuesto del cristal y se dirigirá al detector del espectrómetro. El detector registra el haz IR atenuado como una señal de interferograma, que puede utilizarse entonces para generar un espectro [38].

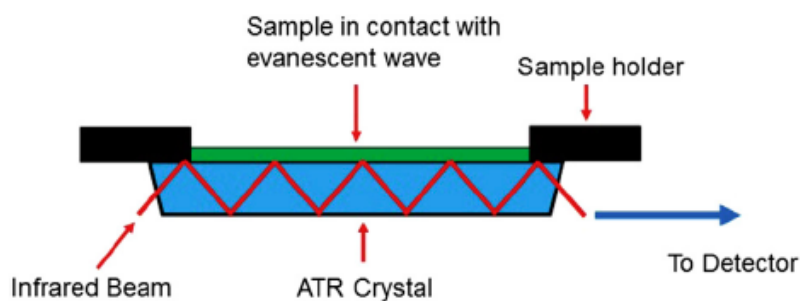


Figura 3.10. Un sistema de reflectancia total atenuada [38].

3.2.3. Espectroscopía de resonancia magnética nuclear

La Resonancia Magnética Nuclear (RMN) es una técnica de espectrometría para determinar estructuras químicas; en la que se aplica un campo magnético a la muestra de estudio. Cuando un núcleo atómico con un momento magnético se coloca en un campo magnético y se somete a una radiación de radiofrecuencia (energía) a la frecuencia apropiada, tiende a alinearse con el campo aplicado y absorbe energía. La frecuencia de la radiación necesaria para la absorción energética depende de tres cosas. En primer lugar, es característica del tipo de núcleo (por ejemplo, ^1H o ^{13}C). En segundo lugar, varía según el entorno químico del núcleo. Por ejemplo, los protones de amida de dos residuos de triptófano diferentes en una proteína nativa se

absorben a diferentes frecuencias ya que su proximidad inmediata en la molécula es diferente. En tercer lugar, la frecuencia de la RMN también podría cambiar con la ubicación espacial del campo magnético en caso de que éste no sea uniforme. Mediante la determinación de i) los niveles de energía de transición para todos los átomos de una molécula y, lo que es más importante, ii) los desplazamientos espectrales debidos a los entornos químicos (comúnmente denominados desplazamientos químicos, δ), es posible determinar la estructura química de una muestra [35].

Los núcleos más comúnmente examinados por RMN son ^1H y ^{13}C , ya que son los núcleos sensibles a la RMN de los elementos más abundantes en los materiales orgánicos. Las resonancias de ^1H son bastante específicas para los tipos de carbono a los que están adheridas y, en menor medida, para los carbonos adyacentes. Estas resonancias pueden dividirse en múltiplos, ya que los núcleos de hidrógeno pueden acoplarse a otros núcleos de hidrógeno cercanos. La magnitud de las divisiones y la multiplicidad se utilizan para determinar la estructura química en las proximidades de un hidrógeno determinado. Cuando todas las resonancias observadas se analizan de forma similar, es posible determinar la estructura de la molécula. Sin embargo, como sólo se observa el hidrógeno, cualquier característica estructural sin un hidrógeno unido sólo se puede inferir. Pueden surgir complicaciones si la molécula es muy compleja porque las diferentes resonancias pueden superponerse y resultar difíciles o imposibles de resolver [35].

En cuanto a los requisitos de la muestra para el análisis, cabe señalar que cualquier gas, líquido o sólido puede ser analizado siempre que pueda ser disuelto en un disolvente deuterado, hasta el nivel del 1% o más. Los sólidos también pueden ser analizados sin disolución; sin embargo, se deben hacer ajustes especiales. En cualquier caso, el análisis es no destructivo, de modo que las muestras pueden ser recuperadas para su posterior análisis si es necesario [35].

3.2.4. Análisis termogravimétrico

El análisis termogravimétrico (TGA) permite el estudio de la degradación térmica del material, así como el cálculo de la masa residual obtenida a una determinada temperatura. La muestra utilizada para el TGA es normalmente de pocos miligramos. El horno debe ser controlado a través de un programa informático para asegurar la velocidad necesaria para el aumento de la temperatura. El análisis térmico puede realizarse en un entorno de diferentes gases como el nitrógeno, el oxígeno, el aire y el argón. Durante la prueba, la termobalanza registra cómo varía la masa de la muestra en función de la temperatura o del tiempo. La primera derivada de la curva TGA con respecto al tiempo (curva DTG); es proporcional a la velocidad de descomposición de la muestra. El TGA es útil para la determinación de la temperatura de descomposición y los cambios de masa durante la descomposición. También proporciona alguna información sobre la composición de la muestra o el porcentaje de agua en algunos polímeros hidrófilos.

3.2.5. Propiedades mecánicas

3.2.5.1. Ensayo de compresión

La herramienta más común utilizada para la caracterización mecánica de los materiales es una máquina universal de ensayos, que es capaz de llevar a cabo una amplia variedad de pruebas experimentales. El ensayo de compresión es una técnica que se ha utilizado para examinar las propiedades mecánicas de los diferentes hidrogeles. Esta técnica consiste en colocar el material entre dos placas y comprimirlo (Fig. 3.11a) [39]. En el ensayo de compresión, los datos de carga y desplazamiento ($F-x$) se convierten en datos de tensión-deformación ($\sigma-\epsilon$) utilizando relaciones geométricas simples y se informa del módulo de Young (E) y de la tensión de fractura (σ_f). Los ensayos habituales se realizan a velocidad constante hasta la rotura de la muestra [40]. Normalmente, la muestra de hidrogel tiene una geometría cilíndrica. Entre las limitaciones

figuran el abombamiento del material y las dificultades para aplicar una presión uniforme a la muestra [41].

3.2.5.2. Ensayos reológicos

La reología es un método apropiado para caracterizar propiedades mecánicas del hidrogel, ya que es rápido, sensible, requiere tamaños de muestra pequeños y es indicativo de diferencias en la estructura como el grado de entrecruzamiento y la homogeneidad/heterogeneidad estructural [42]. El reómetro es el instrumento utilizado para medir y analizar las propiedades reológicas de materiales y su comportamiento bajo determinados parámetros, como la deformación y estrés de cizalla. La muestra, por lo general en una geometría especificada para el instrumento y el tipo de prueba, se carga en el instrumento entre discos paralelos y se pueden realizar diferentes tipos de mediciones de "barrido" (Fig. 3.11b). El más común es un barrido de frecuencia, en el que la oscilación sinusoidal está en una deformación constante (y normalmente bastante pequeña) pero la frecuencia de oscilación es variable. El resultado de la prueba son los módulos de almacenamiento (G') y módulos de pérdida (G'') en función de la frecuencia [40].

Los módulos G' y G'' de las soluciones de polímeros se han utilizado para diferenciar un polímero no reticulado de un polímero reticulado. El G'' es mucho mayor que el G' para las soluciones de polímeros no reticulados y se atribuye principalmente a la propiedad de mayor viscosidad en comparación con la propiedad elástica en todo el rango de frecuencias, mientras que el G' es mayor que el G'' para las soluciones de polímeros parcialmente reticuladas. Además de esto, la pendiente de la G' también aumenta. En el caso de los hidrogeles, que son redes de polímeros altamente reticulados, tanto la G' como la G'' son muy altas y son casi paralelas entre sí. Los valores G' y G'' de un hidrogel se miden en el rango de viscosidad lineal. En el caso de un gel no reticulado, el punto donde el G' y el G'' se cruzan se conoce como punto de cruce y denota la temperatura de transición gel-sol [43].

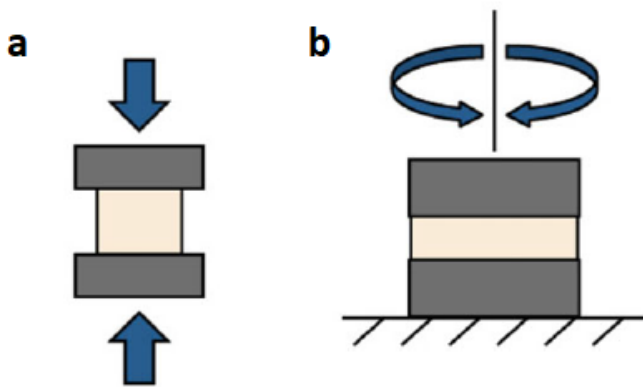


Figura 3.11. Esquemas de pruebas mecánicas utilizadas para evaluar las propiedades mecánicas del hidrogel. Compresión (a) y reometría de cizalla (b) [40].

3.2.6. Porosimetría

Las mediciones de adsorción de gas se utilizan ampliamente para determinar la superficie y la distribución del tamaño de los poros de diversos materiales sólidos. La medición de la adsorción en la interfaz gas/sólido también forma parte esencial de muchas investigaciones fundamentales y aplicadas sobre la naturaleza y el comportamiento de las superficies sólidas. El nitrógeno (a 77 K) es el adsorbente más utilizado para la caracterización de materiales porosos. El método de adsorción de gas Brunauer-Emmett-Teller (BET) se ha convertido en el procedimiento estándar más utilizado para la determinación de la superficie de materiales finamente divididos y porosos. BET se basa en el cálculo del número de moléculas de adsorbato, en este caso de nitrógeno, adsorbidas en monocapa, es decir, el número de moléculas necesario para cubrir la pared del sólido con una única capa [44].

La muestra sólida se enfriá, a vacío, a temperatura criogénica (usando nitrógeno líquido) y a continuación se inicia un proceso de inyección de adsorbato (N_2) en incrementos controlados. Después de cada dosis de adsorbato inyectado, se alcanza la presión de equilibrio entre adsorbato y adsorbente y se calcula la cantidad de gas adsorbido. El volumen de gas adsorbido a cada presión (a una temperatura constante) define una isoterma de adsorción, de la cual se

puede determinar el gas requerido para formar una monocapa sobre la muestra. Conocido el área que ocupa cada molécula de gas absorbido, se puede calcular el área superficial de la muestra. El área de superficie se puede calcular utilizando la ecuación BET.

Continuando este proceso hasta que se produzca la condensación del gas sobre los poros, se puede evaluar la estructura fina porosa de la muestra. Inicialmente la condensación de gas se produce sobre los poros más estrechos, y conforme aumenta la presión se va extendiendo a otros poros más anchos, y termina por alcanzar la saturación, momento en el cual todos los poros están llenos de líquido. A continuación, se va reduciendo gradualmente la presión del gas adsorbato, produciéndose la evaporación del gas condensado sobre el sistema. La evaluación de las ramas de adsorción y desorción de estas isotermas, revela información sobre el volumen de poros y la distribución del tamaño de los poros. El cálculo de BJH (Barrett, Joyner y Halenda) se utiliza para determinar el volumen de poro y la distribución del tamaño de poro [45] .

3.2.7. Espectroscopía ultravioleta-visible

Es un importante método óptico para la determinación cuantitativa de algunos analitos. Se basa en el principio de que las transiciones electrónicas en las moléculas se producen en las regiones visibles y ultravioletas del espectro electromagnético, y que una determinada transición se produce a una longitud de onda característica. El espectrofotómetro UV-vis es el instrumento que mide la intensidad del rayo de luz después de pasar por la muestra y la compara con la intensidad de la luz que pasa por la referencia. La absorbancia (A) se calcula a través del software basado en la ecuación de la ley de Beer-Lambert (Eq.1):

$$A = \log \frac{I_0}{I} = \varepsilon l c \quad (1)$$

Donde I_0 es la intensidad de la luz después de pasar por la referencia, I es la intensidad del rayo de luz después de pasar por la longitud de la muestra l , c es la concentración molar de la muestra y ε es el coeficiente de absorción molar. La longitud de la muestra l es normalmente la longitud

de la cubeta donde se coloca la solución de muestra. La ley de Lambert-Beer indica que la intensidad de la luz que pasa a través de una muestra disminuye exponencialmente con la concentración y el espesor de la muestra. Si el grosor de la muestra es fijo (longitud de la cubeta), la absorbancia será directamente proporcional a la concentración de la muestra. La concentración de la muestra puede calcularse fácilmente midiendo su absorbancia y usando una curva de calibración [46].

3.2.8. Ensayos celulares

3.2.8.1. Ensayo de viabilidad celular

El propósito general del ensayo MTT (bromuro de 3-(4,5-dimetiltiazol-2-il)-2,5 difeniltetrazolio) es medir las células viables con un rendimiento relativamente alto (placas de 96 pocillos) sin necesidad de un recuento celular complejo. El principio del ensayo MTT es que para la mayoría de las células viables la actividad mitocondrial es constante y, por lo tanto, un aumento o disminución del número de células viables está linealmente relacionado con la actividad mitocondrial. La actividad mitocondrial de las células se refleja en la conversión de la sal de tetrazolio, soluble en agua y de color amarillo, en cristales de formazán, de color violeta e insolubles en agua, que pueden solubilizarse para una medición homogénea en un disolvente orgánico como dimetilsulfóxido. Así pues, cualquier aumento o disminución del número de células viables puede detectarse midiendo la concentración de formazán reflejada en la densidad óptica mediante un lector de placas a 550 nm. Dado que para la mayoría de las poblaciones celulares la actividad mitocondrial total está relacionada con el número de células viables, este ensayo se utiliza ampliamente para medir los efectos citotóxicos *in vitro* de un compuesto en líneas celulares o en células primarias de un paciente [47].

3.2.8.2. Ensayo de nitrito

El óxido nítrico (NO) es un mediador endógeno de numerosos procesos fisiológicos que van desde la regulación de la función cardiovascular y la transmisión neurológica hasta las respuestas antipatógenas y tumorales. La formación de NO a partir de la L-arginina es catalizada por una familia diversa de isoenzimas de óxido nítrico sintasa (NOS). La activación del sistema inmunológico puede dar lugar a la expresión de la NOS inducible (iNOS) en numerosos tipos de células (por ejemplo, macrófagos, neutrófilos, hepatocitos). Entonces, los niveles de NO pueden ser útiles marcadores de la inflamación y la patogénesis de una enfermedad. La cuantificación de NO es difícil en medios biológicos, debido a su corta vida media y a sus bajas concentraciones, por eso se cuantifican sus metabolitos estables: nitrito y nitrato [48]. El primer paso en la medición del NO, es la conversión del nitrato en nitrito, catalizado por el nitrato reductasa, con cofactores (NADPH) y compuestos específicos para eliminar las interferencias (exceso de NADPH). Posteriormente, el nitrito convertido puede ser cuantificado por la adición del reactivo Griess, que convierte el nitrito en un compuesto azoico púrpura. La concentración exacta del nitrito puede determinarse mediante la medición fotométrica del compuesto azoico coloreado. El mecanismo del ensayo de Griess se resume en el acoplamiento azoico entre las especies de diazonio, que se producen a partir de la sulfanilamida con NO_2^- y la naftilendiamina.

3.2.8.3. Ensayo de herida (*In vitro scratch wound assay*)

El ensayo de herida *in vitro* es un método sencillo y económico para estudiar la migración celular *in vitro*. Este método se basa en la observación de que, al crearse una nueva separación artificial, llamada "arañazo" (*scratch*) en una monocapa de células confluentes, las células que quedan al borde del arañazo recién creado se moverán hacia el espacio de separación para cerrar el 'rasguño' hasta que se establezcan de nuevos contactos entre células. Los pasos básicos del ensayo implican la creación de un rasguño en la monocapa de células, la captura de imágenes al

principio y a intervalos regulares durante la migración celular para cerrar el rasguño, y la comparación de las imágenes para determinar la tasa de migración celular [49]. La migración celular puede ser determinada a través de la cuantificación del área del cierre de herida (rasguño) a tiempo 0 y a los intervalos definidos, usando el software ImageJ y su *plugin MRI Wound Healing Tool*.

Una de las principales ventajas de este sencillo método es que imita en cierta medida la migración de las células *in vivo*. Por ejemplo, la eliminación de la parte del endotelio en los vasos sanguíneos inducirá la migración de las células endoteliales a la zona despojada para cerrar la herida [49].

3.3. Referencias

- [1] M.S. Hamid Akash, K. Rehman, S. Chen, Natural and synthetic polymers as drug carriers for delivery of therapeutic proteins, *Polym. Rev.* 55 (2015) 371–406. doi:10.1080/15583724.2014.995806.
- [2] A. Muxika, A. Etxabide, J. Uranga, P. Guerrero, K. De Caba, Chitosan as a bioactive polymer : Processing , properties and applications, *Int. J. Biol. Macromol.* 105 (2017) 1358–1368. doi:10.1016/j.ijbiomac.2017.07.087.
- [3] M. Rinaudo, Chitin and chitosan : Properties and applications, *Prog. Polym. Sci.* 31 (2006) 603–632. doi:10.1016/j.progpolymsci.2006.06.001.
- [4] J. Nilsen-Nygaard, S.P. Strand, K.M. Vårum, K.I. Draget, C.T. Nordgård, Chitosan: Gels and interfacial properties, *Polymers (Basel)*. 7 (2015) 552–579. doi:10.3390/polym7030552.
- [5] A. Noreen, Z. i. H. Nazli, J. Akram, I. Rasul, A. Mansha, N. Yaqoob, R. Iqbal, S. Tabasum, M. Zuber, K.M. Zia, Pectins functionalized biomaterials; a new viable approach for biomedical applications: A review, *Int. J. Biol. Macromol.* 101 (2017) 254–272. doi:10.1016/j.ijbiomac.2017.03.029.
- [6] F. Munarin, M.C. Tanzi, P. Petrini, Advances in biomedical applications of pectin gels, *Int. J. Biol. Macromol.* 51 (2012) 681–689. doi:10.1016/j.ijbiomac.2012.07.002.
- [7] S. Sungthongjeen, P. Sriamornsak, T. Pitaksuteepong, A. Somsiri, S. Puttipipatkhachorn, Effect of degree of esterification of pectin and calcium amount on drug release from pectin-based matrix tablets, *AAPS PharmSciTech.* 5 (2004) E9. doi:10.1208/pt050109.
- [8] J. Necas, L. Bartosikova, Carrageenan: A review, *Vet. Med. (Praha)*. 58 (2013) 187–205.
- [9] L. Li, R. Ni, Y. Shao, S. Mao, Carrageenan and its applications in drug delivery, *Carbohydr. Polym.* 103 (2014) 1–11. doi:10.1016/j.carbpol.2013.12.008.
- [10] V.L. Campo, D.F. Kawano, D.B. da Silva, I. Carvalho, Carrageenans: Biological properties, chemical modifications and structural analysis - A review, *Carbohydr. Polym.* 77 (2009) 167–180. doi:10.1016/j.carbpol.2009.01.020.
- [11] L. Cunha, A. Grenha, Sulfated seaweed polysaccharides as multifunctional materials in drug delivery applications, *Mar. Drugs.* 14 (2016) 1–41. doi:10.3390/md14030042.

- [12] I. Gibas, H. Janik, Review: Synthetic polymer hydrogels for biomedical application, *Chem. Chem Technol.* 4 (2010) 297–304.
- [13] D.A. Gyles, L.D. Castro, J.O.. Silva Jr, R.M. Ribeiro-Costa, A review of the designs and prominent biomedical advances of natural and synthetic hydrogel formulations, *Eur. Polym. J.* 88 (2017) 373–392. doi:10.1016/j.eurpolymj.2017.01.027.
- [14] Y. Ramadan, M.I. González-Sánchez, K. Hawkins, J. Rubio-Retama, E. Valero, S. Perni, P. Prokopovich, E. López-Cabarcos, Obtaining new composite biomaterials by means of mineralization of methacrylate hydrogels using the reaction – diffusion method, *Mater. Sci. Eng. C.* 42 (2014) 696–704. doi:10.1016/j.msec.2014.06.017.
- [15] G. Tommasi, S. Perni, P. Prokopovich, An Injectable Hydrogel as Bone Graft Material with Added Antimicrobial Properties, *Tissue Eng. Part A.* 22 (2016) 862–872. doi:10.1089/ten.tea.2016.0014.
- [16] B. Tang, Z. Yang, S. Zhang, Poly(polyethylene glycol methyl ether methacrylate) as Novel Solid-Solid Phase Change Material for Thermal Energy Storage, *J. Appl. Polym. Sci.* 125 (2012) 1377–1381. doi:10.1002/app.
- [17] Y. Chen, A. Venault, J. Jhong, H. Ho, C. Liu, R.-H. Lee, G.-H. Hsiue, Y. Chang, Developing blood leukocytes depletion membranes from the design of bioinert PEGylated hydrogel interfaces with surface charge control, *J. Memb. Sci.* 537 (2017) 209–219. doi:10.1016/j.memsci.2017.05.031.
- [18] S. Eswaramma, N.S. Reddy, K.S.V.K. Rao, Phosphate crosslinked pectin based dual responsive hydrogel networks and nanocomposites: Development, swelling dynamics and drug release characteristics, *Int. J. Biol. Macromol.* 103 (2017) 1162–1172. doi:10.1016/j.ijbiomac.2017.05.160.
- [19] V. Simion, D. Stan, A.M. Gan, M.M. Pirvulescu, E. Butoi, I. Manduteanu, M. Deleanu, E. Andrei, A. Durdureanu-Angheluta, M. Bota, M. Enachescu, M. Calin, M. Simionescu, Development of curcumin-loaded poly(hydroxybutyrate-co-hydroxyvalerate) nanoparticles as anti-inflammatory carriers to human-activated endothelial cells, *J. Nanoparticle Res.* 15 (2013) 2108. doi:10.1007/s11051-013-2108-1.
- [20] I. Chodak, Polyhydroxyalkanoates: Origin, properties and applications, in: *Monomers, Polym. Compos. from Renew. Resour.*, 2008: pp. 451–477. doi:10.1016/B978-0-08-045316-3.00022-3.

- [21] N.B. Javan, N.J. Omid, N.M. Hasab, L.R. Shirmard, M. Rafiee-Tehrani, F. Dorkoosh, Preparation, statistical optimization and in vitro evaluation of pramipexole prolonged delivery system based on poly (3-hydroxybutyrate-co-3-hydroxyvalerate) nanoparticles, *J. Drug Deliv. Sci. Technol.* 44 (2018) 82–90. doi:10.1016/j.jddst.2017.11.026.
- [22] N. Bahari Javan, L. Rezaie Shirmard, N. Jafary Omid, H. Akbari Javar, M. Rafiee Tehrani, F. Abedin Dorkoosh, Preparation, statistical optimisation and in vitro characterisation of poly (3-hydroxybutyrate-co-3-hydroxyvalerate)/poly (lactic-co-glycolic acid) blend nanoparticles for prolonged delivery of teriparatide, *J. Microencapsul.* 33 (2016) 460–474. doi:10.1080/02652048.2016.1208296.
- [23] G. Barouti, C.G. Jaffredo, S.M. Guillaume, Advances in drug delivery systems based on synthetic poly(hydroxybutyrate) (co)polymers, *Prog. Polym. Sci.* 73 (2017) 1–31. doi:10.1016/j.progpolymsci.2017.05.002.
- [24] B.S.T. Gadgil, N. Killi, G. V. Rathna, Polyhydroxyalkanoates as biomaterials, *Med. Chem. Commun.* 8 (2017) 1774–1787. doi:10.1039/C7MD00252A.
- [25] D.P. Pacheco, M.H. Amaral, R.L. Reis, A.P. Marques, V.M. Correlo, Development of an injectable PHBV microparticles-GG hydrogel hybrid system for regenerative medicine, *Int. J. Pharm.* 478 (2015) 398–408. doi:10.1016/j.ijpharm.2014.11.036.
- [26] P. Pahuja, S. Arora, P. Pawar, P. Pahuja, S. Arora, P. Pawar, Ocular drug delivery system : a reference to natural polymers, *Expert Opin. Drug Deliv.* 9 (2012) 837–861. doi:10.1517/17425247.2012.690733.
- [27] S. Barak, D. Mudgil, Locust bean gum : Processing , properties and food applications — A review, *Int. J. Biol. Macromol.* 66 (2014) 74–80. doi:10.1016/j.ijbiomac.2014.02.017.
- [28] A.C. Pinheiro, A.I. Bourbon, C. Rocha, C. Ribeiro, J.M. Maia, M.P. Gonçalves, J.A. Teixeira, A.A. Vicente, Rheological characterization of κ -carrageenan/galactomannan and xanthan/galactomannan gels: Comparison of galactomannans from non-traditional sources with conventional galactomannans, *Carbohydr. Polym.* 83 (2011) 392–399. doi:10.1016/j.carbpol.2010.07.058.
- [29] M.S. Marques, K.M. Zepon, J.M. Heckler, F.D.P. Morisso, M.M. da Silva Paula, L.A. Kanis, One-pot synthesis of gold nanoparticles embedded in polysaccharide-based hydrogel : Physical-chemical characterization and feasibility for large-scale production, *Int. J. Biol. Macromol.* 124 (2019) 838–845. doi:10.1016/j.ijbiomac.2018.11.231.

- [30] M. Dionísio, A. Grenha, Locust bean gum : Exploring its potential for biopharmaceutical applications, *J. Pharm. Bioallied Sci.* 4 (2012) 175–185. doi:10.4103/0975-7406.99013.
- [31] L. Tytgat, M. Vagenende, H. Declercq, J.C. Martins, H. Thienpont, H. Ottevaere, P. Dubruel, S. Van Vlierberghe, Synergistic effect of κ-carrageenan and gelatin blends towards adipose tissue engineering, *Carbohydr. Polym.* 189 (2018) 1–9. doi:10.1016/j.carbpol.2018.02.002.
- [32] Q. Chai, Y. Jiao, X. Yu, Hydrogels for biomedical applications: Their characteristics and the mechanisms behind them, *Gels.* 3 (2017) 6. doi:10.3390/gels3010006.
- [33] S. Kommareddy, D.B. Shenoy, M.M. Amiji, Gelatin Nanoparticles and Their Biofunctionalization, in: *Nanotechnologies Life Sci.*, 2007: pp. 330–352. doi:10.1002/9783527610419.ncbi0011.
- [34] A. Pal, B.L. Vernon, M. Nikkhah, Therapeutic neovascularization promoted by injectable hydrogels, *Bioact. Mater.* 3 (2018) 389–400. doi:10.1016/j.bioactmat.2018.05.002.
- [35] M. Alatorre-Meda, J.F. Mano, General Characterization of Chemical Properties of Natural-Based Biomaterials., in: *Biomater. from Nat. Adv. Devices Ther.*, 2016: pp. 517–531. doi:10.1016/b978-0-444-99697-8.50007-1.
- [36] C. Berthomieu, R. Hienerwadel, Fourier transform infrared (FTIR) spectroscopy, *Photosynth. Res.* 101 (2009) 157–170. doi:10.1007/s11120-009-9439-x.
- [37] V. Tucureanu, A. Matei, A.M. Avram, FTIR Spectroscopy for Carbon Family Study, *Crit. Rev. Anal. Chem.* 46 (2016) 502–520. doi:10.1080/10408347.2016.1157013.
- [38] M.A. Mohamed, J. Jaafar, A.F. Ismail, M.H.D. Othman, M.A. Rahman, Fourier Transform Infrared (FTIR) Spectroscopy, in: *Membr. Charact.*, Elsevier B.V., 2017: pp. 3–29. doi:10.1016/B978-0-444-63776-5.00001-2.
- [39] M. Ahearne, Y. Yang, K.K. Liu, Mechanical characterisation of hydrogels for tissue engineering applications, *Top. Tissue Eng.* 4 (2008) 1–16. doi:10.1016/j.ijsolstr.2018.05.016.
- [40] M.L. Oyen, Mechanical characterisation of hydrogel materials, *Int. Mater. Rev.* 59 (2017) 44–59. doi:10.1179/1743280413Y.0000000022.
- [41] S.L. Wilson, M. Ahearne, A.J. El Haj, Y. Yang, Mechanical characterization of hydrogels

- and its implications for cellular activities, in: Hydrogels Cell-Based Ther., The Royal Society of Chemistry Cambridge, UK., 2014: pp. 171–190.
- [42] J.M. Zuidema, C.J. Rivet, R.J. Gilbert, F.A. Morrison, A protocol for rheological characterization of hydrogels for tissue engineering strategies, *J. Biomed. Mater. Res. - Part B Appl. Biomater.* 102 (2014) 1063–1073. doi:10.1002/jbm.b.33088.
- [43] K. Pal, A.K. Banthia, D.K. Majumdar, Polymeric hydrogels: Characterization and biomedical applications, *Des. Monomers Polym.* 12 (2009) 197–220. doi:10.1163/156855509X436030.
- [44] K.S.W. Sing, Reporting physisorption data for gas/solid systems with special reference to the determination of surface area and porosity (Recommendations 1984), *Pure Appl. Chem.* 57 (1985) 603–619. doi:10.1351/pac198557040603.
- [45] K.S.W. Sing, Adsorption methods for the characterization of porous materials, *Adv. Colloid Interface Sci.* 76–77 (1998) 3–11. doi:10.1016/S0001-8686(98)00038-4.
- [46] J. Daintith, *Dictionary of Chemistry*, Oxford University Press, 2008.
- [47] J. Van Meerloo, G.J. Kaspers, J. Cloos, Cell sensitivity assays: the MTT assay, in: *Cancer Cell Cult.*, Humana Press, 2011: pp. 237–245. doi:10.1007/978-1-61779-080-5.
- [48] K.M. Miranda, M.G. Espey, D.A. Wink, A rapid, simple spectrophotometric method for simultaneous detection of nitrate and nitrite, *Nitric Oxide - Biol. Chem.* 5 (2001) 62–71. doi:10.1006/niox.2000.0319.
- [49] C.C. Liang, A.Y. Park, J.L. Guan, In vitro scratch assay: A convenient and inexpensive method for analysis of cell migration in vitro, *Nat. Protoc.* 2 (2007) 329–333. doi:10.1038/nprot.2007.30.

CAPÍTULO 4: Entrapment of chitosan, pectin or κ-carrageenan within methacrylate based hydrogels: effect on swelling and mechanical properties.

4.1. Introduction

Hydrogels are hydrophilic polymers in three dimensional network with the capability to absorb and retain a large amount of water or biological fluids within their structure without dissolving [1]. Hydrogels can be crosslinked chemically by covalent bonds, physically by non-covalent interactions or by a combination of both. Crosslinking provides structure of network and physical integrity to the hydrogels [2]. The physical crosslinking allows the reversibility, ease of manufacture, reshaping, biodegradation and non-toxicity, properties that sometimes chemically crosslinked hydrogels lack [3]. Chemical crosslinking results in a network with good mechanical stability [4,5].

Hydrogels composed of various polymers interconnected via chemical or physical linkages, interpenetrating polymer network (IPN) hydrogels and nanocomposite hydrogels incorporating organic or inorganic nanoparticles, have emerged as innovative materials for biomedical applications [6]. An interpenetrating polymer network, IPN, is defined as a combination of two or more polymers in network form, at least one of which is polymerized and/or crosslinked in the immediate presence of the other(s). Semi -IPN is a kind of IPN in which one or more polymers are crosslinked, and one or more polymers are linear or branched [7]. IPNs have been developed with the aim to improve at least one property of the constituent networks. The combination of the polymers must effectively produce an advanced multicomponent polymeric system, with a new profile [8]. Natural polymers such as polysaccharides and proteins, and hydrophilic synthetic polymers have been used for the formation of IPN hydrogels [9].

Polysaccharides such as chitosan, pectin and κ -carrageenan are commonly used in biomedical fields. The main advantage of natural polymers is their biocompatibility, biodegradability and non-toxicity [10]. On the other hand, a major advantage of using synthetic polymers is that they can be tailored to suit specific functions and thus exhibit controllable properties [11]. Hydrogels synthesized for biomedical use tend to incorporate synthetic polymers such as polyacrylamide and its derivatives, polyethylene glycol (PEG), among others [12].

Chitosan, a cationic polysaccharide, has been blended with poly(2- hydroxyethyl methacrylate) [13] and poly(acrylamide) [14] for obtaining interpenetrating networks with improved mechanical properties. The pectin, an anionic polysaccharide, has been combined with different compounds and polymers to improve its properties [15]. Biocompatible and biodegradable hydrogels were obtained by the combination of pectin and (2-dimethylamino) ethyl methacrylate indicating that this dual network allows to respond to pH and temperature changes and could be useful for drug delivery and wound healing applications [16]. Other polysaccharide that was considered attractive for the preparation of hydrogels is κ -carrageenan (κ C) since it has strong gel formation ability with high swelling property [17]. It is an unbranched negatively charged hydrophilic polysaccharide with a structure similar to natural glycosaminoglycan which makes it a potential candidate for tissue engineering [18]. It has been combined with poly(vinyl alcohol) (PVA) for enhancing the cell adhesion ability of PVA hydrogels [19,20]. Combining an ionically crosslinked κ -carrageenan network with a covalently cross-linked polyacrylamide network allowed to obtain a hydrogel that exhibited a higher elastic modulus than single hydrogel [21].

Hence, the blending of natural and synthetic polymers allows developing new biomaterials that exhibit combinations of properties that could not be obtained from individual polymers. The aim of this work was to develop a biocompatible hydrogel with improved swelling and mechanical properties. For this, composite hydrogels were obtained by entrapment of chitosan, pectin or κ -carrageenan within two methacrylate monomers previously used in the preparation of hydrogels for medical applications [22–24]. The surface morphologies, swelling, thermogravimetric analysis, mechanical properties and biocompatibility of the prepared hydrogels were analyzed to determine the effect of the entrapment of each polysaccharide on the properties of these hydrogels and their potential characteristics for biomedical applications.

4.2. Materials and methods

4.2.1. Materials

The monomers polyethylene glycol methyl ether methacrylate (PEGMEM) and the 2-dimethylamino ethyl methacrylate (DMAEM), the crosslinker N,N'-methylenebis(acrylamide) (BIS), the pectin from citrus peel (PC) (degree of esterification $\geq 6.7\%$) and the chitosan (CS) (75-85% deacetylated, molar mass: 190–310 kDa) were purchased from Sigma Aldrich, Germany. The κ -carrageenan (κ C) was gifted by Ceamsa, Spain (molar mass distribution as provided by the supplier: 53,3% between 1000 to 5000 kDa; around 21,8% between 500 to 1000 kDa and the rest corresponds to 100 to 500 kDa). The initiator ammonium persulfate (APS) was purchased from Acros Organics, Spain. Potassium chloride used was of analytical grade and purchased from Scharlau, Spain. All chemicals were used without further purification. The water used in the preparation and the dialysis was purified in a Milli-Q ultrapure system (Millipore, France).

4.2.2. Synthesis of the hydrogels

A series of hydrogels were prepared according to the method proposed by Ramadan et al. [23] with modifications (Table 4.1). For the synthetic hydrogel (SH), equimolar amounts of the monomers PEGMEM (0.0065 mol) and DMAEM (0.0065 mol) were added to 5 mL of deionized water. The crosslinker (BIS) was added to the solution in a concentration of 5% molar ratio to the monomers. Afterwards, the mixture was stirred for 20 min at room temperature. The free radical polymerization was initiated by adding 50 μ L of a solution of 100 mg mL^{-1} of APS under stirring. The mixture was allowed to polymerize for 50 min at room temperature.

Table 4.1. Preparation of synthetic and composite hydrogels

Sample code	0.2PC	0.5PC	1PC	0.2CS	0.5CS	1CS	0.2 κ C	0.5 κ C	1 κ C
Polysaccharide	Pectin			Chitosan			κ -carrageenan		
Polysaccharide concentration (% w/v)	0.2	0.5	1	0.2	0.5	1	0.2	0.5	1

For composite hydrogels, the 5 mL of deionized water was replaced by a solution of the same volume of one of the following polysaccharides: PC, CS and κ C of one of the following concentrations: 0.2%, 0.5% and 1% w/v. The monomers PEGMEM (0.0065 mol) and DMAEM (0.0065 mol) were added to the corresponding polysaccharides. The preparation continued under the conditions previously mentioned for the SH, except for the κ C hydrogel solutions which were stirred at 70 °C and finally 100 μ L KCl 0.5 M was added for its gelification.

The solutions of each polysaccharide were prepared from a stock solution with a concentration of 1% w/v. The stock solution of PC was prepared by dissolving 0.5 g of PC powder in 50 mL of deionized water and stirred for 1 h at room temperature. The stock solution of κ C was prepared by dissolving 0.5 g of the κ C powder in 50 mL of deionized water and stirred for 30 min at 70 °C. The stock solution of CS was prepared by dissolving 0.5 g of CS powder in 50 mL of 0.1 M HCl and stirred for 1 h at 60 °C. Then, these stock solutions were used for the preparation of the hydrogels at concentrations of 0.2% w/v, 0.5% w/v and 1% w/v of polysaccharides. To remove the extractables, the hydrogels were immersed in an excess of deionized water until equilibrium of swelling with daily refreshment of water. Thereafter, the swollen hydrogels were freeze dried for use in subsequent assays (LyoQuest, Telstar, Spain). Also, the extractables obtained of each hydrogel were lyophilized and the fraction obtained was weighed to obtain %wt. of the extractable.

4.2.3. Attenuated total reflectance ATR-FTIR spectra

The polymerization of the monomers was checked by ATR-FTIR. The ATR-FTIR spectra of freeze-dried hydrogels were recorded in a FT-IR spectrophotometer (Jasco FT/IR-4700, Japan) using an ATR technique by averaging the signals of 64 scans at a resolution of 4 cm^{-1} in the range from 4000 cm^{-1} to 600 cm^{-1} . The reagents and freeze-dried extractables were analyzed under the same conditions.

4.2.4. ^1H Nuclear magnetic resonance (^1H NMR)

Freeze dried hydrogels were immersed in deuterated water for 24 h. After that, the extractable solution was analyzed in a Bruker Avance 500 spectrometer (frequency of ^1H , 500.13 MHz) (Germany) equipped with a dual cryoprobe $^1\text{H}/^{13}\text{C}$. ^1H spectra (sequence zg) were obtained under standard conditions, using a 10000 Hz spectral window.

4.2.5. Swelling behavior

To determine the water uptake (WU) of the hydrogels, the pre-weighed freeze-dried hydrogels were immersed completely in deionized water at room temperature. The swollen hydrogels were weighed daily after removing the water until equilibrium was reached. The water uptake (WU) was calculated by the equation (1) [25]:

$$\text{WU} = \frac{W_t - W_d}{W_d} \quad (1)$$

where W_t represents the mass of gel in swollen state at equilibrium and W_d is the mass of freeze dried hydrogel.

4.2.6. Field emission scanning electron microscopy

To evaluate the surface morphological structure, the swollen hydrogels were freeze-dried and then sputter-coated with iridium using a QUORUM Q150T-S turbo-pumped sputter coater (Quorum Technologies Ltd, England). The surface morphology was observed using a field emission scanning electron microscope ZEISS FESEM ULTRA Plus (Carl Zeiss, Germany) at an acceleration voltage of 5 kV and 10 kV.

4.2.7. Thermogravimetric analysis

The water content of the swollen hydrogels and the thermal stability of the lyophilized hydrogels were analyzed by a thermogravimetric analyzer (TGA 4000, Perkin Elmer, Netherlands). About 15 mg of each hydrogel was taken into an alumina pan and heated in the temperature ranged from 30 °C to 500 °C with a heating rate of 10 °C min⁻¹ under a nitrogen flow of 20 cm³ min⁻¹. The

water content and the decomposition onset temperature were determined from the TGA curves.

4.2.8. Mechanical properties

The mechanical properties of the fresh prepared hydrogels including the compression load and the compression strain were determined using an Instron Universal Testing Machine 5565 (Instron, England) with a 500 N load cell and a crosshead speed of 2 mm min⁻¹. Cylindrical hydrogel samples with dimensions of 25 mm of diameter and 8 mm of height were used for the compression tests. The compression load corresponds to the maximum compression load applied before the break of the hydrogel and the compression strain corresponds to the strain at the break point. The data were showed as the standard deviation (SD) of the means.

4.2.9. Biocompatibility

4.2.9.1. Cell culture

The J774A.1 cell line from mouse BALB/c monocyte macrophages was a gift from Dr. Oreste Gualillo (Neuroendocrine Interactions in Rheumatology and Inflammatory Diseases, Institute of Biomedical Research of Santiago de Compostela, Spain). The J774A.1 macrophages were cultured in dulbecco's modified eagle medium (DMEM) (Lonza Group Ltd, Switzerland) supplemented with 10% heat-inactivated fetal bovine serum (FBS) (Merck KGaA, Germany), 2% penicillin/streptomycin antibiotics and 2% L-glutamine (Sigma-Aldrich, USA) at 37 °C and 5% CO₂. After overnight incubation of hydrogels in culture medium, the cells were seeded above the hydrogels.

4.2.9.2. MTT viability assay

Toxicity of the hydrogels was determined using the 3-(4,5-dimethylthiazol-2-yl)-2,5-diphenyltetrazolium bromide (MTT) (Sigma-Aldrich, USA) cell viability assay. MTT is a yellow compound that when reduced by functioning mitochondria, produces purple formazan crystals

that can be measured spectrophotometrically. The quantity of formazan is presumably directly proportional to the number of the viable cells and their metabolic activity (Riss et al., 2004). For this purpose, the J774A.1 macrophages were seeded above the hydrogels and kept in culture for 24 h. MTT 0.5 mg mL⁻¹ was added 4 h before the expiry of this period. After overnight incubation at 37 °C, the absorbance at 550 nm was measured in a microplate reader (MultiscanEX, Thermo Fisher Scientific, USA).

4.2.9.3. Nitrite assay

Nitrite accumulation was measured in the culture medium by Griess reaction. Briefly, after 24 h of J774A.1 macrophages exposure to hydrogels, 50 µL of cell culture medium were mixed with 50 µL of Griess reagent (equal volumes of 1% sulfanilamide in 5% phosphoric acid and 0.1% naphtylethylenediamine HCl). Then, absorbance at 550 nm was measured in a microplate reader (MultiscanEX, Thermo Fisher Scientific, USA). Fresh culture medium was used as blank. The amount of nitrite production was calculated from a sodium nitrite standard curve freshly prepared in culture medium. Lipopolysaccharide (LPS) 250 ng mL⁻¹ (E. coli serotype O55:B5, Sigma-Aldrich, USA) was used as positive control, and culture medium from untreated cells as negative control.

4.2.9.4. Hydrogel imaging

Phase contrast microscopy (Zeiss Axio Vert.A1; Zeiss, Germany) was used for image acquisition. Images were taken using a dry 10x objective.

4.2.9.5. Statistical analysis

All experimental data were obtained from six independent experiments. The data are expressed as mean ± standard error of the mean (SEM). Statistical analysis was performed using the Wilcoxon signed-rank test as implemented in Prism 5 (GraphPad Software Inc., USA).

4.3. Results and discussion

4.3.1. Synthesis of the hydrogels

The hydrogels were synthesized by free radical chain polymerizations of the hydrophilic monomers containing carbon double bond. ATR-FTIR spectroscopy was carried out to characterize the chemical structure of the synthetic hydrogel (SH) and to analyze the effect of the incorporation of the polysaccharides on the polymerization process. Figure 4.1 shows the FTIR spectra of the monomers and the synthetic hydrogel. For PEGMEM, the $-\text{CH}_2$ was observed at 2870 cm^{-1} and 1454 cm^{-1} ; $\text{C}=\text{O}$ at 1716 cm^{-1} ; $\text{C}=\text{O}(\text{O})\text{CH}_2$ at 1350 cm^{-1} , 1249 cm^{-1} and 1103 cm^{-1} . For DMAEM, the $-\text{CH}_2$ was observed at 2948 cm^{-1} , 2821 cm^{-1} and 2770 cm^{-1} ; $\text{C}=\text{O}$ at 1716 cm^{-1} ; $\text{C}=\text{O}(\text{O})$ at 1317 cm^{-1} and 1295 cm^{-1} ; $\text{C}-\text{N}$ at 1156 cm^{-1} [26]. For the synthetic hydrogel PEGMEM/DMAEM (SH) the peaks formed at 1245 cm^{-1} and 1102 cm^{-1} are attributed to $\text{C}=\text{O}(\text{O})$ from PEGMEM [27]. The peak at 1724 cm^{-1} corresponds to the stretching of $\text{C}=\text{O}$. For both monomers the $\text{C}=\text{C}$ was observed at 1637 cm^{-1} , bond that then is broken during the polymerization. In addition, the coexistence of absorption at 2940 cm^{-1} , 2870 cm^{-1} , 2821 cm^{-1} and 2770 cm^{-1} shows the PEGMEM/DMAEM polymerization. The formation of copolymer PEGMEM/DMAEM in ratio 1:1 was reported by Ramadan et al. [23]. No changes were observed between the spectra of the synthetic and the composite hydrogels (Supplementary material, Fig.S.4.1). The obtained spectra showed only the peaks corresponding to the abundant chemically bonded synthetic network. The absence of the peaks corresponding to the polysaccharides is due to that the concentrations of which were very low compared to that of synthetic monomers. These results indicate that the polymerization of the synthetic monomers was carried out successfully in all the hydrogels and therefore, the polysaccharides did not interfere with the polymerization. PC and CS formed a network of linear polymers embedded within the first methacrylate network, therefore, these hydrogels are considered semi-IPN. On the other hand, κC hydrogels are considered IPN, because there was a formation of two

nets, the chemically bonded synthetic network and the physically bonded network of κ C and potassium ions.

The %wt. extractables were 7.4%, 7.1%, 7.2% and 17.3% for SH, 1PC, 1CS and 1 κ C, respectively. These %wt of extractables reflect high yield of polymerization of the synthetic monomers for the synthetic hydrogel in the absence of the polysaccharides. The incorporation of the κ C was accompanied with a decrease of the polymerization yield, however both PC and CS did not seem to affect the polymerization yield. The extractable solutions of SH, 1CS, 1PC and 1 κ C were analyzed with ATR-FTIR (Supplementary material, Fig. S.4.2). For all the extractable solutions, the $-\text{CH}_2$ from PEGMEM was observed at 2870 cm^{-1} and the coexistence of absorption at 2940 cm^{-1} , 2870 cm^{-1} , 2821 cm^{-1} and 2770 cm^{-1} from PEGMEM/DMAEM is absent. In addition, C=C at 1637 cm^{-1} from both monomers was observed, that bond was then broken during the polymerization. The peak at 1540 cm^{-1} from BIS was observed in extractable and not in SH. These results were in agreement with the obtained in ^1H NMR (Supplementary material, Fig. S.4.3). Peaks from PEGMEM (6.07 ppm, 4.2 ppm and 3.6 ppm); DAEM (5.2 ppm) and BIS (5.7 ppm, 4.8 ppm) were observed. The FTIR and ^1H NMR analysis indicate that the extractables of all hydrogels are composed mainly of residual synthetic monomers, crosslinker (BIS) and low molecular weight polymeric chains. The absence of the peaks corresponding to the polysaccharides indicates the absence or the very low concentration of the polysaccharides in the extractables of the composite hydrogels, which suggest the successful entrapments of all polysaccharides within the synthetic polymer network.

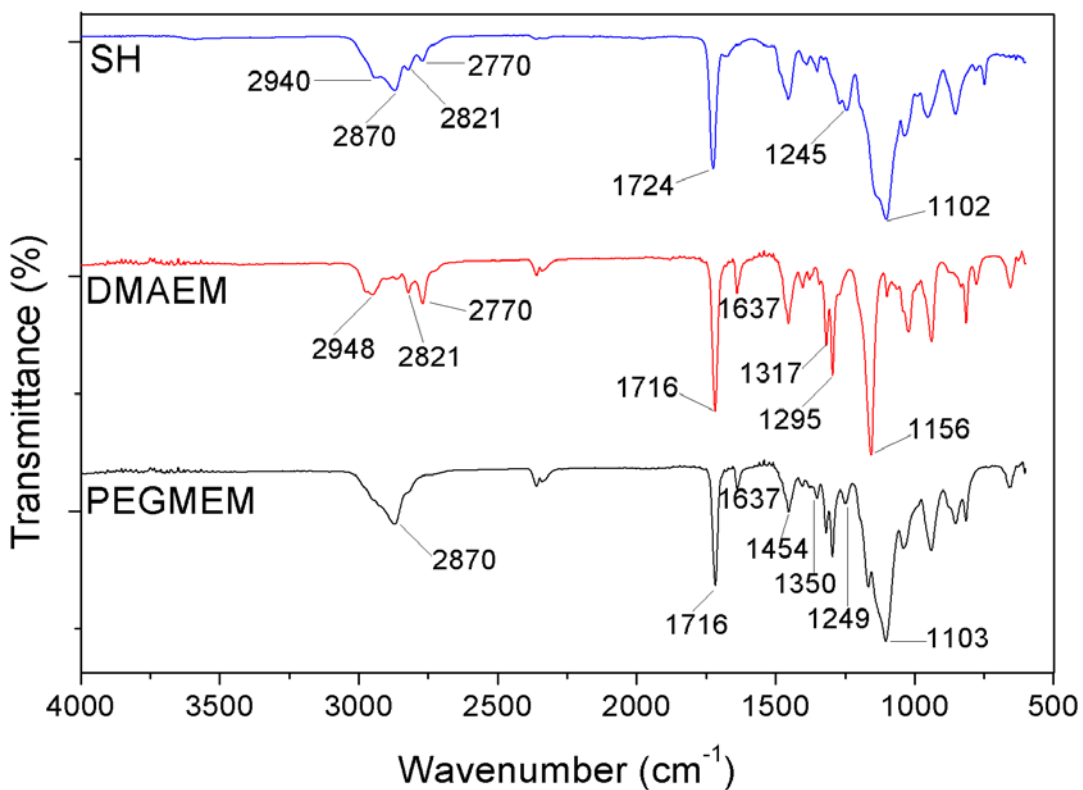


Figure 4.1. FTIR spectra of PEGMEM, DMAEM and SH.

4.3.2. Swelling behavior

Figure 4.2a shows the swelling behavior of the hydrogels according to the composition. The WU of SH was 11.9 g/g and the WU of PC hydrogels were slightly lower and increased with increasing the PC concentration from 9.6 g/g to 11.7 g/g for 0.2% and 1%, respectively. The PC hydrogels have carboxylic groups forming hydrogen bond between PC and monomers that reduce the flexibility of the network which does not favor swelling [28,29]. The WU of CS hydrogels was higher than the WU of SH and increased with increasing the CS concentration from 17.8 g/g to 26.0 g/g for 0.2% and 1%, respectively. The CS hydrogels have amine groups deprotonated and swelling increase due to a decrease in electrostatic interaction [30]. Maximum WU were observed for κC hydrogels, which increased with increasing of κC from 0.2% to 1% from 29.1 g/g to 41.5 g/g, respectively. These hydrogels can be classified as superabsorbent hydrogels since

they have an absorption above 200% [31]. The κC hydrogels have sulfate groups (very hydrophilic) that contribute to its high swelling ability in deionized water [18]. The WU of hydrogels increases as κC content increases due to increasing the hydrophilicity of hydrogel. Therefore, incorporation of κC and CS in synthetic hydrogel produces an increase in the swelling behavior. The κC hydrogels showed an appreciable WU and may be considered as candidates to design novel drug delivery systems.

The effect of the crosslinker concentration N,N'-methylenebis(acrylamide) (BIS) on the WU was evaluated in this work with 0.5κC hydrogel, which presented a high swelling (Fig. 4.2b). It was observed that a slight increase in the crosslinker concentration from 5% to 6% decreased the WU from 36.2 g/g to 28.3 g/g; and an increase to 10% and 15% of crosslinker decreased markedly the WU to 11.3 g/g and 7.3 g/g, respectively. This is due to crosslinking hinders the mobility of the polymer chain, hence lowering the WU [2]. It has been reported that swelling behavior in PEGMEM/DMAEM hydrogels [23] and κC/methacrylamide hydrogels [32] is controlled by the concentration of crosslinker. Therefore, the swelling behavior of κC hydrogels can be controlled according to its desired application.

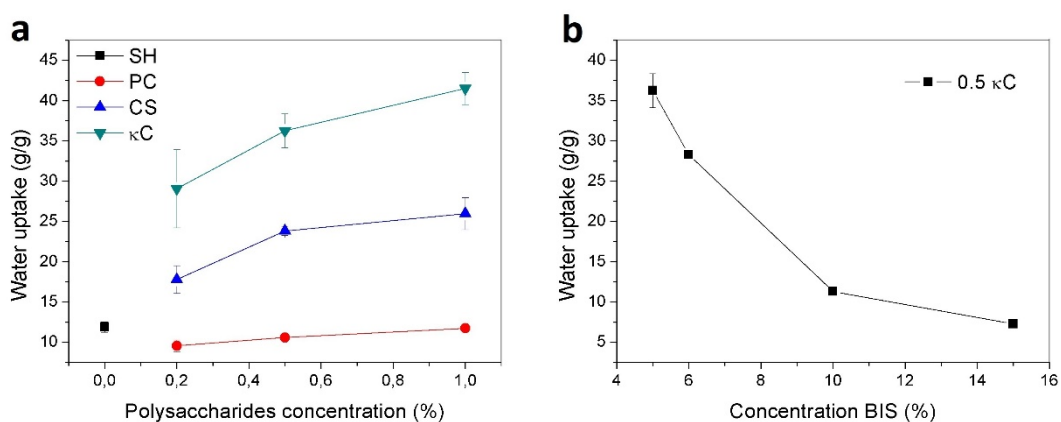


Figure 4.2. Water uptake of prepared hydrogels (a) and effect the crosslinker concentration on water uptake of 0.5κC hydrogel (b).

4.3.3. Field emission scanning electron microscopy

Fig. 4.3 shows the morphologies of the surfaces of the freeze-dried swollen hydrogels. The figure showed the porous structure of the prepared hydrogels. SH showed a non-uniform structure evidenced by its uneven pore size and wall thickness. 1CS hydrogel was not uniform, with similar wall thickness of pores and pore size larger than SH. 1kC hydrogel had the largest average pore size and a relatively uniform wall thickness of pores. For 1PC hydrogel, its pore size decreases in comparison with 1kC hydrogel while the pores density increases. These results show that the incorporation of polysaccharides produced changes in the surface morphology of the synthetic hydrogel. The PC and kC favors the formation of larger and more defined pores. The porous structure of hydrogels can provide a matrix for drug loading and could allow the passage of nutrients and low molecular weight solutes necessary for the survival and growth of cells [33]. For instance, it has been demonstrated that the optimum pore size for ingrowth of hepatocytes is 20 μm , 20–125 μm for regeneration of adult mammalian skin and 200–350 μm for osteoconduction [34].

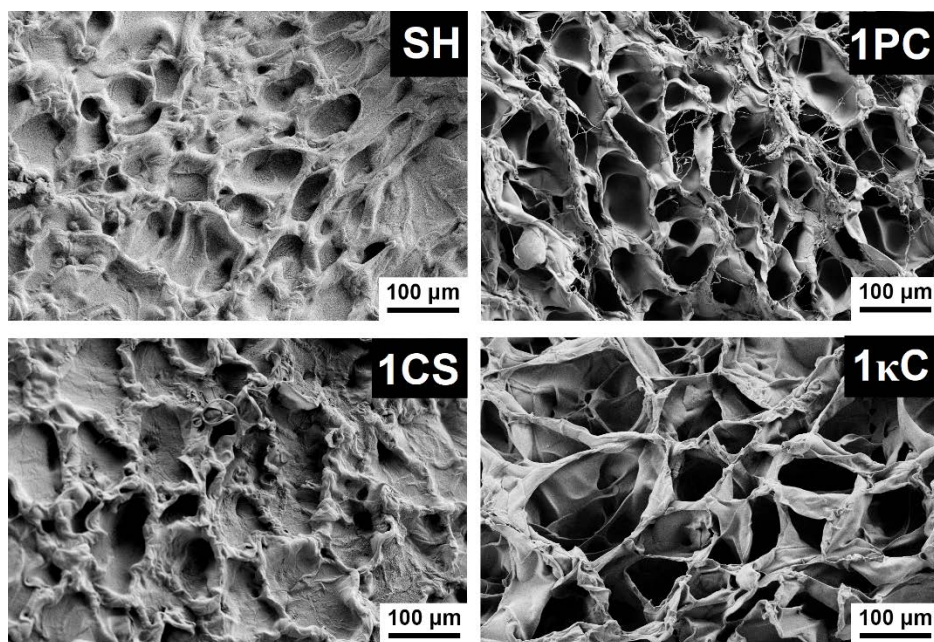


Figure 4.3. FESEM images of freeze-dried swollen hydrogels SH, 1PC, 1CS and 1kC.

4.3.4. Thermogravimetric analysis

The water content of the prepared hydrogels is presented in Fig. 4.4a. The percentage of water content in the swollen hydrogels obtained was 90.0%; 90.2%; 96.2% and 96.7% for SH, 1PC, 1CS and 1 κ C, respectively. All hydrogels presented good holding water capabilities without dissolving. The water content of a swollen hydrogel plays a key role in the biomedical applications of hydrogels, as it can significantly influence the solute diffusion and the mechanical properties of the hydrogels[35].

The thermogravimetric analysis of the lyophilized hydrogels was carried out and the TGA curves are presented in Fig. 4.4b. The decomposition onset temperature for SH was the highest at 267 °C. The entrapment of PC, CS and κ C decreased the decomposition onset temperature at 249 °C, 259 °C and 238 °C, respectively, which can be attributed to the decomposition of polysaccharides. It was reported [36] that κ C showed low thermal stability with three maximum decomposition rate at 92.5 °C, 201 °C and 321 °C.

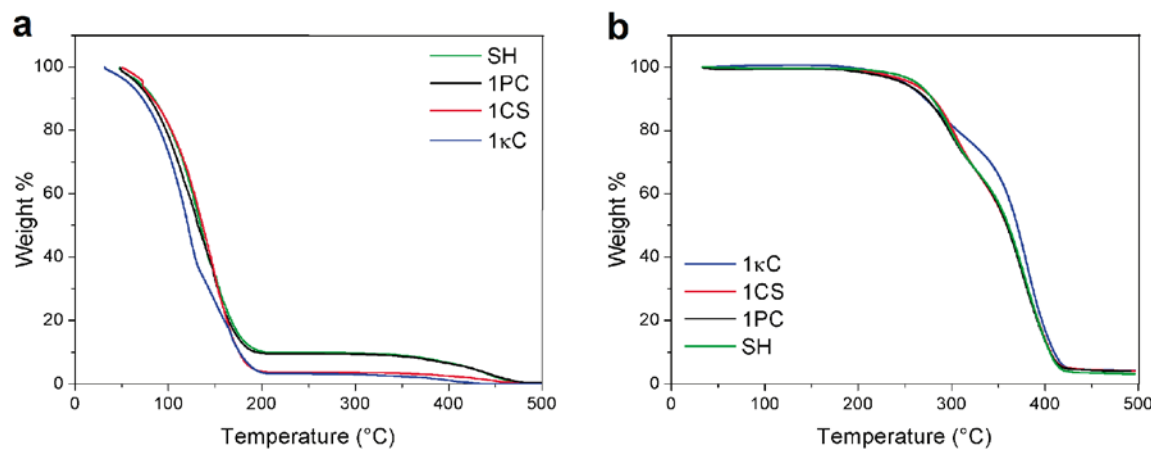


Figure 4.4. TGA of swollen hydrogels (a) and TGA curves of lyophilized hydrogels (b).

4.3.5. Mechanical properties

To investigate the effects of the entrapment of polysaccharides within synthetic hydrogel on the mechanical properties, the compression load and the compression strain were determined and

compared with the values for the SH. The results are summarized in Table 4.2. SH had 100.1 N and 83.1% of compression load and compression strain, respectively. PC hydrogels presented compression load and compression strain values similar to SH, increasing their values with the increase of the PC concentration. In the CS hydrogels the compression load and the compression strain decreased with values of 82.5 N and 77.4%, respectively for 1CS. κC hydrogels showed the highest deformations, exceeding 100% and the highest values of compression load, reaching up 400 N approximately for 0.2κC. It has been reported a κC /polyacrylamide hydrogel that exhibited high toughness and the results were attributed to the unzipping of double-helical aggregates and dissociation of double helices of κC, which produced continuous fracture process of the first κC network and the toughening mechanism of the physically and chemically crosslinked κC/polyacrylamide hydrogel [21]. Thereby, the κC improves the mechanical properties of a synthetic hydrogel suggesting a potential application as biomaterial in tissue engineering.

Table 4.2. Mechanical properties of hydrogels

Sample	Compression load (N)	Compression strain (%)
SH	100.1 ± 22.1	83.1 ± 2.7
0.2PC	98.1 ± 11.9	80.6 ± 5.8
0.5PC	119.7 ± 13.1	85.2 ± 5.6
1PC	127.9 ± 22.1	86.8 ± 7.6
0.2CS	59.1 ± 6.9	74.9 ± 2.7
0.5CS	74.5 ± 7.3	78.3 ± 3.1
1CS	82.5 ± 7.1	77.4 ± 2.2
0.2κC	398.3 ± 13.0	109.5 ± 6.1
0.5κC	266.4 ± 14.4	107.2 ± 7.8
1κC	307.4 ± 15.4	102.2 ± 4.7

4.3.6. Biocompatibility

To evaluate the potential application as biomaterials, the biocompatibility of the prepared hydrogels was investigated with *in vitro* cytotoxicity assay. The viability of the macrophages seeded on the hydrogels was assessed with the MTT assay (Fig. 4.5). The macrophages viability was reduced until approximately 70% with SH and 1PC; and it was not affected with 1CS and 1kC (no significant differences). Thus, the cell viability of the prepared hydrogels was within the established acceptance limit of 70% of the value of the control [37]. The nitrite production assay (Fig. 4.6) showed that all hydrogels did not induce nitrite production in these cells, this means that the prepared hydrogels did not induce an inflammatory response. Besides, cells were attached to the bottom of the culture plate, not to hydrogels surface in SH, 1CS and 1kC; only 1PC hydrogel allowed cell attachment to material surface (Fig. 4.7). The ideal is that the macrophages do not adhere to the gel, since their accumulation could trigger a chronic inflammation. These results suggest that the prepared hydrogels did not contain any toxic substrate influencing cellular growth and mainly the 1CS and 1kC could be considered as valid candidates for biomedical use.

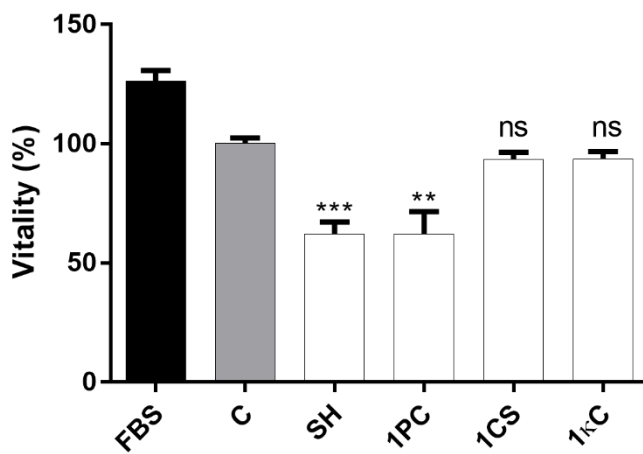


Figure 4.5. MTT assay. Effect of SH, 1PC, 1CS and 1kC hydrogels on J774.A1 macrophages vitality ($n = 6$) for 24 h. Culture medium with 10% of FBS was used as positive control.

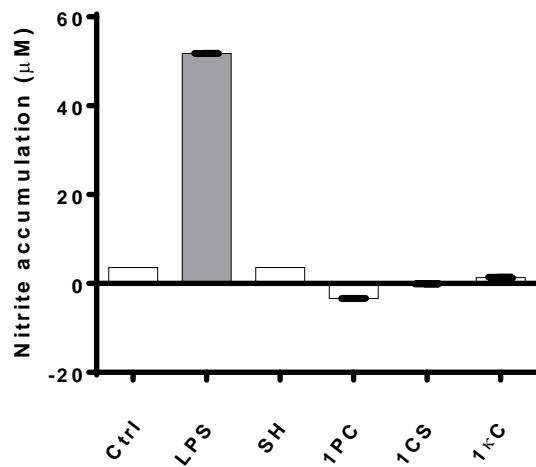


Figure 4.6. Nitrite assay. Effect of SH, 1PC, 1CS and 1kC hydrogels on J774.A1 macrophages nitrite production. LPS 250 ng mL⁻¹ was used as positive control, and culture medium from untreated cells as negative control (n=6).

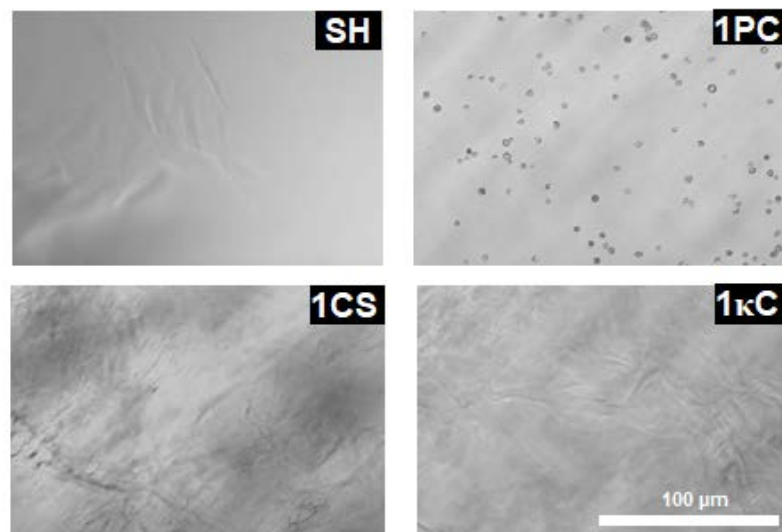


Figure 4.7. Microscopy images of hydrogels surfaces after cell seeding.

4.4. Conclusions

Biocompatible composite hydrogels with improved swelling and mechanical properties were obtained. The results showed that CS hydrogels had higher WU and lower mechanical properties than the SH. The PC hydrogels presented the lowest WU of all hydrogels and compression load and compression stress values similar than the SH. The κ C hydrogels showed the highest water uptake and they can be classified as superabsorbent hydrogels. Also, the κ C improved considerably the mechanical properties of the SH. The results of MMT assay and nitrite assay for the composite hydrogels showed a good biocompatibility, mainly for CS and κ C hydrogels. Therefore, the entrapment of κ C within SH improves both the swelling and the mechanical properties and they could be considered as a potential biomaterial in tissue engineering and drug delivery.

Supplementary material

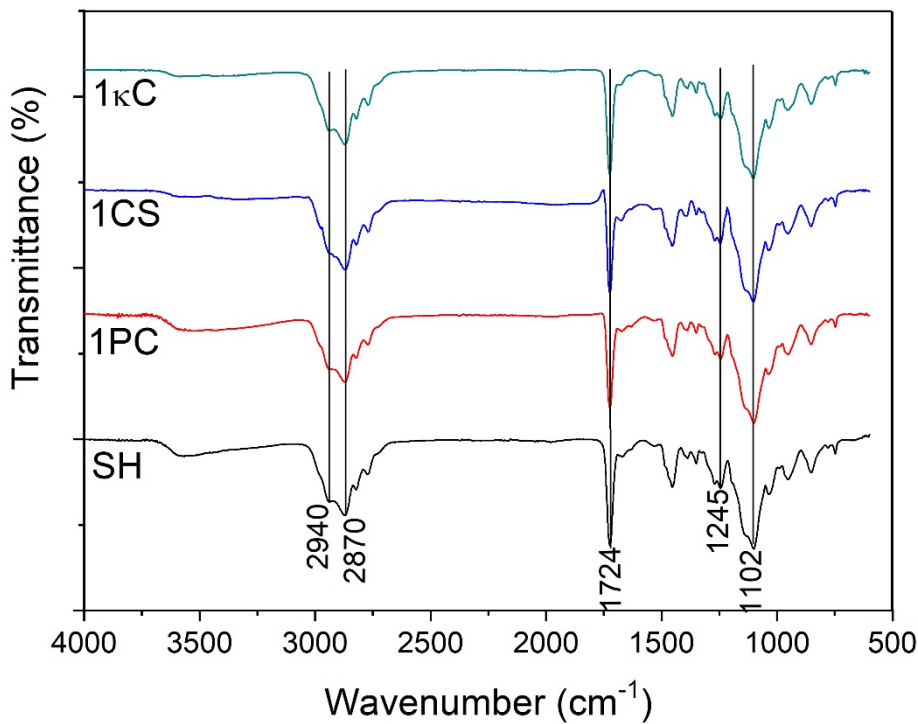


Figure S. 4.1. FTIR spectra of SH, 1PC, 1CS and 1 κ C hydrogel.

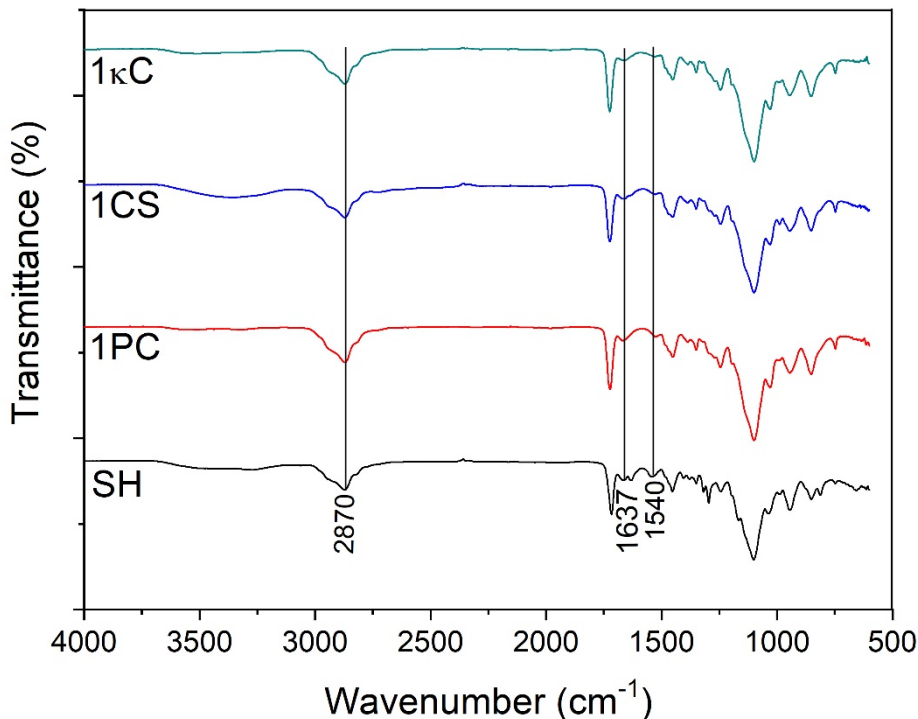


Figure S. 4.2. FTIR spectra of extractables from SH, 1PC, 1CS and 1 κ C hydrogel

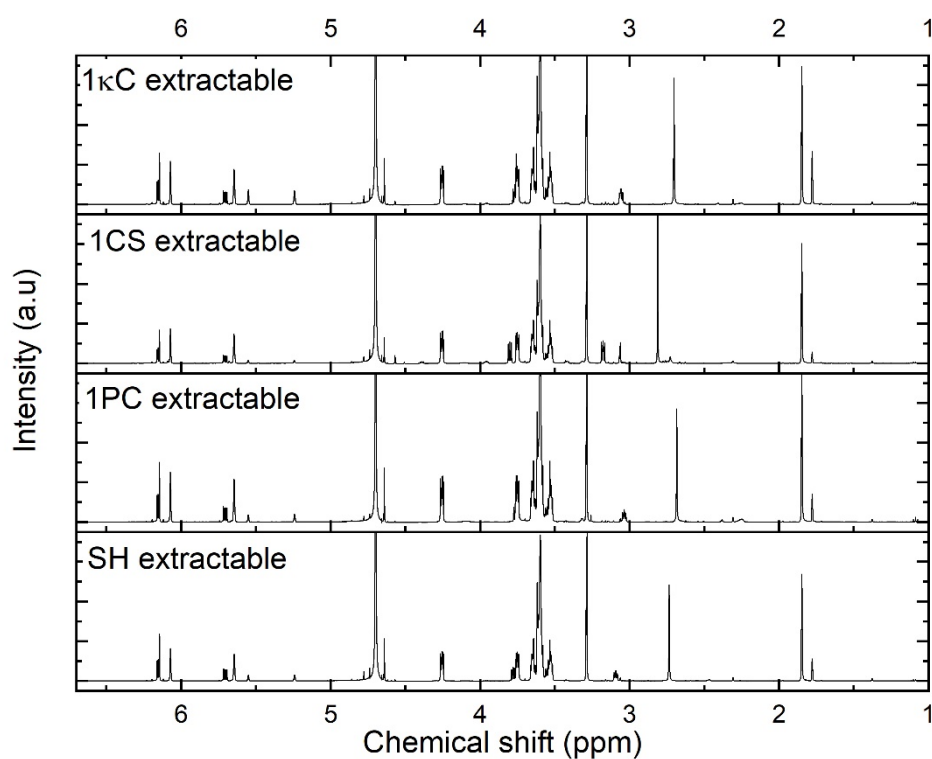


Figure S. 4.3. ^1H RMN spectra of extractables from SH, 1PC, 1CS and 1kC hydrogel

4.5. References

- [1] N.A. Peppas, J.Z. Hilt, A. Khademhosseini, R. Langer, Hydrogels in biology and medicine : from molecular principles to bionanotechnology, *Adv. Mater.* 18 (2006) 1345–1360. doi:10.1002/adma.200501612.
- [2] N.A. Peppas, P. Bures, W. Leobandung, H. Ichikawa, Hydrogels in pharmaceutical formulations, *Eur. J. Pharm. Biopharm.* 50 (2000) 27–46. doi:10.1016/S0939-6411(00)00090-4.
- [3] F. Ullah, M.B.H. Othman, F. Javed, Z. Ahmad, H.M. Akil, Classification, processing and application of hydrogels: A review, *Mater. Sci. Eng. C* 57 (2015) 414–433. doi:10.1016/j.msec.2015.07.053.
- [4] K. Varaprasad, G.M. Raghavendra, T. Jayaramudu, M.M. Yallapu, R. Sadiku, A mini review on hydrogels classification and recent developments in miscellaneous applications, *Mater. Sci. Eng. C* 79 (2017) 958–971. doi:10.1016/j.msec.2017.05.096.
- [5] W.E. Hennink, C.F. Van Nostrum, Novel crosslinking methods to design hydrogels, *Adv. Drug Deliv. Rev.* 64 (2012) 223–236. doi:10.1016/j.addr.2012.09.009.
- [6] L. Racine, I. Texier, R. Auzély-Velty, Chitosan-based hydrogels: Recent design concepts to tailor properties and functions, *Polym. Int.* 66 (2017) 981–998. doi:10.1002/pi.5331.
- [7] L.H. Sperling, V. Mishra, The current status of interpenetrating polymer networks, *Polym. Adv. Technol.* 7 (1996) 197–208. doi:10.1002/(SICI)1099-1581(199604)7:4<197::AID-PAT514>3.0.CO;2-4.
- [8] E.S. Dragan, Design and applications of interpenetrating polymer network hydrogels . A review, *Chem. Eng. J.* 243 (2014) 572–590. doi:10.1016/j.cej.2014.01.065.
- [9] E.S. Dragan, Advances in interpenetrating polymer network hydrogels and their applications, *Pure Appl. Chem.* 86 (2014) 1707–1721. doi:10.1515/pac-2014-0713.
- [10] J. Duan, L. Zhang, Robust and Smart Hydrogels Based on Natural Polymers, *Chinese J. Polym. Sci.* 35 (2017) 1165–1180. doi:10.1007/s10118-017-1983-9.
- [11] O. Robles-Vazquez, I. Orozco-Avila, J.C. Sánchez-Díaz, E. Hernandez, An Overview of Mechanical Tests for Polymeric Biomaterial Scaffolds Used in Tissue Engineering, *J. Res. Updat. Polym. Sci.* 4 (2015) 168–178.

- [12] D.A. Gyles, L.D. Castro, J.O.C.S. Júnior, R.M. Ribeiro-Costa, A review of the designs and prominent biomedical advances of natural and synthetic hydrogel formulations, *Eur. Polym. J.* 88 (2017) 373–392. doi:10.1016/j.eurpolymj.2017.01.027.
- [13] J. García, E. Ruiz-Durández, N.E. Valderruten, Interpenetrating polymer networks hydrogels of chitosan and poly(2-hydroxyethyl methacrylate) for controlled release of quetiapine, *React. Funct. Polym.* 117 (2017) 52–59. doi:10.1016/j.reactfunctpolym.2017.06.002.
- [14] M. Zeng, Z. Feng, Y. Huang, J. Liu, J. Ren, Q. Xu, L. Fan, Chemical structure and remarkably enhanced mechanical properties of chitosan-graft-poly(acrylic acid)/polyacrylamide double-network hydrogels, *Polym. Bull.* 74 (2017) 55–74. doi:10.1007/s00289-016-1697-0.
- [15] A. Noreen, Z. i. H. Nazli, J. Akram, I. Rasul, A. Mansha, N. Yaqoob, R. Iqbal, S. Tabasum, M. Zuber, K.M. Zia, Pectins functionalized biomaterials; a new viable approach for biomedical applications: A review, *Int. J. Biol. Macromol.* 101 (2017) 254–272. doi:10.1016/j.ijbiomac.2017.03.029.
- [16] S. Eswaramma, N.S. Reddy, K.S.V.K. Rao, Phosphate crosslinked pectin based dual responsive hydrogel networks and nanocomposites: Development, swelling dynamics and drug release characteristics, *Int. J. Biol. Macromol.* 103 (2017) 1162–1172. doi:10.1016/j.ijbiomac.2017.05.160.
- [17] L. Li, R. Ni, Y. Shao, S. Mao, Carrageenan and its applications in drug delivery, *Carbohydr. Polym.* 103 (2014) 1–11. doi:10.1016/j.carbpol.2013.12.008.
- [18] J. Nourmohammadi, F. Roshanfar, M. Farokhi, M. Haghbin, Silk fibroin / kappa - carrageenan composite scaffolds with enhanced biomimetic mineralization for bone regeneration applications, *Mater. Sci. Eng. C* 76 (2017) 951–958. doi:10.1016/j.msec.2017.03.166.
- [19] Y. Zhang, L. Ye, J. Cui, B. Yang, H. Sun, J. Li, F. Yao, A Biomimetic Poly(vinyl alcohol)-Carrageenan Composite Scaffold with Oriented Microarchitecture, *ACS Biomater. Sci. Eng.* 2 (2016) 544–557. doi:10.1021/acsbiomaterials.5b00535.
- [20] G.F. El-fawal, A.M. Yassin, N.M. El-deeb, The Novelty in Fabrication of Poly Vinyl Alcohol / κ -Carrageenan Hydrogel with *Lactobacillus bulgaricus* Extract as Anti-inflammatory Wound Dressing Agent, *AAPS PharmSciTech.* 18 (2017) 1605–1616. doi:10.1208/s12249-

016-0628-6.

- [21] S. Liu, L. Li, Recoverable and self-healing double network hydrogel based on k-Carrageenan, *ACS Appl. Mater. Interfaces.* 8 (2016) 29749–29758. doi:10.1021/acsami.6b11363.
- [22] Y. Chen, A. Venault, J. Jhong, H. Ho, C. Liu, R.-H. Lee, G.-H. Hsiue, Y. Chang, Developing blood leukocytes depletion membranes from the design of bioinert PEGylated hydrogel interfaces with surface charge control, *J. Memb. Sci.* 537 (2017) 209–219. doi:10.1016/j.memsci.2017.05.031.
- [23] Y. Ramadan, M.I. González-Sánchez, K. Hawkins, J. Rubio-Retama, E. Valero, S. Perni, P. Prokopovich, E. López-Cabarcos, Obtaining new composite biomaterials by means of mineralization of methacrylate hydrogels using the reaction – diffusion method, *Mater. Sci. Eng. C* 42 (2014) 696–704. doi:10.1016/j.msec.2014.06.017.
- [24] G. Tommasi, S. Perni, P. Prokopovich, An Injectable Hydrogel as Bone Graft Material with Added Antimicrobial Properties, *Tissue Eng. Part A.* 22 (2016) 862–872. doi:10.1089/ten.tea.2016.0014.
- [25] E.S. Dragan, A.I. Cocarta, Smart Macroporous IPN Hydrogels Responsive to pH, Temperature, and Ionic Strength: Synthesis, Characterization, and Evaluation of Controlled Release of Drugs, *ACS Appl. Mater. Interfaces.* 8 (2016) 12018–12030. doi:10.1021/acsami.6b02264.
- [26] L.C. Bonkovoski, A.F. Martins, I.C. Bellettini, F.P. Garcia, C. V Nakamura, A.F. Rubira, E.C. Muniz, Polyelectrolyte complexes of poly [(2-dimethylamino) ethyl methacrylate]/ chondroitin sulfate obtained at different pHs : I . Preparation , characterization , cytotoxicity and controlled release of chondroitin sulfate, *Int. J. Pharm.* 477 (2014) 197–207. doi:10.1016/j.ijpharm.2014.10.017.
- [27] G.A. Titaux, A. Contreras-García, E. Bucio, Surface modification by g -ray-induced grafting of PDMAEMA / PEGMEMA onto PE films, *Radiat. Phys. Chem.* 78 (2009) 485–488. doi:10.1016/j.radphyschem.2009.03.031.
- [28] K.D. Yao, H. Tu, F. Cheng, J.W. Zhang, J. Liu, pH-sensitivity of the swelling of a chitosan-pectin polyelectrolyte complex, *Die Angew. Makromol. Chemie.* 245 (1997) 63–72. doi:10.1002/apmc.1997.052450106.

- [29] N. Sivagangi Reddy, K. Madhusudana Rao, T.J. Sudha Vani, K.S. V Krishna Rao, Y.I. Lee, Pectin/poly(acrylamide-co-acrylamidoglycolic acid) pH sensitive semi-IPN hydrogels: selective removal of Cu²⁺ and Ni²⁺, modeling, and kinetic studies, Desalin. Water Treat. 57 (2016) 6503–6514. doi:10.1080/19443994.2015.1008053.
- [30] G.R. Mahdavinia, A. Mosallanezhad, M. Soleymani, M. Sabzi, Magnetic- and pH-responsive kappa-carrageenan/chitosan complexes for controlled release of methotrexate anticancer drug, Elsevier B.V., 2017. doi:10.1016/j.ijbiomac.2017.01.012.
- [31] S. Sharma, A. Dua, A. Malik, Polyaspartic acid based superabsorbent polymers, Eur. Polym. J. 59 (2014) 363–376. doi:10.1016/j.eurpolymj.2014.07.043.
- [32] A. Pourjavadi, M. Sadeghi, H. Hosseinzadeh, Modified carrageenan. 5. Preparation, swelling behavior, salt- and pH-sensitivity of partially hydrolyzed crosslinked carrageenan-graft-polymethacrylamide superabsorbent hydrogel, Polym. Adv. Technol. 15 (2004) 645–653. doi:10.1002/pat.524.
- [33] Q. Chai, Y. Jiao, X. Yu, Hydrogels for biomedical applications: Their characteristics and the mechanisms behind them, Gels. 3 (2017) 6. doi:10.3390/gels3010006.
- [34] I.M. El-Sherbiny, M.H. Yacoub, Hydrogel scaffolds for tissue engineering: Progress and challenges, Glob. Cardiol. Sci. Pract. (2013) 38. doi:10.5339/gcsp.2013.38.
- [35] F. Zhao, D. Yao, R. Guo, L. Deng, A. Dong, J. Zhang, Composites of Polymer Hydrogels and Nanoparticulate Systems for Biomedical and Pharmaceutical Applications, Nanomaterials. 5 (2015) 2054–2130. doi:10.3390/nano5042054.
- [36] G.R. Mahdavinia, A. Massoudi, A. Baghban, E. Shokri, Study of adsorption of cationic dye on magnetic kappa-carrageenan/PVA nanocomposite hydrogels, J. Environ. Chem. Eng. 2 (2014) 1578–1587. doi:10.1016/j.jece.2014.05.020.
- [37] O. Guaresti, C. García-Astrain, T. Palomares, A. Alonso-Varona, A. Eceiza, N. Gabilondo, Synthesis and characterization of a biocompatible chitosan – based hydrogel cross – linked via ‘click’ chemistry for controlled drug release, Int. J. Biol. Macromol. 102 (2017) 1–9. doi:10.1016/j.ijbiomac.2017.04.003.

CAPÍTULO 5: Poly(hydroxybutyrate-co-hydroxyvalerate) microparticles embedded in κ -carrageenan/locust bean gum hydrogel as a dual drug delivery carrier.

5.1. Introduction

Currently the development of new drug delivery systems has been intensified. In recent years, pharmaceutical and biomedical strategies require the delivery of more than one drug in a controlled and localized manner. Combined drug therapy can have the advantage of producing a drug synergistic effect, minimize the amount of each drug and reduce the side effects. In order to comply with this requirement, different vehicles have been developed to allow the multiaction of different drugs from a single formulation [1]. For this reason, the development of vehicles capable of encapsulating and delivering multiple drugs is an important aspect in smart drug delivery [2]. Nowadays different dual drug delivery systems have been investigated, such as hydrogel beads [1], nanoparticles [3,4], nanocomposite fibrous [5], hydrogel [6], hydrogel/micelle composite [7] or microspheres/hydrogel [8].

Within drug delivery systems, hydrogels have been widely applied due to their high water content allowing the enhancement of drugs permeation [9,10]. Moreover, hydrogels can control drug release due to changes (swelling, dissolution or degradation) in the gel structure in response to internal or external stimuli [11]. However, despite their favorable characteristics, there are still certain limitations for using these hydrogels as drug delivery systems. For example, the homogeneity and quantity of the drug loaded on the hydrogels may be limited, particularly in the case of hydrophobic or poorly water soluble drugs [12]. To overcome these limitations different strategies have been adopted to modify the hydrogels, one is the incorporation of micro or nanoparticles to create composite hydrogels with custom properties [13]. The combination of particles and hydrogels create synergistic, unique and potentially useful properties that are not found in the individual components [14]. For instance, mupirocin silica microspheres loaded collagen scaffold [15] and PHBV microparticles in gellan gum hydrogel [16] have been reported as synergistic composites for localized delivery of drugs.

Among the hydrogels that can be used for drug delivery, polysaccharide-based hydrogels have received special attention due to their biocompatibility, similarity to native extracellular matrix,

low toxicity and susceptibility to degradation by human enzymes or by hydrolysis [17,18]. Also, polysaccharide-based hydrogels can be physically crosslinked, which make them attractive for the development of drug delivery vehicles since their preparation do not involve any toxic compounds [19]. An ideal polysaccharide for controlled drug delivery applications is κ -carrageenan since it has a strong gel formation ability with a high swelling property and has a structure that resembles glycosaminoglycans, which are major components of native extracellular matrices [20]. Microcapsules, microspheres, beads, nanoparticles and gels based on κ -carrageenan have been developed for drug delivery systems [21]. κ -carrageenan forms a network of three-dimensional double helices upon cooling and in presence of a suitable cation, typically potassium [22,23]. On the other hand, locust bean gum (LBG) shows a synergistic effect with κ -carrageenan and forms a gel with more elasticity and strength [24]. The combination of LBG and κ -carrageenan is widely utilized in various industries such as foods and cosmetics, and more recently in the biopharmaceutical and biomedicine fields. For example, κ -carrageenan/LBG hydrogels for wound dressing have been developed with gold nanoparticles [25] or cranberry extract [26].

The aim of this work was to prepare a novel composite hydrogel combining microparticles and hydrogel for simultaneous dual delivery of two hydrophobic drugs. In addition to showing that it can be obtained a prolonged and slower drug release with this composite hydrogel than the obtained release from the microparticles or the hydrogel separately. The purpose is also to show that this composite hydrogel may be used as a model for dual delivery of hydrophobic drugs. κ -carrageenan and LBG were the biopolymers chosen to prepare a physical hydrogel and poly(hydroxybutyrate-co-hydroxyvalerate (PHBV) was selected to elaborate microparticles to encapsulate two hydrophobic drugs. PHBV belongs to the polyhydroxyalkanoates (PHAs) family, well known for their biodegradability, biocompatibility and mechanical strength [27]. Also, nanoparticles, microparticles and nanofibers of PHBV have been prepared to encapsulate and release various therapeutic agents [28]. Specifically, it has been reported the encapsulation of

hydrophobic drugs in nano [29] or microparticles [16] of PHBV. Ketoprofen, a nonsteroidal anti-inflammatory and mupirocin, a commonly used antibiotic, both used in wound healing, were selected as model drugs due to their hydrophobicity.

Therefore, a dual drug encapsulation of ketoprofen and mupirocin was achieved in PHBV microparticles and then incorporated in κ -carrageenan/locust bean gum hydrogels. The surface morphologies, particle size, porosity, drug loading and entrapment efficiency of the microparticles were determined. The surface morphologies, swelling behavior and rheological properties were determined for the composite hydrogel. Also, *in vitro* drug release and biocompatibility assays were studied for the purpose of analyzing the potential of this composite hydrogel as a novel dual drug delivery carrier, mainly for wound healing applications.

5.2. Materials and Methods

5.2.1. Materials

κ -carrageenan (κ C) (molar mass distribution as provided by the supplier: 53.3% between 1000 and 5000 kDa; around 21.8% between 500 and 1000 kDa and the rest corresponds to 100 to 500 kDa) and locust bean gum (LBG) (viscosity 3500 cps, 25 °C) were gifted by Ceamsa, Spain. Poly(3-hydroxybutyrate-co-3-hydroxyvalerate) (PHBV) (12% hydroxyvalerate (HV) content, Mw: 240,000) was supplied by Goodfellow Cambridge limited, UK. Dichloromethane was purchased from VWR Chemicals, France. Poly (vinyl alcohol) (PVA) (86.7–88.7 mol% hydrolysis, Mw: 31,000), (Mowiol® 4-88) and phosphate buffered saline (PBS) (0.01 M, pH 7.4) were purchased from Sigma-Aldrich, Germany. Tween®80, ethanol absolute and potassium chloride used were of analytical grade and purchased from Scharlau, Spain. Ketoprofen (MW: 254.28 Da) was purchased from Carbosynth, UK. Mupirocin (MW: 500.63 Da) was purchased from Thermo Fisher, Germany. All chemicals were used without further purification. The water used in the preparations and washings was purified on a Milli-Q ultrapure system (Millipore, France).

5.2.2. Preparation of PHBV microparticles

PHBV microparticles carrying ketoprofen and mupirocin (KM-MPs) were prepared by using emulsification/solvent evaporation method previously described [30] with modifications. Briefly, PHBV was dissolved in dichloromethane at a concentration of 1% w/v using stirring and heating at 40 °C. Then, the drugs were added to the solution in a concentration of 0.1% w/v and 0.2% w/v, respectively. 10% w/v PVA solution in water was prepared by stirring at 90 °C until complete dissolution and was used as aqueous phase of the emulsion. Afterwards, the emulsion was formed by mechanical stirring at 750 rpm for 1h at room temperature. Subsequently, the organic solvent was evaporated by rotary evaporator at 40 °C and 30 rpm for 1 h. The particles were collected in the aqueous solution, washed several times with deionized water and then lyophilized to be characterized. Lyophilization was performed with a Lyoquest-85 (Azbil Telstar Technologies, S. L. U., Spain) at 0.2 mbar for at least 2 days. Unloaded microparticles of PHBV (unloaded MPs) were prepared without drugs with the same procedure described above. Fig. 5.1a shows a general schematic diagram of the preparation of PHBV microparticles.

5.2.3. Preparation of the hydrogels

Three samples of the κ -carrageenan/locust bean gum hydrogels were prepared. The first was the hydrogel without drugs or particles (κ CLH). The second was the hydrogel directly loaded with both drugs without the microparticles (KM- κ CLH). The third was the hydrogel loaded with the PHBV microparticles containing both drugs (KM-MPs- κ CLH). For the preparation of κ CLH, a stock solution was prepared with κ C and LBG as following. 0.334 g of LBG was dissolved in 50 mL of distilled water at 85 °C with magnetic stirring. Then, 1 g of κ C was added and heated at 85 °C about 30 min until completely dissolved. Afterwards, 375 μ L KCl 0.5 M was added to 10 mL stock solution to promote gelation of κ CLH hydrogel. The mixture was left at room temperature during approximately 1 h, allowing the formation of the gel.

For the preparation of KM- κ CLH, 0.014% w/v of ketoprofen and 0.016% w/v of mupirocin were added to 10 mL stock solution of κ C and LBG. Then, the drugs were dispersed in the solution using ultrasonication for 2 min with an ultrasonic processor SONOPULS HD 3200 (Bandelin electronics, Germany) equipped with a titanium microtip of 3 mm diameter. The ultrasonic power is up to 200 W and the processing frequency is 20 kHz. Subsequently, 375 μ L KCl 0.5 M was added to the solution and hydrogel formation was allowed.

For the preparation of KM-MPs- κ CLH, 32 mg KM-MPs were added to 10 mL stock solution. Then, the microparticles were suspended using ultrasonication and prepared under the conditions previously mentioned for KM- κ CLH. Fig. 5.1b shows a general schematic diagram of the preparation of the composite hydrogel.

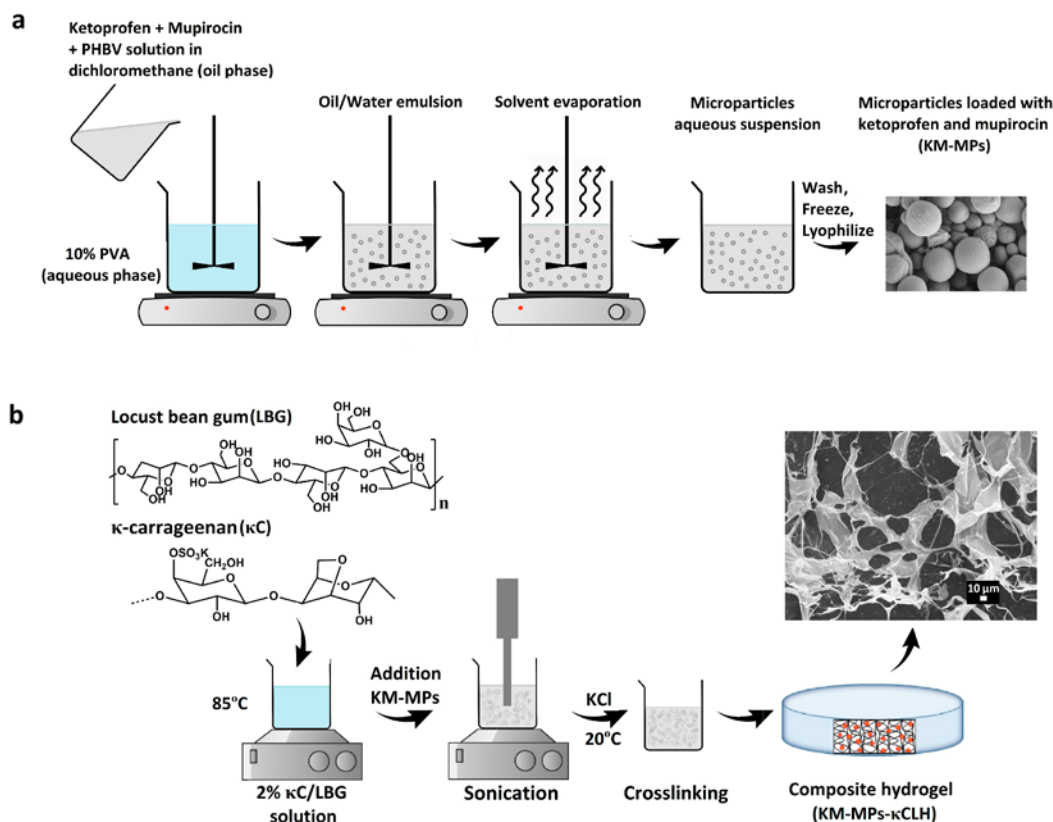


Figure 5.1. Schematic diagram showing the microparticles (a) and composite hydrogel (b) preparation.

5.2.4. Characterization of the microparticles

5.2.4.1. Field emission scanning electron microscopy (FESEM) and particle size analysis

To evaluate the surface morphological structure, the microparticles were sputter-coated with platinum/palladium using a Cressington 208HR High Resolution sputter coater (Cressington Scientific Instruments, UK). The surface morphology was observed using a field emission scanning electron microscope JSM 7200F (Jeol, USA) at an acceleration voltage of 10 kV and 15 kV. The size of the particles was determined using software Nis Elements of Nikon.

5.2.4.2. Zeta potential, surface area and pore size analysis

Zeta potential of KM-MPs was measured by Electrophoretic Light Scattering (ELS) using a Zetasizer Nano ZS90 (Malvern Instruments, Worcestershire, UK). A suspension of 1 mg polymeric microparticles was prepared in sufficient Milli-Q water to ensure that the signal intensity was suitable for the instrument. The measurements were performed at 25 °C with a detection angle of 173° in distilled water. The Brunauer-Emmett-Teller (BET) surface area and the pore size of the lyophilized KM-MPs were measured using a surface area analyzer MicroActive for TriStar II Plus (Micromeritics, USA) through N₂ adsorption at 77 K and then applied to determine the pore size distribution using the Barret-Joyner-Halenda (BJH) method.

5.2.4.3. Drug loading and entrapment efficiency

For the entrapment (%EE) and the drug loading (%DL) efficiency measurements, lyophilized KM-MPs were weighed and dispersed in absolute ethanol. Then, these dispersions were magnetically stirred for 4 days to allow the complete release of the loaded drugs. Afterwards, the dispersions were centrifuged at 14500 rpm for 5 min and the ketoprofen and mupirocin in the supernatant were quantified spectrophotometrically using an UV–Vis spectrophotometer SPECORD 200 PLUS (Analytikjena, Germany) at a wavelength of 225 nm and 260 nm, respectively. A series of standard solutions of ketoprofen and mupirocin in ethanol were used

for obtaining the calibration curve. The measurements were performed in triplicate. The %EE and %DL were calculated using the following equations (Eq. 1 and Eq. 2) [31]:

$$EE\% = (\text{Entrapped drug amount}/\text{Total drug amount}) \times 100 \quad (1)$$

$$DL\% = (\text{Entrapped drug amount}/\text{Weight of microparticles}) \times 100 \quad (2)$$

5.2.5. Characterization of the hydrogels

5.2.5.1. Swelling behavior

The swelling behaviors of κ CLH and KM-MPs- κ CLH were determined by immersing the weighed and fresh hydrogels in PBS at 25°C and 37°C. The swollen hydrogels were weighed daily after removing the water until equilibrium was reached. The swelling ratio (SR) was calculated by the Eq. 3 [32]:

$$SR (\%) = (W_s - W_d)/W_d \times 100 \quad (3)$$

where W_s is the weight of swollen hydrogel and W_d is the weight of fresh hydrogel.

5.2.5.2. Morphological properties

To evaluate the surface morphological structure, the swollen hydrogels were freeze-dried and analyzed by field emission scanning electron microscopy (FESEM) under the same conditions described in 5.2.4.1.

5.2.5.3. Rheological properties

Rheological characterization was performed for κ CLH and KM-MPs- κ CLH using a rheometer Ares (TA Instruments, USA) in a parallel plate geometry (diameter 25 mm) cell with a gap between plates of 1 mm. All the hydrogel samples were cut in a cylindrical shape. The elastic modulus (G') and the viscous modulus (G'') over a frequency range of 0.1-100 rad/s were recorded at a constant strain of 1% and 0.5% for κ CLH and KM-MPs- κ CLH, respectively, which were in the

linear range of the viscosity. All measurements were carried out in triplicate for each sample at 25 °C and 37 °C.

5.2.6. *In vitro* drug release studies

The release of ketoprofen and mupirocin from KM-MPs, KM-κCLH and KM-MPs-κCLH was studied at 25 °C and 37 °C. For the release studies from KM-MPs, 3 mg of KM-MPs were suspended in 1.5 mL PBS 0.1 M containing Tween®80 0.02% (as release medium) [33]. After predetermined intervals, the samples were centrifuged (5 min, 14.500 rpm). Afterwards, aliquots of the supernatant were withdrawn at various time intervals and replaced by the same volume of fresh medium. The amount of ketoprofen and mupirocin in the supernatant was determined spectrophotometrically as described above in 5.2.4.3.

For the release studies from KM-κCLH and KM-MPs-κCLH, freshly prepared samples of 15 mm diameter were weighed and placed in a glass beaker containing 4 mL of release medium. The drug release assays were made at 25 °C and 37 °C with a constant vibration of 70 rpm (Incubator 1000 Heidolph, Germany). The release of both drugs was determined as described above in 2.4.3. All the assays were performed in triplicate.

The Add-in program DDSolver was used for making the fitting calculations and for the calculation of the highest adjusted coefficient of determination R^2_{adj} [34].

5.2.7. Biocompatibility

5.2.7.1. Cell culture

The embryonic fibroblast cell line (NIH 3T3) was a gift from Dr. Oreste Gualillo (Neuroendocrine Interactions in Rheumatology and Inflammatory Diseases, Institute of Biomedical Research of Santiago de Compostela, Spain). Cells were cultured in Dulbecco's Modified Eagle Medium (DMEM) 4.5 g L⁻¹ glucose (Lonza Group Ltd, Switzerland) supplemented with 10% heat-inactivated fetal bovine serum (FBS) (Merck KGaA, Germany), 2% penicillin/streptomycin

antibiotics and 2% L-glutamine (Sigma-Aldrich, USA) in a humidified atmosphere at 37 °C and 5% CO₂. Cells were seeded at a density of 20×10³ cells per well in 96-well tissue culture plates.

5.2.7.2. Cell treatment

Unloaded MPs were washed in ethanol 70° and centrifuged at 10.000 xg/5 min at room temperature. The pelleted MPs were resuspended in the culture medium. Ketoprofen and mupirocin were dissolved in ethanol, and cells treated with the unloaded MPs were used as control for these treatments. Hydrogels were previously sterilized under UV light for 1 h, minced and added to the culture medium as previously described [35]. The different treatments applied for 24 h to the cells were the following: Unloaded MPs 1 mg mL⁻¹, ketoprofen 0.138 mg mL⁻¹, mupirocin 0.2 mg mL⁻¹, 120 mg mL⁻¹ of minced KM-MPs- κ CLH.

On the other hand, hydrogels were incubated in the culture medium for 24 h and subsequently cells were treated for 24 h with serial dilutions (1:2) of the extracts obtained as previously described [26].

5.2.7.3. MTT viability assay

Cytotoxicity of the different treatments was determined using the 3-(4,5-dimethylthiazol-2-yl)-2,5-diphenyltetrazolium bromide (MTT) cell viability assay. MTT is a yellow compound that when reduced by functioning mitochondria, produces purple formazan crystals that can be measured spectrophotometrically. The quantity of formazan is presumably directly proportional to the number of viable cells and their metabolic activity [36]. For this purpose, cells were treated for 24 h and 4 h before the expiry of this period with 0.5 mg mL⁻¹ MTT (Sigma-Aldrich, USA). At the end of the treatment, a solubilization solution (10% SDS solution in 0.01 M HCl) was added to dissolve the formazan crystals. After overnight incubation at 37 °C, absorbance at 550 nm was measured in a microplate reader (MultiscanEX, Thermo Fisher Scientific, USA). Data are represented as percentage of control (untreated cells).

5.2.7.4. Statistical analysis

All experimental data were obtained from six independent experiments. Data are expressed as mean \pm standard error of the mean. Statistical analysis was performed using the Mann–Whitney U test as implemented in Prism 5 (GraphPad Software Inc., USA).

5.3. Results and discussion

5.3.1. Microparticles characterization

KM-MPs were prepared by the emulsification/solvent evaporation technique. Fig. 5.2 shows the morphologies of the surfaces of unloaded MPs and KM-MPs. As shown in Fig. 5.2a and 5.2b, the microparticles showed spherical shape. The FESEM analysis of KM-MPs shows that the spherical shape of unloaded MPs is maintained after the incorporation of the drugs. Particle size distribution analysis showed that unloaded MPs were in the size range of 0.4–2.8 μm and the average mean particle size was 1.5 μm , while for KM-MPs the size range was 0.3–1.8 μm and the average mean particle size was 1.0 μm . This may be because when a drug is incorporated into the fabrication process, the drug molecules can influence the particle size depending on the molecular weight of drugs, drug/polymer ratio or drug/polymer interactions [37]. The addition of a low MW drug may not change or even reduce the particle size compared to an unloaded particle. It was reported that a dual encapsulation of dexamethasone and diclofenac sodium in PLGA nanoparticles slightly reduce the nanoparticle dimensions [2].

Zeta potential value of KM-MPs was -14.1 mV, while that for unloaded MPs was -34.1 mV. The negative surface charge is attributed to the presence of free carboxylic acid groups at the chain ends of the PHBV polymer exposed on the particle surface. The lower zeta potential value for KM-MPs could be due to the adsorption of some quantity of drugs on their surfaces, which could produce masking effect on the terminal carboxylic groups and reduce the negative zeta potential value [38].

BET is an important tool to study the surface and internal variations in physical structure by determining the surface area and porosity of materials. Porosity analysis indicated that the KM-MPs exhibited a surface area of $3.36 \text{ m}^2\text{g}^{-1}$, pore volume of $0.0046 \text{ cm}^3\text{g}^{-1}$ and pore size of 5.54 nm, while a decrease in the surface area ($2.31 \text{ m}^2\text{g}^{-1}$) and pore volume ($0.00034 \text{ cm}^3\text{g}^{-1}$) was observed in unloaded MPs. Both microparticles were of similar pore size (5.81 nm, unloaded MPs) indicating a mesoporous material, according to the International Union of Pure and Applied Chemistry (IUPAC) standard [39]. Also, the microparticles seem to have an inner pore structure as can be seen in Fig. 5.2c. Previous results reported about other PHBV MPs showed images with higher pore size [16] and higher values of surface area [40,41]. These results were probably due to the larger size of the PHBV MPs studied.

The entrapment efficiency (% EE) and the drug loading (% DL) for both drugs in KM-MPs were calculated by Eq 1 and Eq 2. The % EE for ketoprofen was $5.93\% \pm 0.29\%$ and for mupirocin was $4.33\% \pm 0.18\%$. The % DL for ketoprofen was $3.41\% \pm 0.17\%$ and for mupirocin was $4.97\% \pm 0.21\%$. Then, it was possible to encapsulate both drugs in the PHBV microparticles.

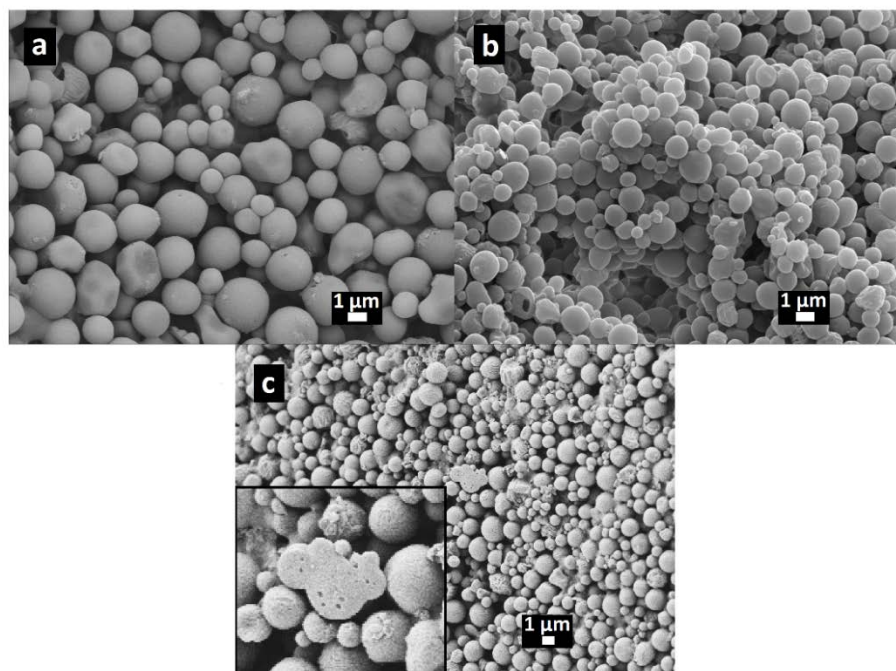


Figure 5.2. FESEM images of unloaded MPs (a) and KM-MPs (b, c). Fig.5.2c present an enlargement of the central region of the image showing the inner pore structure.

5.3.2. Characterization of hydrogels

5.3.2.1 *Swelling behavior*

The swelling behaviors of the hydrogel (κ CLH) and composite hydrogel (KM-MPs- κ CLH) were evaluated at 25 °C and 37 °C for a period of one week. The obtained results showed that the swelling behavior was sensitive to the change of the temperature. At 25 °C there was no swelling observed for both hydrogels. However, at 37 °C both hydrogels showed swelling ratios of 223.46% ± 19.26% and 183.59% ± 14.96% for κ CLH and KM-MPs- κ CLH, respectively. The increase of the swelling ratio may be due to the fact that an increase in temperature increases the mobility of the polymeric chains, thus more water molecules can penetrate the network, resulting in a higher swelling capacity [32]. The swelling ratio at 37 °C of KM-MPs- κ CLH was less than that of κ CLH, which may be attributed to the hydrophobic nature of the incorporated PHBV microparticles.

5.3.2.2. *Morphologies of the hydrogels*

Fig. 5.3 shows the morphologies of the surfaces of the hydrogel (κ CLH) and composite hydrogel (KM-MPs- κ CLH). κ CLH showed a rough and non-uniform surface (Fig. 5.3a and 5.3b). For KM-MPs- κ CLH the surface observed was smoother and uniform than for κ CLH (Fig. 5.3c). In both cases, structures like threads were observed. The microparticles were completely embedded within of the hydrogel and maintained their spherical shape (Fig. 5.3d). Thus, the incorporation of KM-MPs produced changes in the surface morphology of κ CLH making it more uniform.

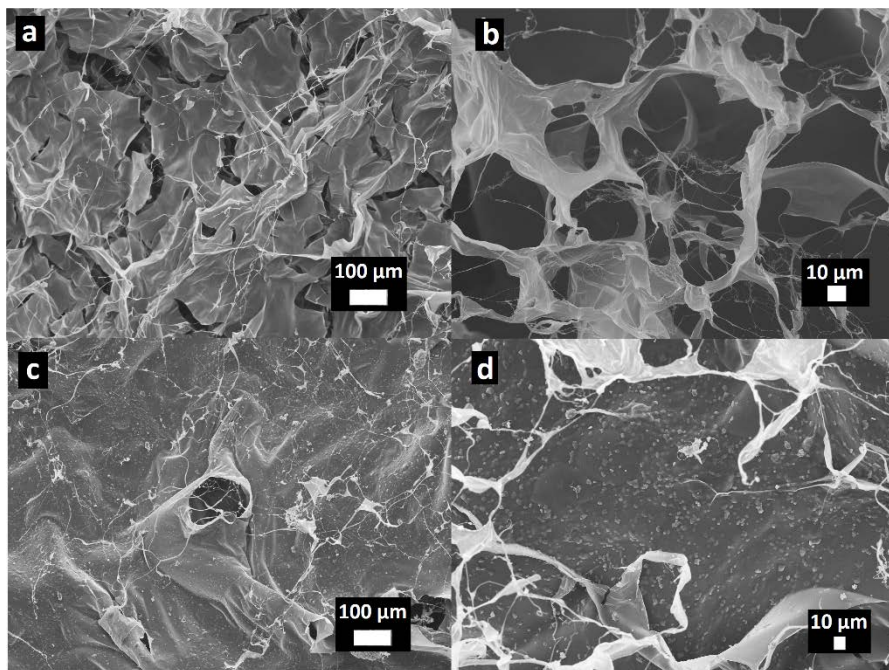


Figure 5.3. FESEM images of κCLH (a), κCLH (cross-section) (b), KM-MPs-κCLH (c) and KM-MPs-κCLH (cross-section) (d).

5.3.2.3. Rheological behavior

Mechanical properties of hydrogels are very important for pharmaceutical applications [42]. The rheological properties of the hydrogel (κCLH) and composite hydrogel (KM-MPs-κCLH) were measured by monitoring the elastic (G') and the viscous modulus (G'') as a function of the angular frequency at 25 °C and 37 °C (Fig. 5.4a and 5.4b). A typical rheological behavior of a hydrogel is that the elastic modulus dominates over the viscous modulus ($G' > G''$). Also, a typical behavior for cross-linked materials in a frequency sweep at low frequencies is that the G' and G'' curves are almost parallel straight lines in a constant limiting values [43]. According to Fig. 5.4 for both hydrogels at 25 °C and 37 °C, $G' > G''$ indicating characteristic of a strong hydrogel [44], thereby constituting a stable structure for drug loading. The elastic modulus slightly increased with increasing the frequency for both hydrogels, while the viscous modulus was nearly constant with the changing frequency for both hydrogels at 25 °C and 37 °C. At 37 °C, the addition of KM-MPs increased the G' and G'' compared to κCLH. The rheological behavior indicated that the composite hydrogel can be used for drug delivery applications.

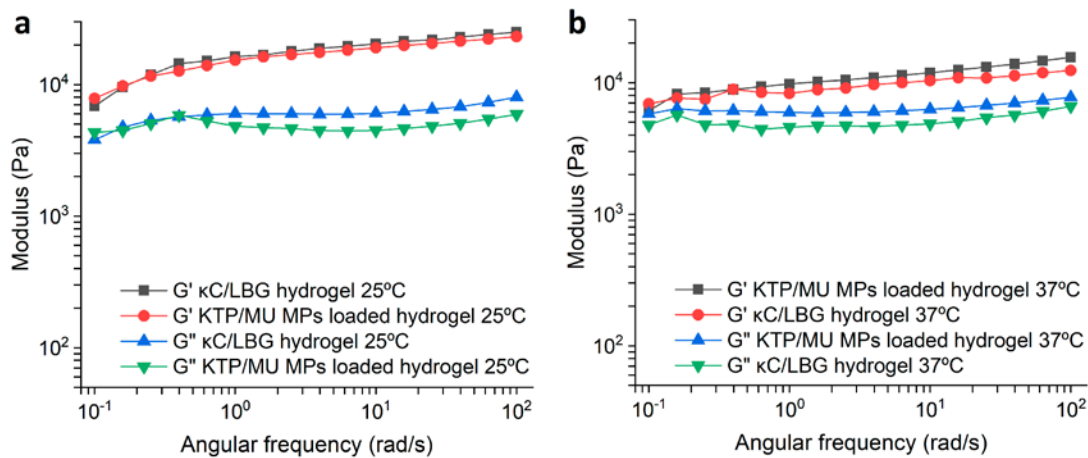


Figure 5.4. Rheological measurements of κCLH and KM-MPs- κCLH at 25 °C (a) and 37 °C (b).

5.3.3. *In vitro* drug release studies

The drug release profiles of both drugs from the microparticles (KM-MPs), the hydrogel (KM-κCLH) and the composite hydrogel (KM-MPs- κCLH) were evaluated at 25 °C and 37 °C (Fig. 5.5). Drug release studies from these different systems were carried out to compare the release profiles and prove that a delivery system combining microparticles and hydrogel (composite hydrogel) allows a slower release than the obtained for each other system separately.

The drug release data for KM-MPs at 25 °C showed that within the first 5 min 79% of ketoprofen and 86% of mupirocin were released and that almost 100% of both drugs were released within 7 h. While at 37 °C, 70% of ketoprofen and 62% mupirocin were released within the first 5 min and 100% of both drugs were released within 4 h (Fig. 5.5a and 5.5b). This rapid initial release rate has been attributed to either non encapsulated drug molecules on the surface of the microparticles or drug molecules that are close to the surface (immersed in the polymer matrix) [2].

The drug release data for KM- κ CLH at 25 °C showed that at 7 h 95% of ketoprofen (Fig. 5.5c) and 100% of mupirocin (Fig. 5.5d) were released. While, at 37 °C it was observed that 95% of both drugs were released at 7 h and 100% were released during 24 h (Fig. 5.5c and 5.5d).

On the other hand, the drug release from the composite hydrogel showed a slower release than the obtained release from the microparticles and the hydrogel. The release profile from the composite hydrogel at 25 °C showed that 90% of ketoprofen and mupirocin was released at 7 h and 100% during 72 h. At 37 °C a slower release was observed, 84% of ketoprofen was released at 7 h, while 76% of mupirocin was released at 7 h. Finally, 100% of both drugs were released during 168 h (Fig. 5.5e and 5.5f). This result indicated that the composite hydrogel at 37 °C can deliver both drugs during 7 days. It was shown that a system based on PHBV microparticles incorporated in the hydrogel allows a release of both drugs slower than the obtained release from the microparticles or the hydrogel. Therefore, the composite hydrogel improved the dual release kinetics of ketoprofen and mupirocin, hydrophobic drugs, used as models.

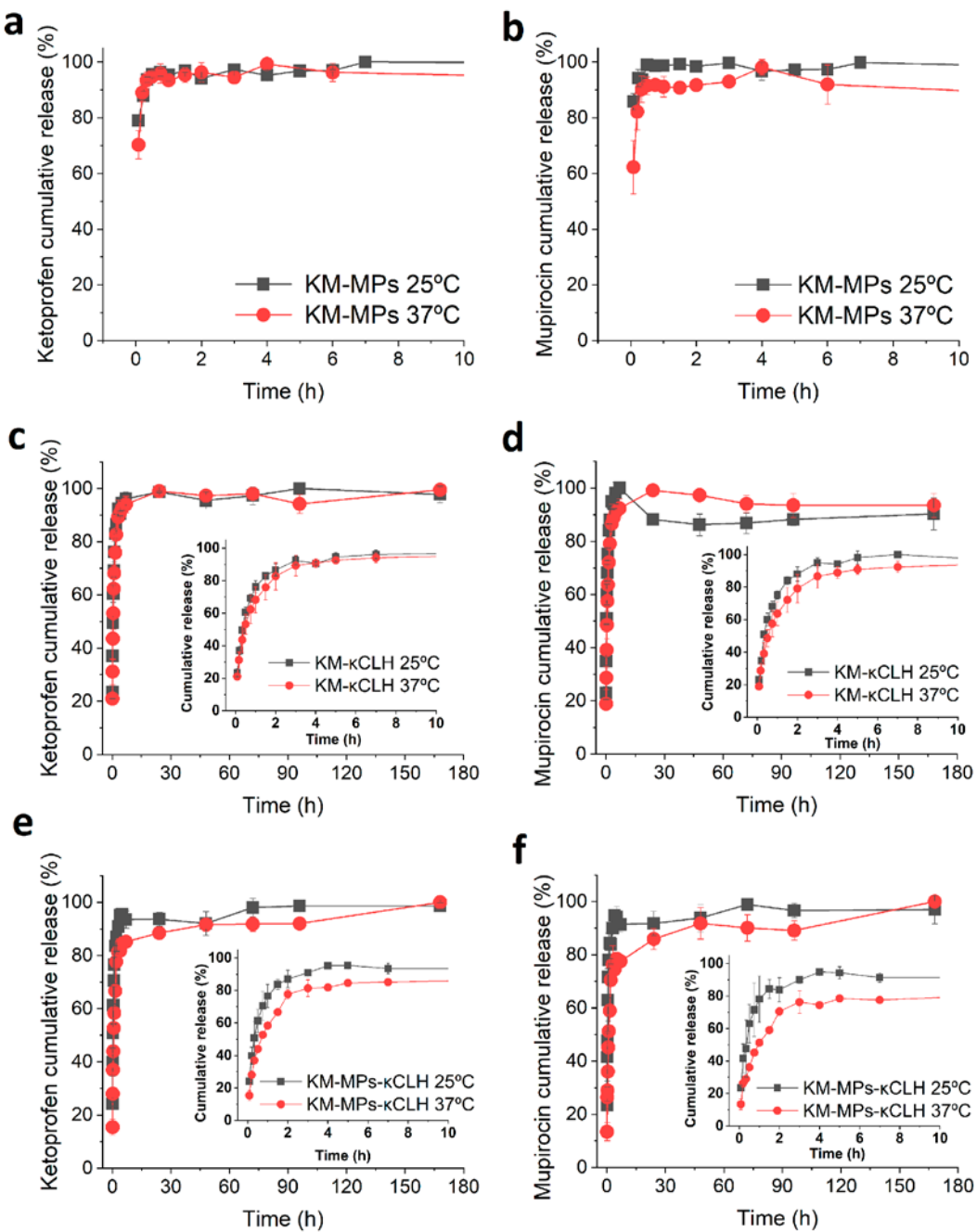


Figure 5.5. Ketoprofen release from microparticles at 25 °C and 37 °C (a), mupirocin release from microparticles at 25 °C and 37 °C (b), ketoprofen release from κ CLH at 25 °C and 37 °C (c), mupirocin release from κ CLH at 25 °C and 37 °C (d), ketoprofen release from KM-MPs- κ CLH at 25 °C and 37 °C (e), mupirocin release from KM-MPs- κ CLH at 25 °C and 37 °C (f).

The most important kinetic mechanisms that regulate the rate of controlled release of a drug are diffusion, swelling and erosion [45]. The drug release mechanism of the composite hydrogel (KM-MPs-κCLH) was analyzed. The cumulative drug release data were fitted to different release models such as first-order kinetics, Higuchi and Korsmeyer-Peppas. The best model was selected according to the highest adjusted coefficient of determination (R^2_{adj}) determined from the linear regression fit for each model [46]. The parameters of the different release models in addition to the coefficient of determination R^2_{adj} from KM-MPs-κCLH at 25 °C and 37 °C are summarized in Table 5.1.

The release of ketoprofen and mupirocin at 25 °C and 37 °C from KM-MPs-κCLH showed the best fitting to a Higuchi model (Eq. 4). In a general way it is possible to resume the Higuchi model to the following expression (generally known as the simplified Higuchi model) [46]:

$$f_t = K_H t^{1/2} \quad (4)$$

where f_t is the released amount of drug in time t , K_H is the Higuchi dissolution constant treated in a different manner by different authors and theories. Higuchi described the drug release as a diffusion process based on Fick's law, square root time dependent [47]. Therefore, the good fitting of the release data to this model suggests that the release of both drugs from KM-MPs-κCLH at 25 °C and 37 °C was mostly controlled by diffusion through the hydrogel matrix. One hypothesis of this model is that swelling and dissolution of the release matrix (the hydrogel network in this case) are negligible [45]. In Table 5.1, it is observed that the swelling of the hydrogels at 37 °C has negligible effect on the release behavior of both drugs according to this model.

For a further verification, the release data of the drugs at 25 °C and 37 °C were fitted to the model of Peppas –Sahlin (Eq.5). This model considers the release kinetics to be affected by two additive mechanisms: Fickian diffusion and case-II relaxation, i.e. the relaxation in hydrophilic polymers which undergo swelling in water [45].

$$C_t/C_\infty = K_1 t^m + K_2 t^{2m} \quad (5)$$

where C_t/C_∞ is the portion of drug release (< 0.6 should only be used) in time t , K_1 and K_2 are the release constants and m is the release exponent. The first term of the right hand of Eq. 5 represents the Fickian diffusion contribution and the second term represents the case-II relaxation contribution to the release process. As it is shown in Table 5.1, the R^2_{adj} values showed very good fitting of the release data to this model too. The K_2 constant that corresponds to the polymer relaxation contribution to the release process is very low in comparison with K_1 at both at 25 °C and 37 °C. This also indicates that the release of both drugs from KM-MPs- κ CLH at 25 °C and 37 °C is dominated mainly by Fickian diffusion as suggested before by the application of the Higuchi model.

Table 5.1. The parameters of the different release models in addition to the coefficient of determination R^2_{adj} at 25 °C and 37 °C from fitting into first-order, Higuchi, Korsmeyer-Peppas and Peppas-Sahlin equations for the composite hydrogel.

Release temperature	Drugs	First-order		Higuchi		Korsmeyer-Peppas		Peppas-Sahlin		
		K_F	R^2_{adj}	K_H	R^2_{adj}	n	R^2_{adj}	K_1	K_2	R^2_{adj}
25°C	Ketoprofen	0.030	0.856	11.280	0.997	0.521	0.995	11.382	0.438	0.989
	Mupirocin	0.028	0.832	11.265	0.978	0.532	0.967	10.826	0.576	0.935
37°C	Ketoprofen	0.013	0.786	7.810	0.988	0.472	0.980	8.773	0.110	0.979
	Mupirocin	0.012	0.722	6.520	0.982	0.499	0.978	7.802	0.020	0.980

5.3.4. Cytotoxicity assays

NIH 3T3 fibroblasts were treated with the different hydrogels to study their effect on cell viability. The cells were cultured on culture plates and then incubated with the presence of unloaded MPs, ketoprofen, mupirocin, 120 mg mL⁻¹ of κ CLH or KM-MPs- κ CLH for 24 h. The MTT viability assay showed that the unloaded MPs decreased cell proliferation vs. control. However, when hydrogels were added at 120 mg mL⁻¹ to the cells, no significant effect on cell proliferation

was observed between KM-MPs- κ CLH and κ CLH. On the other hand, both drugs showed a significant increase on cell viability vs. control (Fig. 5.6a).

Cells were also treated with the extracts obtained from KM-MPs- κ CLH and κ CLH incubation in culture medium for 24 h. NIH 3T3 fibroblasts were treated with 100% - 1.56% dilution of the extracts for 24 h. It must be noted that according to ISO 10993-5 recommendations [48], cells viability higher than 70% assessed by MTT indicates non cytotoxicity for the tested material. As shown in figure 5.6b, the effect on cell viability of 25% - 1.56% extracts treatments of both hydrogels is above this threshold.

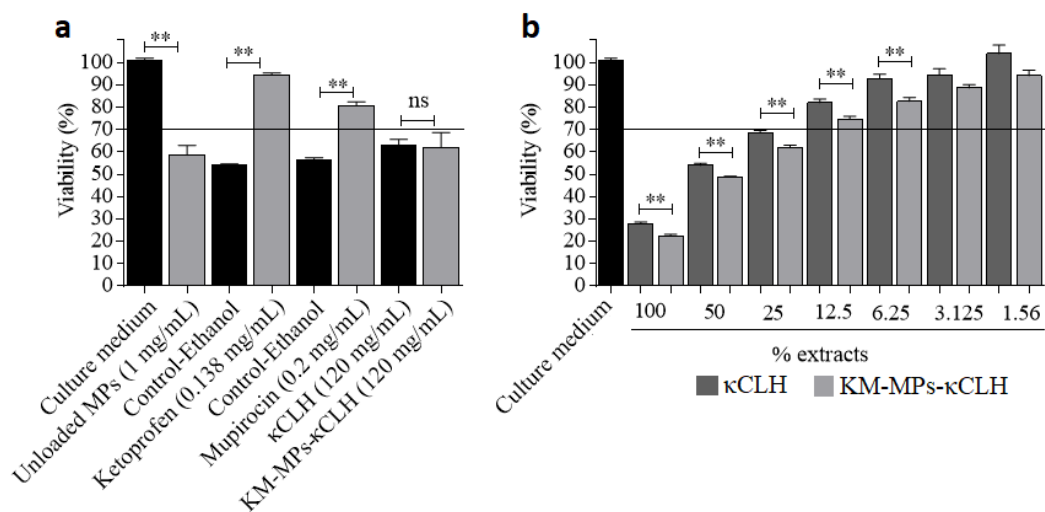


Figure 5.6. MTT assay showing the effect of the treatment for 24 h with unloaded MPs, ketoprofen, mupirocin, κ CLH and KM-MPs- κ CLH (a) and serial dilutions of the hydrogels extracts (b) on NIH 3T3 fibroblast viability. Solid black line highlights the cytotoxicity threshold. N=6. *p<0.05, **p<0.01.

5.4. Conclusion

A novel biocompatible dual drug delivery carrier based on PHBV microparticles loaded in κ -carrageenan/locust bean gum hydrogel able to release simultaneously ketoprofen and mupirocin was prepared. The composite hydrogel improved the dual release kinetics of both drugs showing a slower release than the obtained release from microparticles and hydrogel at

37 °C. The drug release at 37 °C was observed during 7 days. A prolonged release of the drugs was obtained thanks to the system that combines microparticles and hydrogel. The release behavior of the composite hydrogel was well adjusted to a Higuchi kinetic model. Also, this composite hydrogel has thermosensitive swelling behavior, appropriate rheological properties and biocompatibility with fibroblast cells. Therefore, PHBV microparticles loaded in κ -carrageenan/locust bean gum hydrogel can be considered as a potential delivery carrier of poorly water soluble drugs, mainly for wound healing applications.

5.5. References

- [1] D. Zhong, Z. Liu, S. Xie, W. Zhang, Y. Zhang, W. Xue, Study on poly (D, L-lactic) microspheres embedded in calcium alginate hydrogel beads as dual drug delivery systems, *J. Appl. Polym. Sci.* 129 (2013) 767–772. doi:10.1002/app.38797.
- [2] L. Español, A. Larrea, V. Andreu, G. Mendoza, M. Arruebo, V. Sebastian, M.S. Aurora-Prado, E.R.M. Kedor-Hackmann, M.I.R.M. Santoro, J. Santamaria, Dual encapsulation of hydrophobic and hydrophilic drugs in PLGA nanoparticles by a single-step method: drug delivery and cytotoxicity assays, *RSC Adv.* 6 (2016) 111060–111069. doi:10.1039/C6RA23620K.
- [3] T. Khuroo, D. Verma, A. Khuroo, A. Ali, Z. Iqbal, Simultaneous delivery of paclitaxel and erlotinib from dual drug loaded PLGA nanoparticles: Formulation development, thorough optimization and in vitro release, *J. Mol. Liq.* 257 (2018) 52–68. doi:10.1016/j.molliq.2018.02.091.
- [4] H. Nosrati, F. Abhari, J. Charmi, S. Davaran, H. Danafar, Multifunctional nanoparticles from albumin for stimuli-responsive efficient dual drug delivery, *Bioorg. Chem.* 88 (2019) 102959. doi:10.1016/j.bioorg.2019.102959.
- [5] S. Kuttappan, D. Mathew, J. ichiro Jo, R. Tanaka, D. Menon, T. Ishimoto, T. Nakano, S. V. Nair, M.B. Nair, Y. Tabata, Dual release of growth factor from nanocomposite fibrous scaffold promotes vascularisation and bone regeneration in rat critical sized calvarial defect, *Acta Biomater.* 78 (2018) 36–47. doi:10.1016/j.actbio.2018.07.050.
- [6] T.S. Anirudhan, A.M. Mohan, Novel pH sensitive dual drug loaded-gelatin methacrylate/methacrylic acid hydrogel for the controlled release of antibiotics, *Int. J. Biol. Macromol.* 110 (2018) 167–178. doi:10.1016/j.ijbiomac.2018.01.220.
- [7] T.S. Anirudhan, J. Parvathy, A.S. Nair, A novel composite matrix based on polymeric micelle and hydrogel as a drug carrier for the controlled release of dual drugs, *Carbohydr. Polym.* 136 (2016) 1118–1127. doi:10.1016/j.carbpol.2015.10.019.
- [8] F. Wang, Q. Zhang, X. Li, K. Huang, W. Shao, D. Yao, C. Huang, Redox-responsive blend hydrogel films based on carboxymethyl cellulose/chitosan microspheres as dual delivery carrier, *Int. J. Biol. Macromol.* 134 (2019) 413–421. doi:10.1016/j.ijbiomac.2019.05.049.

- [9] L.F. Santos, I.J. Correia, A.S. Silva, J.F. Mano, Biomaterials for drug delivery patches, *Eur. J. Pharm. Sci.* 118 (2018) 49–66. doi:10.1016/j.ejps.2018.03.020.
- [10] N.A. Peppas, Hydrogels and drug delivery, *Curr. Opin. Colloid Interface Sci.* 2 (1997) 531–537. doi:10.1016/S1359-0294(97)80103-3.
- [11] S. Merino, C. Martin, K. Kostarelos, M. Prato, E. Vazquez, Nanocomposite Hydrogels: 3D Polymer-Nanoparticle Synergies for On-Demand Drug Delivery, *ACS Nano.* 9 (2015) 4686–4697. doi:10.1021/acsnano.5b01433.
- [12] F. Zhao, D. Yao, R. Guo, L. Deng, A. Dong, J. Zhang, Composites of polymer hydrogels and nanoparticulate systems for biomedical and pharmaceutical applications, *Nanomaterials.* 5 (2015) 2054–2130. doi:10.3390/nano5042054.
- [13] D. Gu, A.J. O'Connor, G. G.H. Qiao, K. Ladewig, Hydrogels with smart systems for delivery of hydrophobic drugs, *Expert Opin. Drug Deliv.* 14 (2017) 879–895. doi:10.1080/17425247.2017.1245290.
- [14] P. Thoniyot, M.J. Tan, A.A. Karim, D.J. Young, X.J. Loh, Nanoparticle–hydrogel composites: concept, design, and applications of these promising, multi-functional materials, *Adv. Sci.* 2 (2015) 1–13. doi:10.1002/advs.201400010.
- [15] S. Perumal, S.K. Ramadass, B. Madhan, Sol-gel processed mupirocin silica microspheres loaded collagen scaffold: A synergistic bio-composite for wound healing, *Eur. J. Pharm. Sci.* 52 (2014) 26–33. doi:10.1016/j.ejps.2013.10.006.
- [16] D.P. Pacheco, M.H. Amaral, R.L. Reis, A.P. Marques, V.M. Correlo, Development of an injectable PHBV microparticles-GG hydrogel hybrid system for regenerative medicine, *Int. J. Pharm.* 478 (2015) 398–408. doi:10.1016/j.ijpharm.2014.11.036.
- [17] S. Van Vlierberghe, P. Dubrule, E. Schacht, Biopolymer-based hydrogels as scaffolds for tissue engineering applications: A review, *Biomacromolecules.* 12 (2011) 1387–1408. doi:10.1021/bm200083n.
- [18] A. Basu, K.R. Kunduru, E. Abtew, A.J. Domb, Polysaccharide-based conjugates for biomedical applications, *Bioconjug. Chem.* 26 (2015) 1396–1412. doi:10.1021/acs.bioconjchem.5b00242.

- [19] L. Neufeld, H. Bianco-Peled, Pectin–chitosan physical hydrogels as potential drug delivery vehicles, *Int. J. Biol. Macromol.* 101 (2017) 852–861. doi:10.1016/j.ijbiomac.2017.03.167.
- [20] R. Yegappan, V. Selvapritchiviraj, S. Amirthalingam, R. Jayakumar, Carrageenan based hydrogels for drug delivery , tissue engineering and wound healing, *Carbohydr. Polym.* 198 (2018) 385–400. doi:10.1016/j.carbpol.2018.06.086.
- [21] L. Li, R. Ni, Y. Shao, S. Mao, Carrageenan and its applications in drug delivery, *Carbohydr. Polym.* 103 (2014) 1–11. doi:10.1016/j.carbpol.2013.12.008.
- [22] J. Liu, X. Zhan, J. Wan, Y. Wang, C. Wang, Review for carrageenan-based pharmaceutical biomaterials : Favourable physical features versus adverse biological effects, *Carbohydr. Polym.* 121 (2015) 27–36. doi:10.1016/j.carbpol.2014.11.063.
- [23] V.L. Campo, D.F. Kawano, D.B. da Silva, I. Carvalho, Carrageenans: Biological properties, chemical modifications and structural analysis - A review, *Carbohydr. Polym.* 77 (2009) 167–180. doi:10.1016/j.carbpol.2009.01.020.
- [24] S. Barak, D. Mudgil, Locust bean gum : Processing , properties and food applications — A review, *Int. J. Biol. Macromol.* 66 (2014) 74–80. doi:10.1016/j.ijbiomac.2014.02.017.
- [25] M. Souza, K. Modolon, J. Maia, F. Dal, P. Morisso, M. Marques, L. Alberto, One-pot synthesis of gold nanoparticles embedded in polysaccharide-based hydrogel : Physical-chemical characterization and feasibility for large-scale production, *Int. J. Biol. Macromol.* 124 (2019) 838–845. doi:10.1016/j.ijbiomac.2018.11.231.
- [26] K.M. Zepon, M.M. Martins, M.S. Marques, J.M. Heckler, F.D.P. Morisso, M.G. Moreira, A.L. Ziulkoski, L.A. Kanis, F. Dal Pont Morisso, M.G. Moreira, A.L. Ziulkoski, L.A. Kanis, Smart wound dressing based on κ -carrageenan/locust bean gum/cranberry extract for monitoring bacterial infections, *Carbohydr. Polym.* 206 (2019) 362–370. doi:S014486171831347X.
- [27] B.S. Thorat Gadgil, N. Killi, G.V.N. Rathna, Polyhydroxyalkanoates as biomaterials, *Med. Chem. Commun.* 8 (2017) 1774–1787. doi:10.1039/C7MD00252A.
- [28] G. Barouti, C.G. Jaffredo, S.M. Guillaume, Advances in drug delivery systems based on synthetic poly(hydroxybutyrate) (co)polymers, *Prog. Polym. Sci.* 73 (2017) 1–31. doi:10.1016/j.progpolymsci.2017.05.002.

- [29] L. Álvarez-Álvarez, L. Barral, R. Bouza, Y. Farrag, F. Otero-Espinar, S. Feijóo-Bandín, F. Lago, Hydrocortisone loaded poly-(3-hydroxybutyrate-co-3-hydroxyvalerate) nanoparticles for topical ophthalmic administration: Preparation, characterization and evaluation of ophthalmic toxicity, *Int. J. Pharm.* 568 (2019) 118519. doi:10.1016/j.ijpharm.2019.118519.
- [30] Y. Farrag, B. Montero, M. Rico, L. Barral, R. Bouza, Preparation and characterization of nano and micro particles of poly (3-hydroxybutyrate-co-3-hydroxyvalerate) (PHBV) via emulsification / solvent evaporation and nanoprecipitation techniques, *J. Nanoparticle Res.* 20 (2018). doi.org/10.1007/s11051-018-4177-7.
- [31] Z. Naghizadeh, A. Karkhaneh, A. Khojasteh, Simultaneous release of melatonin and methylprednisolone from an injectable in situ self-crosslinked hydrogel/microparticle system for cartilage tissue engineering, *J. Biomed. Mater. Res. - Part A.* 106 (2018) 1932–1940. doi:10.1002/jbm.a.36401.
- [32] C. Siangsanoh, S. Ummartyotin, K. Sathirakul, P. Rojanapanthu, W. Treesuppharat, Fabrication and characterization of triple-responsive composite hydrogel for targeted and controlled drug delivery system, *J. Mol. Liq.* 256 (2018) 90–99. doi:10.1016/j.molliq.2018.02.026.
- [33] G. Rezvan, G. Pircheraghi, R. Bagheri, Curcumin incorporated PVA-borax dual delivery hydrogels as potential wound dressing materials — Correlation between viscoelastic properties and curcumin release rate, *J. Appl. Polym. Sci.* 135 (2018) 46734. doi:10.1002/app.46734.
- [34] Y. Zhang, M. Huo, J. Zhou, A. Zou, W. Li, C. Yao, S. Xie, DDSolver: an add-in program for modeling and comparison of drug dissolution profiles, *AAPS J.* 12 (2010) 263–271. doi:10.1208/s12248-010-9185-1.
- [35] D. Jeong, S.W. Joo, Y. Hu, V.V. Shinde, E. Cho, S. Jung, Carboxymethyl cellulose-based superabsorbent hydrogels containing carboxymethyl β-cyclodextrin for enhanced mechanical strength and effective drug delivery, *Eur. Polym. J.* 105 (2018) 17–25. doi:10.1016/j.eurpolymj.2018.05.023.
- [36] T.L. Riss, R.A. Moravec, A.L. Niles, S. Duellman, H.A. Benink, T.J. Worzella, L. Minor, Cell viability assays, *Assay Guid. Man.* 740 (2004) 33–43. doi:10.1007/978-1-61779-108-6_6.
- [37] A. Budhian, S.J. Siegel, K.I. Winey, Haloperidol-loaded PLGA nanoparticles: Systematic study of particle size and drug content, *Int. J. Pharm.* 336 (2007) 367–375. doi:10.1016/j.ijpharm.2006.11.061.

- [38] F. Masood, P. Chen, T. Yasin, N. Fatima, F. Hasan, A. Hameed, Encapsulation of ellipticine in poly- (3-hydroxybutyrate-co-3-hydroxyvalerate) based nanoparticles and its in vitro application, *Mater. Sci. Eng. C*. 33 (2013) 1054–1060. doi:10.1016/j.msec.2012.11.025.
- [39] K.S.W. Sing, Reporting physisorption data for gas/solid systems with special reference to the determination of surface area and porosity (Recommendations 1984), *Pure Appl. Chem.* 57 (1985) 603–619. doi:10.1351/pac198557040603.
- [40] M.I.Z. Lionzo, M.I. Ré, S.S. Guterres, A.R. Pohlmann, Microparticles prepared with poly(hydroxybutyrate-co-hydroxyvalerate) and poly(ϵ -caprolactone) blends to control the release of a drug model, *J. Microencapsul.* 24 (2007) 175–186. doi:10.1080/02652040701233556.
- [41] F.S. Poletto, E. Jäger, M.I. Ré, S.S. Guterres, A.R. Pohlmann, Rate-modulating PHBV/PCL microparticles containing weak acid model drugs, *Int. J. Pharm.* 345 (2007) 70–80. doi:10.1016/j.ijpharm.2007.05.040.
- [42] N.A. Peppas, P. Bures, W. Leobandung, H. Ichikawa, Hydrogels in pharmaceutical formulations, *Eur. J. Pharm. Biopharm.* 50 (2000) 27–46. doi:10.1016/S0939-6411(00)00090-4.
- [43] C. Yan, D.J. Pochan, Rheological properties of peptide-based hydrogels for biomedical and other applications, *Chem. Soc. Rev.* 39 (2010) 3528–3540. doi:10.1039/b919449p.
- [44] H. Chen, X. Xing, H. Tan, Y. Jia, T. Zhou, Y. Chen, Z. Ling, X. Hu, Covalently antibacterial alginate-chitosan hydrogel dressing integrated gelatin microspheres containing tetracycline hydrochloride for wound healing, *Mater. Sci. Eng. C*. 70 (2017) 287–295. doi:10.1016/j.msec.2016.08.086.
- [45] H.K. Shaikh, R. V Kshirsagar, S.G. Patil, Mathematical models for drug release characterization: A review, *World J. Pharm. Pharm. Sci.* 4 (2015) 324–338.
- [46] J.M.S. Costa, P., & Lobo, Modelling and comparison of dissolution profiles, *Eur. J. Pharm. Sci.* 13 (2001) 123–133. doi:10.1016/S0928-0987(01)00095-1.
- [47] Higuchi T, Rate of release of medicaments from ointment bases containing drugs in suspension., *J. Pharm. Sci.* 50 (1961) 874–875.
- [48] International Organization for Standardization, ISO 10993-5 . Biological evaluation of medical devices. Part 5: Tests for in vitro cytotoxicity. Geneva, Switzerland, 2009.

CAPÍTULO 6: Carrageenan-based physically crosslinked injectable hydrogel for wound healing and tissue repairing applications.

6.1. Introduction

Hydrogels are three-dimensional, hydrophilic polymer networks that are able to absorb and retain a large amount of water or biological fluids within their structure without dissolving [1].

Hydrogels are promising alternative for a wide range of biomedical applications owing to their biocompatibility, excellent permeability for transport of nutrients and metabolites, and similarity to native extracellular matrix [2].

Over the past decades, injectable hydrogels have attracted special attention because their application is minimally invasive eliminating the need for complicated surgical procedures and their ability to form a desired shape which allows cavities or defects in the body to be completely filled. They can reduce patient discomfort, recovery time, and the risk of infection [3]. Especially, injectable hydrogels are commonly applied for tissue engineering, wound dressing and healing and treating injuries or disease which are practically difficult to access [4]. Furthermore, injectable hydrogels can be useful vehicles for the localized delivery of cells, growth factors, and other molecules improving their retention at the injection site [5]. Injectable hydrogels are extremely useful for growth factor delivery since they protect them from degradation in the harsh environment of the wounds. Additionally, the delivery of the growth factor is localized and the biomaterial can provide a structural support for the cells to migrate and facilitate tissue regeneration [6].

An injectable hydrogel needs to satisfy certain requirements for its biomedical application. These requirements include that the injectable solution must flow under modest pressure, set rapidly at the target site and to maintain sufficient integrity and strength as required. Also, the hydrogel components need to be biocompatible with minimal cytotoxicity. Finally, the hydrogel should have controlled biodegradability [7]. Hydrogels based on natural biopolymers such as polysaccharides and polypeptides allow these requirements to be satisfied due to their low immunogenicity, high biocompatibility and susceptibility to degradation by human enzymes or

by hydrolysis. Also, they have the potential to lead the migration, growth, and organization of cells [4,8].

Among natural biopolymers, carrageenan is currently an ideal candidate in tissue engineering, wound healing and drug delivery applications [9]. Carrageenan is a linear, sulfated, hydrophilic polysaccharide, consisting of disaccharide repeat units of galactose and (3,6)-anhydrogalactose connected by alternating α -(1,3)- and β -(1,4)-glycosidic links [10]. There are different types of carrageenan, of which κ -carrageenan (kappa) in presence of potassium ions and ι -carrageenan (iota) with calcium ions form thermoreversible gels. κ -carrageenan forms strong rigid gels while elastic, dry, soft gels are produced by the ι -carrageenan [11]. It has been reported that the stiffness of the mixed iota/kappa gels is much higher than the sum of the corresponding individual gels [12]. The thixotropic behavior of κ -carrageenan makes it suitable for injectable hydrogels for cell delivery and inclusion of other macromolecules [8]. Carrageenan hydrogels can be combined with other polymers or molecules to improve the properties of a hydrogel under physiological conditions. For instance, the addition of kappa and iota carrageenan to hyaluronic acid/fibrin injectable hydrogel to improve the elasticity and stiffness [13], 2D nanosilicate reinforced κ -carrageenan injectable hydrogel to enhance cell adhesion for wound healing and tissue regeneration [14] and an injectable ι -carrageenan hydrogel with whitlockite to promoted osteogenesis and angiogenesis *in vitro* [15]. Locust bean gum shows a synergistic effect with κ -carrageenan and forms a gel with more elasticity and strength [16]. In our previous work, κ -carrageenan/locust bean gum hydrogel loaded with PHBV microparticles was prepared for drug delivery [17].

Another natural biopolymer that has been combined with carrageenan is gelatin. Both are capable of forming thermoreversible hydrogels through coil/helix conformational transitions [18]. Gelatin is a protein obtained from the acidic or alkaline denaturation of collagen [19]. Gelatin lacks significant mechanical strength and is subject to rapid enzymatic degradation which is commonly overcome by chemical or physical crosslinking [20]. A synergistic effect has

been observed in mixtures with κ -carrageenan for potential use in adipose tissue [21]. It was reported that in carrageenan/gelatin hydrogels an increase in carrageenan content increased the mechanical strength [22] and the hydrogels are flexible and porous having high water retention capacity [23].

The aim of this study was the development of a novel injectable hydrogel using natural biopolymers physically crosslinked for wound healing and tissue repairing. The main requirements that were considered for the design of the injectable hydrogel were mechanical stability, biocompatibility, suitability for the delivery of a growth factor and also to provide mechanical support to the cells. The biopolymers selected to prepare the injectable hydrogel were kappa and iota carrageenan, locust bean gum and gelatin. The ability to provide a structural support for the cells and promote *in vitro* wound healing were evaluated in fibroblasts and human umbilical vein endothelial cells. Also, the physical interactions, surface morphologies, swelling behavior, physiological stability and mechanical properties of the prepared hydrogel were analyzed to determine their potential characteristics for wound healing and tissue repairing.

6.2. Materials and methods

6.2.1. Materials

The κ -carrageenan (κ C) (MW= aprox. 500 kDa, low viscosity, as provided by the supplier), ι -carrageenan (ι C) (MW= 300 kDa, low viscosity, as provided by the supplier) and locust bean gum (LB) (viscosity 3500 cps, 25 °C, as provided by the supplier) were kindly gifted by Ceamsa, Spain. Gelatin (G) was obtained from Difco, USA (Ref.214320). Potassium chloride and calcium chloride were of analytical grade and purchased from Scharlau, Spain. All chemicals were used without further purification. The water used in the preparation and the dialysis was purified in a Milli-Q ultrapure system (Millipore, France).

6.2.2. Preparation of hydrogel

A stock solution of 2% w/v of ι C was prepared by dissolving 1 g of ι -carrageenan in 50 mL of deionized water and stirred for 30 min at 60°C. A stock solution of 1% w/v of κ C:LB was prepared by dissolving 0.167 g of LB in 50 mL of deionized water at 70°C with stirring and then, 0.5 g of κ -carrageenan was added and heated at 70 °C about 30 min until completely dissolved. Also, 1% w/v of κ C solution was prepared by dissolving 0.5 g of κ -carrageenan in 50 mL of deionized water and stirred for 30 min at 70 °C. A stock solution of 1% w/v of gelatin was prepared by dissolving 0.5 g of gelatin in 50 mL of deionized water and stirred for 30 min at 50 °C. Then, for the preparation of the injectable hydrogel (CAR:LB:G) were mixed 6 mL of κ C:LB solution, 3 mL of ι C solution and 1 mL gelatin solution with magnetic stirring at 50°C. Afterwards, 300 μ L KCl 0.5 M and 150 μ L CaCl₂ 0.5 M were added to the mixed solution to promote gelation of the carrageenan-based injectable hydrogel. The mixture was left at room temperature during approximately 1 h, allowing the formation of the gel. In addition, the following mixtures were prepared as blank control: 5 mL of ι C solution and 5 mL of κ C solution (CAR) and, 5 mL of ι C solution and κ C:LB solution (CAR:LB). For each solution, 225 μ L KCl 0.5 M and 150 μ L CaCl₂ 0.5 M were added.

6.2.3. Characterization

6.2.3.1. Attenuated total reflectance ATR-FTIR spectroscopy

The ATR-FTIR spectroscopy was performed for the freeze-dried hydrogels and pure compounds to analyze the physical interactions. The ATR-FTIR spectra of samples were recorded in a FTIR spectrophotometer (Jasco FT/IR-4700, Japan) using an ATR technique by averaging the signals of 64 scans at a resolution of 4 cm⁻¹ in the range from 4000 cm⁻¹ to 600 cm⁻¹.

6.2.3.2. Field emission scanning electron microscopy (FESEM)

To evaluate the surface morphological structure, the swollen hydrogels were sputter-coated with platinum/palladium using a Cressington 208HR High Resolution sputter coater (Cressington

Scientific Instruments, UK). The surface morphology was observed using a field emission scanning electron microscope JSM 7200F (Jeol, USA) at an acceleration voltage of 10 kV and 15 kV.

6.2.3.3. Swelling behavior

The swelling behaviors of hydrogels were determined by immersing the weighed lyophilized hydrogels in PBS at 37 °C under static conditions. The swollen hydrogels were weighed daily after removing the water until equilibrium was reached. The equilibrium swelling ratio (SR) was calculated by the Eq. 1 [15]:

$$SR (\%) = (W_s - W_i/W_i) \times 100 \quad (1)$$

where W_s is the weight of swollen hydrogel and W_i is the initial weight of lyophilized hydrogel.

6.2.3.4. Physiological stability

To determine the degradation of the hydrogels, hydrogel samples were prepared and freeze-dried. Then, each hydrogel was weighed and placed in PBS solution at 37 °C under static conditions. These hydrogels were removed, freeze dried and weighed again at 24 h, 48 h, 72 h and 7 days of incubation to determine the final dry weight. The weight loss of the samples was calculated by the Eq. 2 [24]:

$$Weight loss (\%) = (W_i - W_f/W_i) \times 100 \quad (2)$$

where W_i and W_f are the dried weights of the hydrogels before and after the incubation in the PBS solution, respectively.

6.2.3.5. Rheological properties

Rheological characterization was performed for the hydrogels using a rheometer Ares (TA Instruments, USA) in a parallel plate geometry (diameter 25 mm) cell with a gap between plates of 1 mm. All the hydrogel samples were cut in a cylindrical shape. The elastic modulus (G') and

viscous modulus (G'') over a frequency range of $0.1\text{-}100 \text{ rad s}^{-1}$ were recorded at a constant strain of 1%, which were in the linear range of the viscosity. All measurements were carried out in triplicate for each sample at 25°C .

To evaluate the smoothness and injectability visually, CAR:LB:G hydrogel was loaded into 10 mL syringe with 21G needle and injected by hand [15].

6.2.4. Cell assays

6.2.4.1. Cell cultures

All the procedures were approved by the Ethics Committee for Clinical Research at Galicia (Spain), according to the World Medical Association Declaration of Helsinki.

The American Type Culture Collection (ATCC) 3T3-L1 fibroblasts were a gift from Dr. Oreste Gualillo (Health Institute of Biomedical Research, Santiago de Compostela, Spain). 3T3-L1 fibroblast were cultured in high glucose (4.5 g L^{-1}) Dulbecco's modified eagle medium (DMEM) (Lonza Group Ltd, CH) supplemented with 10% heat-inactivated fetal bovine serum (FBS) (Merck KGaA, DE), 2% penicillin/streptomycin antibiotics and 2% L-glutamine (Sigma-Aldrich, USA) at 37°C and 5% CO_2 .

Human Umbilical Vein Endothelial Cells (HUVECs) were a gift from Dr. Ezequiel Álvarez (Health Institute of Biomedical Research, Santiago de Compostela, Spain). Briefly, HUVECs were isolated from freshly obtained human umbilical cords donated under informed consent from mothers and following the method previously described [25]. HUVECs were cultured on 0.2% (w/v) gelatin (Sigma-Aldrich, USA) pre-coated dishes and grown in complete endothelial growth medium (EGM-2) (Lonza Group Ltd, CH) in a humidity-saturated atmosphere with 5% CO_2 at 37°C . Before the experiments, cells were starved in endothelial basal medium (EBM-2) (Lonza Group Ltd, CH) for 3 h. Cells for the experiments were used between the second and seventh passage.

6.2.4.2. MTT viability assay

Toxicity of the hydrogels was determined using the 3-(4,5-dimethylthiazol-2-yl)-2,5-diphenyltetrazolium bromide (MTT) cell viability assay. MTT is a yellow compound that when reduced by functioning mitochondria, produces purple formazan crystals that can be measured spectrophotometrically. The quantity of formazan is directly proportional to the number of viable cells and their metabolic activity [26]. For this purpose, the hydrogels were prepared under sterile conditions in 96 well plates, and 3T3-L1 fibroblasts were seeded on the hydrogels at a density of 1×10^6 cells/well and cultured for 16 h. MTT 0.5 mg mL⁻¹ (Sigma-Aldrich, USA) was added 4 h before the expiry of this period. After overnight incubation at 37 °C with 10% SDS + 0.08% HCl, absorbance at 550 nm was measured in a microplate reader (MultiscanEX, Thermo Fisher Scientific, USA).

6.2.4.3. Cell adhesion

Hydrogels were prepared in a thin monolayer on 35 mm dishes with glass bottom (Ibidi, DE). 3T3-L1 fibroblasts were seeded at a density of 7×10^5 cells/dish on the hydrogel and allowed to adhere for 48 h. Cells were simultaneously stained with 40 µg mL⁻¹ propidium iodide (Sigma-Aldrich, USA) and with 55 µg mL⁻¹ calcein-AM (Invitrogen, USA) to identify dead and viable cells, respectively. Images were taken using the confocal microscope Leica TCS SP8 MP (Leica Microsystems AG, DE).

6.2.4.4. In vitro scratch wound assay

HUVECs were cultured in 24 well plates until confluence. A thin "wound" was manually made by scratching with a sterile 200 µL micropipette tip to create a straight-edged, cell-free zone across the cell monolayer and, subsequently, wells were washed with EBM-2 to remove cell debris. To perform the assay, cells were cultured in EGM-2 medium lacking vascular endothelial growth factor (VEGF) (Lonza Group Ltd, CH). Hydrogels entrapping VEGF (Thermo Fisher Scientific, USA) to a final concentration of 50 ng mL⁻¹ prepared in transwell inserts were added to the 24 well

plates (VWR International, USA). EGM-2 medium lacking VEGF and supplemented with 50 ng mL⁻¹

¹ VEGF (Thermo Fisher Scientific, USA) was used as positive control. Microscope images were taken at 0 h and 24 h using the inverted phase contrast microscope Leica DMi1 with a Leica MC170 HD camera (Leica Microsystems AG, DE). The scratch closure rate (%) was calculated by the Eq.3 [27]:

$$\text{Scratch closure rate (\%)} = (A_0 - A_t / A_0) \times 100 \quad (3)$$

where A_0 and A_t are the scratch area at 0 h and 24 h, respectively. The scratch area was calculated using ImageJ software.

6.2.4.5. Statistical analysis

All experimental data were obtained from six independent experiments. Data were expressed as mean \pm standard error of the mean. Statistical analysis was performed using the Mann-Whitney U test as implemented in Prism 5 (GraphPad Software Inc., USA).

6.3. Results and discussion

6.3.1. Physical interactions and surface morphologies characterization

In the present study an injectable hydrogel was prepared by the mixing of carrageenans, locust bean gum and gelatin solutions followed by an ionic crosslinking through KCl and CaCl₂. Carrageenan forms a thermoreversible gel in aqueous solution by a transition from a random coil to a helical conformation followed by aggregation of the helices to form a network [28]. Thus, the coil-helix transition is induced by cooling of the solution in the presence of cations; potassium chloride promotes gel formation of κC and calcium ion promotes gel formation of ιC [29]. Interaction of cations with carrageenan sulphate groups reduces electrostatic repulsions between the polysaccharide chains, which allow the chains to adopt double helix conformations

resulting in gel formation [10]. A strong synergy was observed between the two types of carrageenans and it has been suggested that the mixtures formed homogeneously interpenetrated or interconnected networks [12]. On the other hand, locust bean gum shows a synergistic effect with κ -carrageenan and forms a gel with more elasticity and strength. It was suggested that LB interferes with the gel structure by the formation of a secondary network [30]. Finally, gelatin with abundant amino groups forms polyelectrolyte complexes with carrageenan via electrostatic interactions [31]. Hydrophobic interactions, electrostatic interactions and hydrogen bonds play a defining role in complex formation [32]. Gelatin chains in helical and coil form could connect the double helices of carrageenan and stabilize the carrageenan network [18,33].

The physical interactions of injectable hydrogels were characterized using FTIR analysis and the obtained spectra are shown in Fig. 6.1. Characteristic bands of the carrageenans and LB were observed in the region between 1300 cm^{-1} and 800 cm^{-1} , that is, within the so-called carbohydrate fingerprint region, where the position and intensity of the bands are specific for every polysaccharide [34] (more details in Supplementary material Fig. S.6.1). The FT-IR spectra of the carrageenans show a typical absorption bands at 1222 cm^{-1} that is attributed to the ester sulphate groups (O=S=O). The bands at $842\text{-}844\text{ cm}^{-1}$ are assigned to the galactose-4-sulfate (C-O-S), at $924\text{-}927\text{ cm}^{-1}$ for 3,6-anhydrogalactose (C-O-C) and at $1024\text{-}1034\text{ cm}^{-1}$ for glycoside bands of saccharide moiety [35,36]. For the gelatin, characteristic bands of protein were observed at 1626 cm^{-1} for the amide, at 1525 cm^{-1} for the amide II and 1235 cm^{-1} for the amide III [21,37]. The spectra of CAR:LB:G hydrogel showed the bands between 1300 cm^{-1} and 800 cm^{-1} due to the presence of carrageenans. In addition, the band corresponding to the ester sulphate groups from carrageenan also shifted from 1222 cm^{-1} to 1226 cm^{-1} in CAR:LB:G indicating the interaction between the biopolymers. Furthermore, the bands of the amide I at 1644 cm^{-1} and amide II at 1556 cm^{-1} in CAR:LB:G shifted to higher wavelengths compared with

the gelatin spectra. These shifts suggest the interaction between carrageenans and gelatin with formation of polyelectrolyte complexes [37,38].

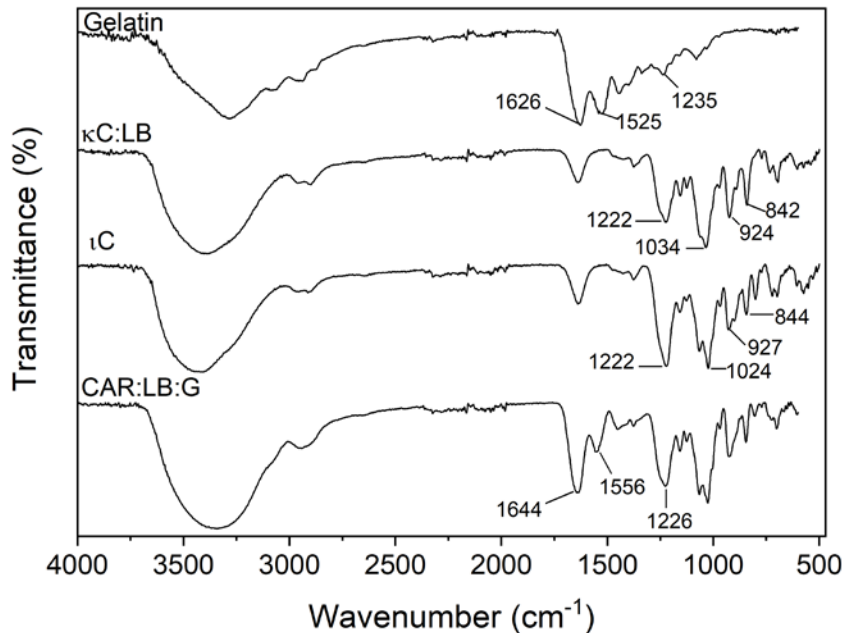


Figure 6.1. FTIR spectra of gelatin, κ C:LB, ι C and CAR:LB:G hydrogel.

The surface morphological properties of the CAR, CAR:LB and CAR:LB:G hydrogels were examined by FESEM and the surface and cross section surface images are shown in Fig. 6.2. CAR and CAR:LB hydrogels showed a non-uniform and irregular surface with some porous structures (Fig. 6.2a and 6.2c). While, the cross section surface was similar in both hydrogels with a non-porous and irregular surface (Fig. 6.2b and 6.2d). On the other hand, CAR:LB:G hydrogel showed different surface and cross-section morphologies. The irregular morphologies were characterized by membrane-like structure, namely a porous network (Fig. 6.2e and 6.2f). Hence, the incorporation of gelatin produced changes in the surface morphology of hydrogel promoting the formation of pores. It has been reported that combination of gelatin and carrageenan forms porous hydrogels with a three dimensional interconnected microstructure and the ratio gelatin-carrageenan influences the porosity of the hydrogels [33]. Pore formation may be due to an

increase in the repulsive forces between amino group, carboxyl groups, hydroxyl groups of gelatin and carrageenan, as reported for a silk fibroin / kappa -carrageenan composite [39]. The 3D structure and pores is fundamental for providing enough space for cell migration, vascularization and allowing the diffusion of nutrients, metabolites and wastes [20].

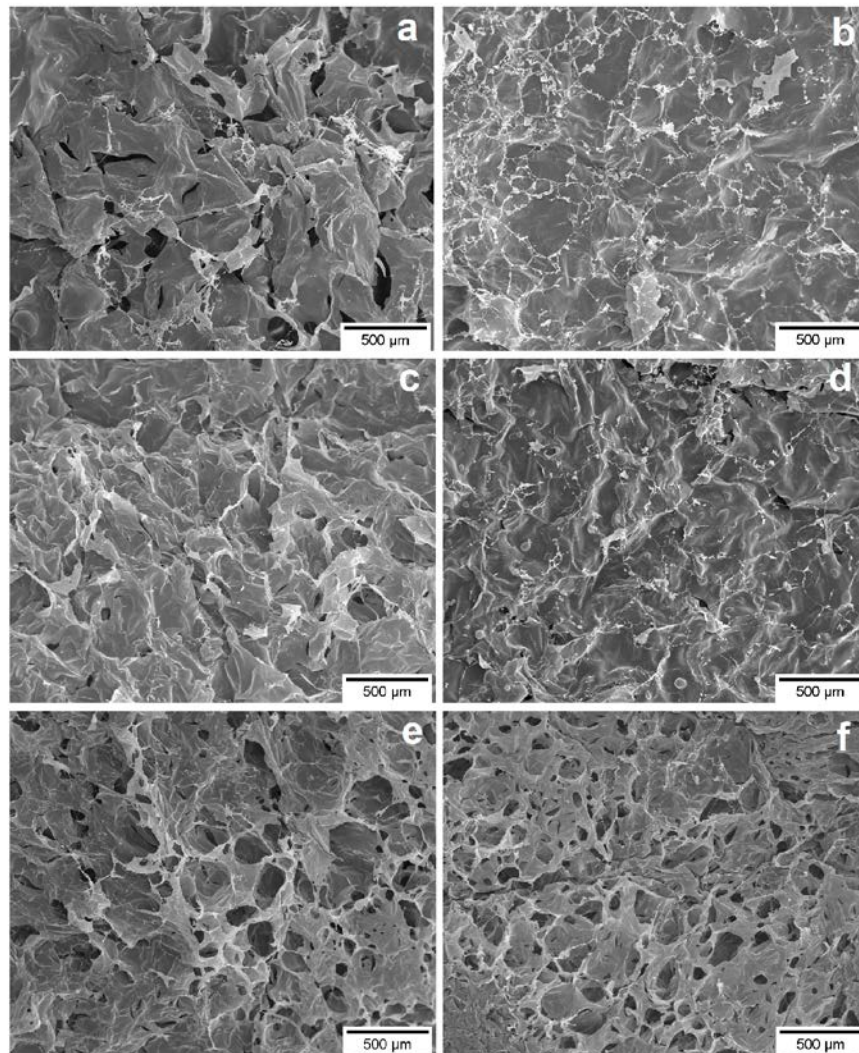


Figure 6.2. FESEM images of surface of the CAR (a), CAR:LB (c) and CAR:LB:G (e) hydrogels, and cross section surface of the CAR (b), CAR:LB (d) and CAR:LB:G (f) hydrogels.

6.3.2. Swelling behavior and physiological stability

The swelling behaviors of the injectable hydrogel (CAR:LB:G) and control hydrogels (CAR:LB and CAR) were evaluated at 37 °C in PBS solution. The obtained results of SR indicated that all hydrogels were able to absorb large quantities of water. The hydrogels showed SR of 5397% ± 284%, 6247% ± 310% and 5131% ± 335% for CAR, CAR:LB and CAR:LB:G, respectively. The SR of CAR:LB:G was slightly lower, this may be due to an increase of ionic crosslinking within the network. Whereas, CAR and CAR:LB have a higher carrageenan content which produces an increase in electrostatic repulsion between sulfate groups. The swelling capacity is provided by the interactions through hydrogen bonds between water molecules with the amino groups, carboxyl groups, hydroxyl groups of gelatin and polysaccharides [40]. Besides, the addition of LB in mixtures with κC is highly effective in reducing syneresis which allows a high water holding capacity [29]. The high water-holding capacity is useful for the transport of nutrients, products or bioactive agents, such as growth factors [19].

The physiological stability of hydrogels was evaluated by incubating the samples in PBS solution at 37 °C. The three hydrogel compositions showed similar weight loss within 48 h. At the end of 7 days, CAR:LB:G and CAR hydrogels evidenced about 60% degradation (Fig. 6.3). Therefore, the addition of LB to the CAR hydrogel led to a slower weight loss, but at the same time the addition of gelatin increases the degradation. Other degradation rates of previously reported carrageenan-based hydrogels physically cross-linked are about 20% weight loss in 72 h for κC/nanosilicates hydrogels [14] and approximately 40% weight loss in 7 days for iC/whitlockite nanoparticles composite [15]. Biodegradation of biopolymers involves the action of enzymes, microorganisms and pH action, entailing complex biological, physical and chemical processes [30].

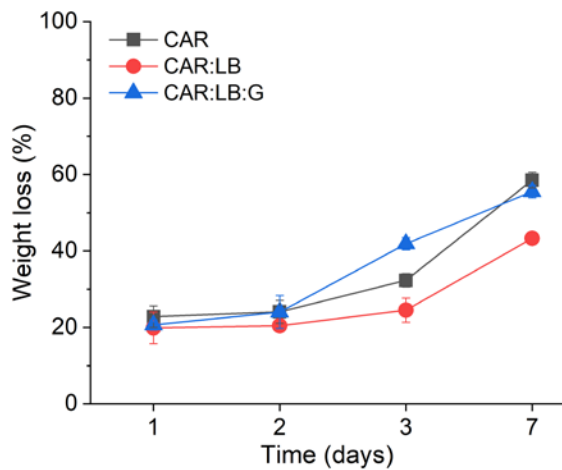


Figure 6.3. Weight loss of CAR, CAR:LB and CAR:LB:G hydrogels in PBS solution over a period of 7 days at physiological temperature (37°C).

6.3.3. Rheological properties

The rheological experiments were performed to analyze the viscoelastic behavior and mechanical strength of the prepared hydrogels. The elastic (G') and the viscous modulus (G'') of the CAR, CAR:LB and CAR:LB:G injectable hydrogels were measured (Fig. 6.4a). A typical rheological behavior of a hydrogel is that the elastic modulus dominates over the viscous modulus ($G' > G''$). According to Fig. 6.4a for CAR:LB and CAR:LB:G hydrogels, $G' > G''$ indicating the predominance of elastic characteristics than viscous characteristics. The value of the elastic modulus observed for CAR:LB:G is higher than that reported in other previous works of physical hydrogels based on carrageenan for medical applications [14,15]. Comparable values in the elastic modulus at frequencies above 1 Hz are due to the fact that all hydrogels have carrageenan as their main component. About the mixture of ι C and κ C has been reported that the gel stiffness of mixed gels was much larger than the sum of the elastic modulus of the ι C and κ C individual gels [12]. Additionally, it has been reported that application of gelatin/k-carrageenan mixtures results in an increase in values of viscoelastic parameters and strength of hydrogels [38].

Shear thinning hydrogels can be potential candidates for injectable vehicles, since they are easily injected by a syringe, filling and adapting to the shape of the cavity or tissue [41]. To determine

the shear thinning property, the viscosity of injectable hydrogels was measured with respect to the shear rate (Fig. 6.4b). The results showed that the viscosity of CAR:LB:G, CAR:LB and CAR hydrogels decreased with increasing shear rate, which means that the injectable hydrogel have shear thinning behavior. The shear thinning behavior is a result of reversible physical crosslinks [42]. The injectability of the CAR:LB:G hydrogel was visually evaluated through the application of a manual shear force by a syringe needle (Fig. 6.4c). When the shear force was applied the CAR:LB:G hydrogel flowed through the needle of the syringe. Therefore, the rheological behavior and shear thinning property indicate that CAR:LB:G hydrogel can be a potential candidate for applications requiring localized injectability.

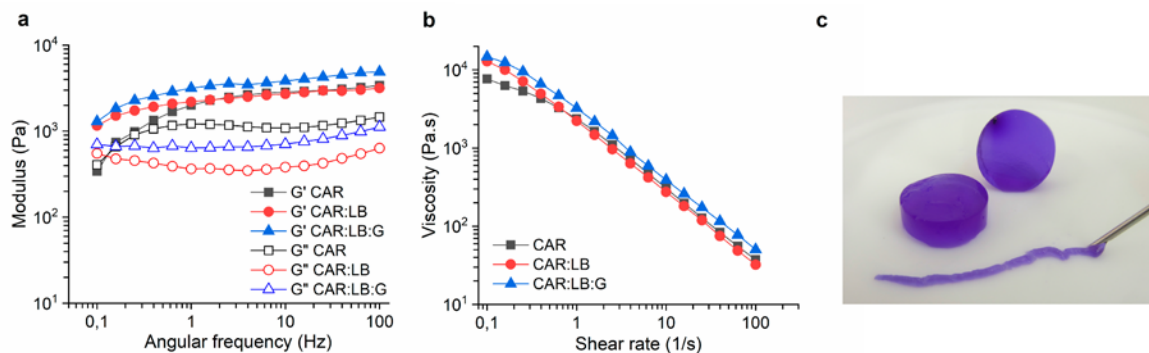


Figure 6.4. Rheological measurements of injectable hydrogel CAR:LB:G and control hydrogels CAR and CAR:LB. The elastic (G') and the viscous modulus (G'') of hydrogels (a), shear-thinning characteristics of hydrogels (b) and injectability by hand of CAR:LB:G, the injectable hydrogel was stained with bromophenol blue to enhance visualization (c).

6.3.4. *In vitro* biological evaluation

To evaluate the potential application as biomaterials in wound healing and tissue repairing, the biocompatibility of the prepared hydrogels was investigated with *in vitro* cytotoxicity assay. The viability of 3T3-L1 fibroblasts seeded on the hydrogels was assessed with the MTT assay (Fig. 6.5). The results showed that cell viability of components and CAR:LB:G higher than 70% indicates non cytotoxicity according to ISO 10993-5 recommendations [43]. The cells treated

with CAR:LB:G hydrogel presented higher metabolic activity showing a significant increase with regard to κ C:LB and CAR:LB.

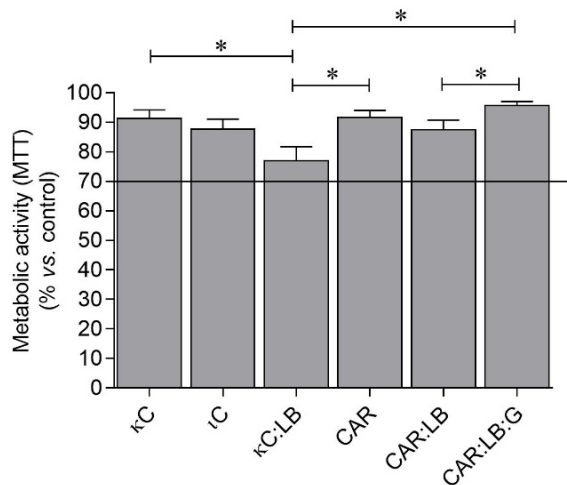


Figure 6.5. MTT assay showing the effect of the components and the hydrogels on 3T3-L1 fibroblasts for 16 h. Solid black line highlights the cytotoxicity threshold. N=6. * $p < 0.05$.

Cell adhesion after 48 h was performed by fluorescence microscopy after live/dead cell staining.

Fig. 6.6 showed the viable cells and their morphologies on the hydrogels. CAR:LB:G hydrogel exhibited more proliferation, attached and spreading fibroblasts compared to CAR and CAR:LB. CAR:LB:G and CAR:LB hydrogels showed a significant increase in cell proliferation compared to CAR hydrogel (Fig. 6.7). Cell spreading is a positive signal of appropriate cell attachment meaning that the hydrogel will more closely resemble the extracellular matrix, which is preferred in biomaterials [44]. The improved adhesion and spreading observed in the CAR:LB:G hydrogel may be due to the RGD sequences (arginine-glycine-aspartate) presented in the gelatin, which enhance cell adhesion and proliferation [45,46]. Cells that have been found to bind favorably to RGD include fibroblasts, endothelial cells, smooth muscle cells, osteoblasts and chondrocytes [47]. Thus, the addition of gelatin promotes the cell attachment which is relevant for the tissue repairing. Therefore, the results indicate that the injectable hydrogel CAR:LB:G can support cell survival and promoting cell adhesion. According to these results, hydrogel CAR:LB:G was selected for the entrapment of a growth factor to evaluate its potential to promote wound healing.

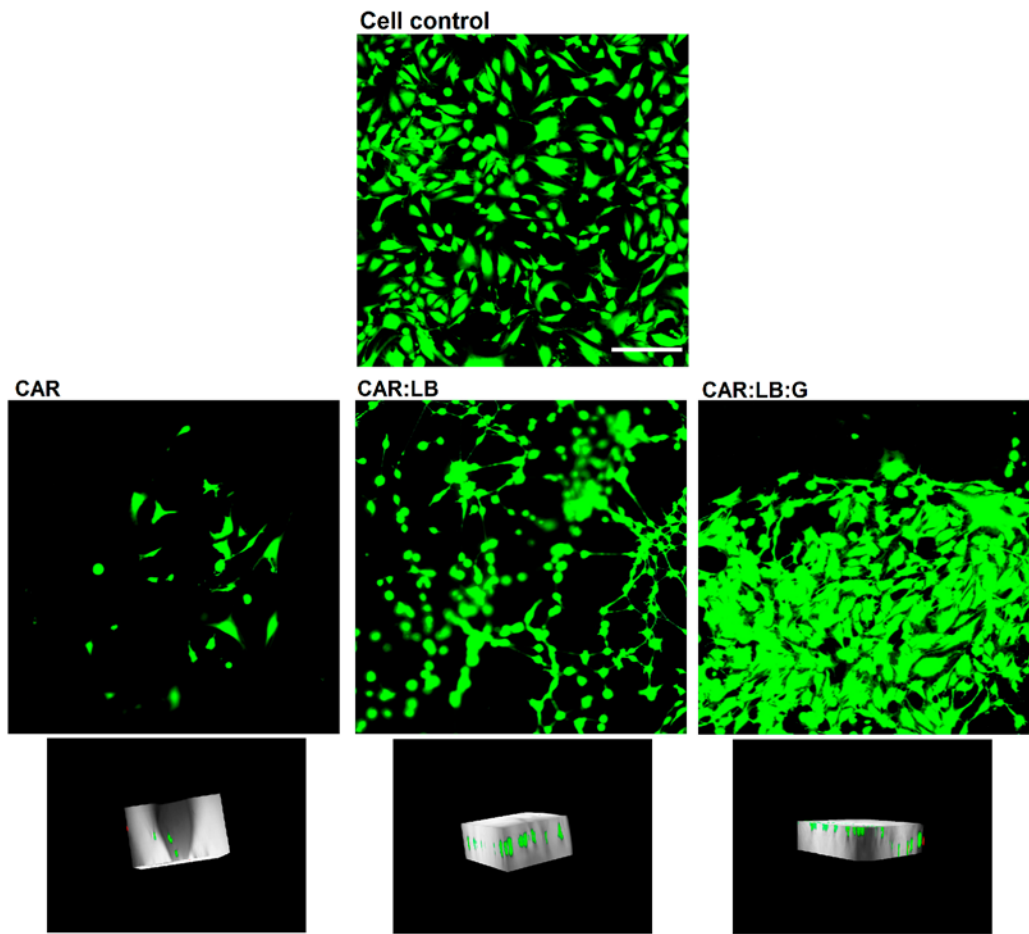


Figure 6.6. Fluorescence microscopy images obtained after 48 h to visualize live/dead staining of 3T3-L1 fibroblasts cultured onto glass bottom (cell control) and CAR, CAR:LB and CAR:LB:G hydrogels. The images below show a 3D projection of the hydrogels with viable cells inside. Scale bar represents 250 µm.

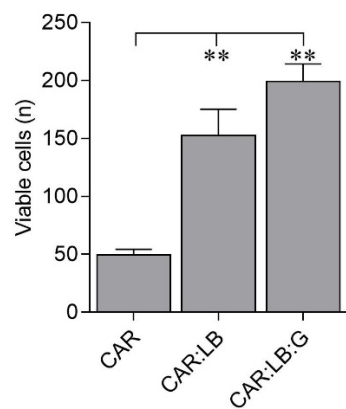


Figure 6.7. Number of viable 3T3-L1 fibroblasts cultured on CAR, CAR:LB and CAR:LB:G hydrogels. Viable cells were stained with calcein-AM. Six fluorescence images from each treatment were considered for cell count using ImageJ. **p < 0.01.

The potential of the injectable hydrogel CAR:LB:G as delivery carrier to promote wound healing was evaluated by the release of the vascular endothelial growth factor (VEGF) loaded within hydrogel. VEGF is one of the most potent mediators of angiogenesis produced by cell types including endothelial cells and osteoblasts. An absent or reduced angiogenesis may be the reason for unsuccessful healing or osteogenesis [48]. VEGF is positively charged at physiological pH which can interact electrostatically with negatively charged molecules [49]. *In vitro* scratch assay was used to evaluate the activity of VEGF released from CAR:LB:G hydrogel. The *in vitro* scratch assay is an easy, low-cost and well-developed method to measure cell migration *in vitro* [50]. Cell migration is vital to many physiological processes such as tissue development, repair, and regeneration [51]. The scratch closure rate was calculated and the results are showed in Fig. 6.8. VEGF released from CAR:LB:G allowed to improve significantly the migration of HUVEC after 24 h, compared with CAR:LB:G without VEGF. The scratch was almost completely closed after 24 h of treatment. Furthermore, according to the results of scratch assays VEGF released maintains its bioactivity since the wound closure caused by VEGF released from CAR:LB:G hydrogel was similar to that caused by treatment with free VEGF (no significant difference). Therefore, a continuous release of VEGF from injectable hydrogel CAR:LB:G can promote cell migration, accelerating wound closure and improving healing.

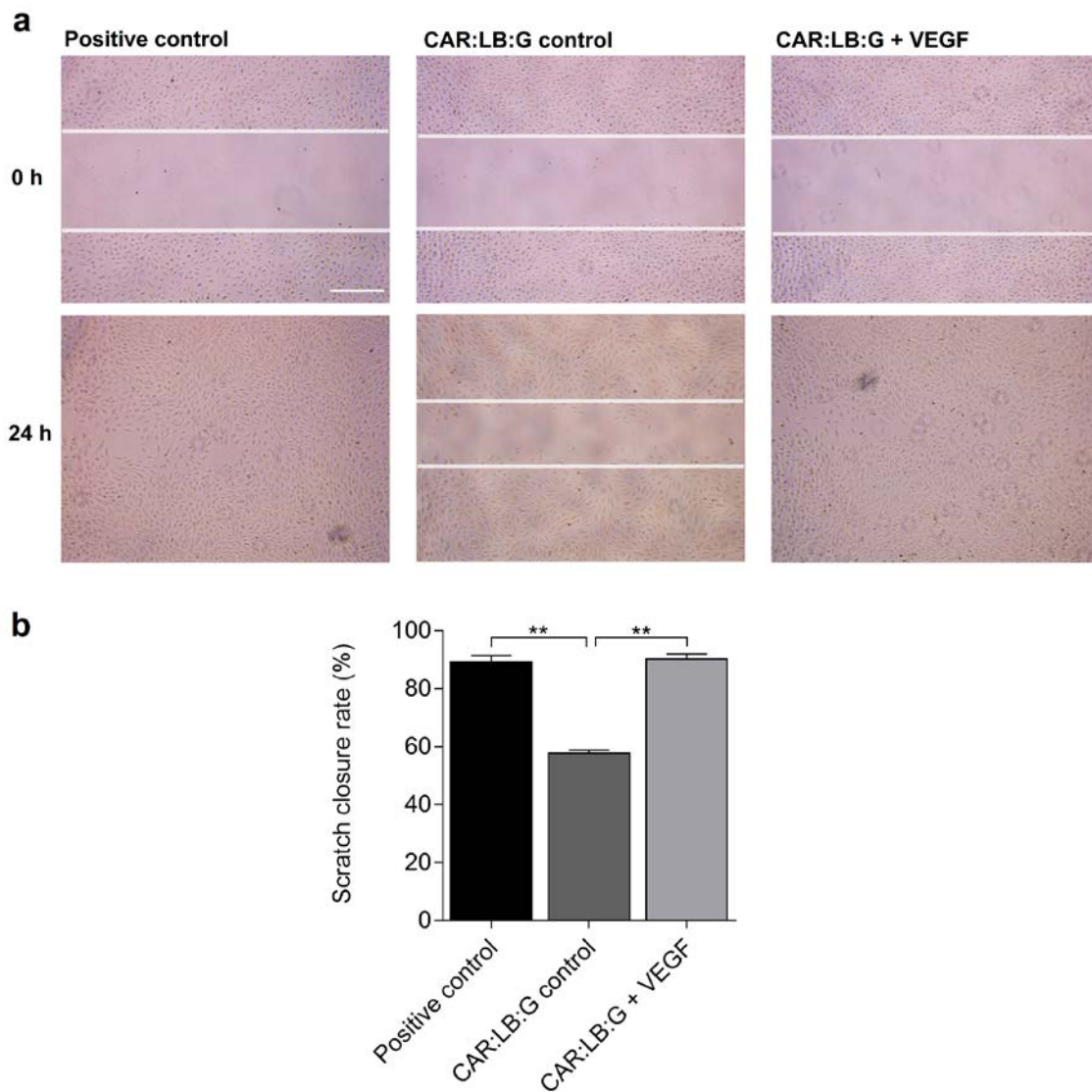


Figure 6.8. Effect of VEGF released from CAR:LB:G hydrogel was evaluated using a scratch wound healing assay after 24 h. Microscope images of the *in vitro* scratches for the different treatments. The scratch was produced by scratching a confluent cell monolayer with a sterile 200 μL pipette tip. Scale bar represents 1 mm. (a). Quantified *in vitro* scratch closure area results for the different treatments after 24 h (b). Positive control: 50 $\mu\text{g ml}^{-1}$ free VEGF; CAR:LB:G control: hydrogel without VEGF; CAR:LB:G + VEGF: hydrogel loaded with 50 $\mu\text{g ml}^{-1}$ VEGF. N=6. **p <0.01.

6.4. Conclusion

A novel biocompatible injectable hydrogel combining kappa and iota carrageenans, locust bean gum and gelatin was prepared and showed a good potential for use in wound healing and tissue repairing. The developed injectable hydrogel showed mechanical and physiological stability, cell

adhesion and ability to release a growth factor to promote cell migration. It has been determined that the incorporation of locust bean gum to carrageenan-based hydrogel improves the mechanical and swelling properties, and also the physiological stability. While, the addition of gelatin enhances cell adhesion and proliferation. 3T3-L1 fibroblasts were able to grow, adhere and spread on the hydrogel. Whereas, the prepared injectable hydrogel accelerated the migration of HUVEC cells by releasing the growth factor VEGF and therefore could be useful for delivery of biomolecules. Consequently, the injectable hydrogel CAR:LB:G could be potentially used in wound healing and tissue repairing.

Supplementary material

FTIR analysis

Characteristics bands of the LB were observed at 810 cm^{-1} and 870 cm^{-1} indicating the presence of α -linked D-galactopyranose units and β -linked D-mannopyranose units, respectively [1]. The broad absorption band ranging between 3750 and 3000 cm^{-1} was assigned to O-H stretching vibration of hydroxyl groups [1,2]. The absorption bands found in κ C are indicated in the main text of section 5.3.1 of manuscript.

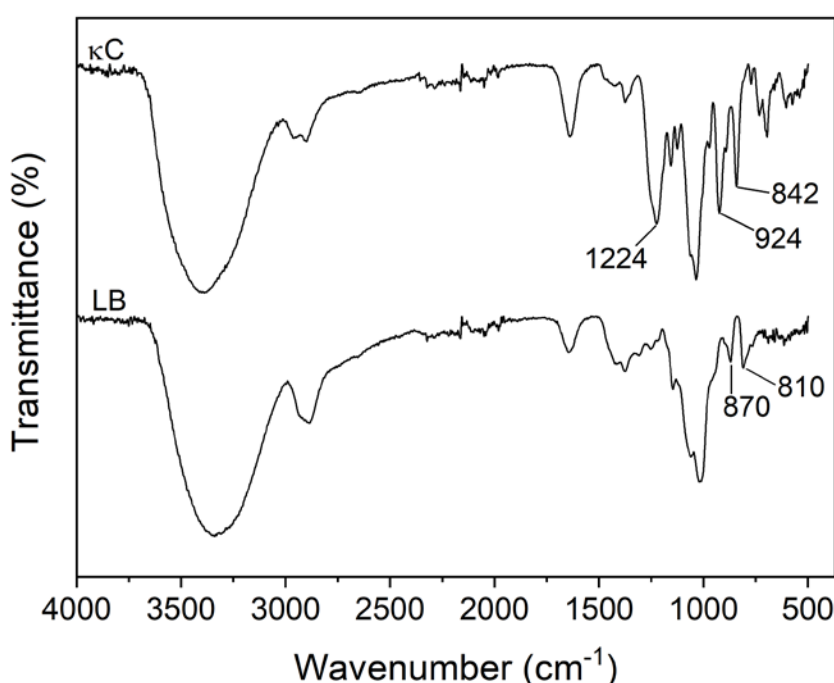


Figure S. 6.1. FTIR spectra of κ -carrageenan (κ C) and locust bean gum (LB).

- [1] J.T. Martins, M.A. Cerqueira, A.I. Bourbon, A.C. Pinheiro, B.W.S. Souza, A.A. Vicente, Synergistic effects between κ -carrageenan and locust bean gum on physicochemical properties of edible films made thereof, *Food Hydrocoll.* 29 (2012) 280–289. doi:10.1016/j.foodhyd.2012.03.004.
- [2] K.M. Zepon, M.M. Martins, M.S. Marques, J.M. Heckler, F.D.P. Morisso, M.G. Moreira, A.L. Ziulkoski, L.A. Kanis, F. Dal Pont Morisso, M.G. Moreira, A.L. Ziulkoski, L.A. Kanis, Smart wound dressing based on κ -carrageenan/locust bean gum/cranberry extract for monitoring bacterial infections, *Carbohydr. Polym.* 206 (2019) 362–370. doi:S014486171831347X.

6.5. References

- [1] N.A. Peppas, J.Z. Hilt, A. Khademhosseini, R. Langer, Hydrogels in biology and medicine : from molecular principles to bionanotechnology, *Adv. Mater.* 18 (2006) 1345–1360. doi:10.1002/adma.200501612.
- [2] D.P. Pacheco, L. Zorzetto, P. Petrini, Soft tissue application of biocomposites, Second Edi, Elsevier Ltd., 2017. doi:10.1016/b978-0-08-100752-5.00004-4.
- [3] K.H. Bae, L.-S. Wang, M. Kurisawa, Injectable biodegradable hydrogels: progress and challenges, *J. Mater. Chem. B.* 1 (2013) 5371. doi:10.1039/c3tb20940g.
- [4] H.F. Darge, A.T. Andrgie, H.C. Tsai, J.Y. Lai, Polysaccharide and polypeptide based injectable thermo-sensitive hydrogels for local biomedical applications, *Int. J. Biol. Macromol.* 133 (2019) 545–563. doi:10.1016/j.ijbiomac.2019.04.131.
- [5] M.H. Chen, L.L. Wang, J.J. Chung, Y.H. Kim, P. Atluri, J.A. Burdick, Methods to Assess Shear-Thinning Hydrogels for Application As Injectable Biomaterials, *ACS Biomater. Sci. Eng.* 3 (2017) 3146–3160. doi:10.1021/acsbiomaterials.7b00734.
- [6] P. Koria, Delivery of growth factors for tissue regeneration and wound healing, *BioDrugs.* 26 (2012) 163–175. doi:10.2165/11631850-000000000-00000.
- [7] M. Guvendiren, H.D. Lu, J.A. Burdick, Shear-thinning hydrogels for biomedical applications, *Soft Matter.* 8 (2012) 260–272. doi:10.1039/c1sm06513k.
- [8] D. Diekjürgen, D.W. Grainger, Polysaccharide matrices used in 3D in vitro cell culture systems, *Biomaterials.* 141 (2017) 96–115. doi:10.1016/j.biomaterials.2017.06.020.
- [9] R. Yegappan, V. Selvapritchivraj, S. Amirthalingam, R. Jayakumar, Carrageenan based hydrogels for drug delivery , tissue engineering and wound healing, *Carbohydr. Polym.* 198 (2018) 385–400. doi:10.1016/j.carbpol.2018.06.086.
- [10] S. Graham, P.F. Marina, A. Blencowe, Thermoresponsive polysaccharides and their thermoreversible physical hydrogel networks, *Carbohydr. Polym.* 207 (2019) 143–159. doi:10.1016/j.carbpol.2018.11.053.
- [11] J. Radhakrishnan, A. Subramanian, U.M. Krishnan, S. Sethuraman, Injectable and 3D Bioprinted Polysaccharide Hydrogels: From Cartilage to Osteochondral Tissue Engineering, *Biomacromolecules.* 18 (2017) 1–26. doi:10.1021/acs.biomac.6b01619.

- [12] V.T.N.T. Bui, B.T. Nguyen, F. Renou, T. Nicolai, Rheology and microstructure of mixtures of iota and kappa-carrageenan, *Food Hydrocoll.* 89 (2019) 180–187. doi:10.1016/j.foodhyd.2018.10.034.
- [13] R.C. Pereira, M. Scaranari, P. Castagnola, M. Grandizio, H.S. Azevedo, R.L. Reis, R. Cancedda, C. Gentili, Novel injectable gel (system) as a vehicle for human articular chondrocytes in cartilage tissue regeneration, *J. Tissue Eng. Regen. Med.* 3 (2009) 97–106. doi:10.1002/term.
- [14] G. Lokhande, J.K. Carrow, T. Thakur, J.R. Xavier, M. Parani, K.J. Bayless, A.K. Gaharwar, Nanoengineered injectable hydrogels for wound healing application, *Acta Biomater.* 70 (2018) 35–47. doi:10.1016/j.actbio.2018.01.045.
- [15] R. Yegappan, V. Selvapritchiviraj, S. Amirthalingam, A. Mohandas, N.S. Hwang, R. Jayakumar, Injectable angiogenic and osteogenic carrageenan nanocomposite hydrogel for bone tissue engineering, *Int. J. Biol. Macromol.* 122 (2019) 320–328. doi:10.1016/j.ijbiomac.2018.10.182.
- [16] S. Barak, D. Mudgil, Locust bean gum : Processing , properties and food applications — A review, *Int. J. Biol. Macromol.* 66 (2014) 74–80. doi:10.1016/j.ijbiomac.2014.02.017.
- [17] N. Pettinelli, S. Rodríguez-Llamazares, Y. Farrag, R. Bouza, L. Barral, S. Feijoo-Bandín, F. Lago, Poly(hydroxybutyrate-co-hydroxyvalerate) microparticles embedded in κ-carrageenan/locust bean gum hydrogel as a dual drug delivery carrier, *Int. J. Biol. Macromol.* 146 (2020) 110–118. doi:10.1016/j.ijbiomac.2019.12.193.
- [18] S.R. Derkach, N.G. Voron'ko, Y.A. Kuchina, D.S. Kolotova, A.M. Gordeeva, D.A. Faizullin, Y.A. Gusev, Y.F. Zuev, O.N. Makshakova, Molecular structure and properties of κ-carrageenan-gelatin gels, *Carbohydr. Polym.* 197 (2018) 66–74. doi:10.1016/j.carbpol.2018.05.063.
- [19] Q. Chai, Y. Jiao, X. Yu, Hydrogels for biomedical applications: Their characteristics and the mechanisms behind them, *Gels.* 3 (2017) 6. doi:10.3390/gels3010006.
- [20] S. Naahidi, M. Jafari, M. Logan, Y. Wang, Y. Yuan, H. Bae, B. Dixon, P. Chen, Biocompatibility of hydrogel-based scaffolds for tissue engineering applications, *Biotechnol. Adv.* 35 (2017) 530–544. doi:10.1016/j.biotechadv.2017.05.006.
- [21] L. Tytgat, M. Vagenende, H. Declercq, J.C. Martins, H. Thienpont, H. Ottevaere, P.

- Dubrule, S. Van Vlierberghe, Synergistic effect of κ -carrageenan and gelatin blends towards adipose tissue engineering, *Carbohydr. Polym.* 189 (2018) 1–9. doi:10.1016/j.carbpol.2018.02.002.
- [22] C. Wen, L. Lu, X. Li, Enzymatic and Ionic Crosslinked Gelatin / K-Carrageenan IPN Hydrogels as Potential Biomaterials, *J. Appl. Polym. Sci.* 131 (2014) 40975. doi:10.1002/app.40975.
- [23] J.R. Padhi, D. Nayak, A. Nanda, P.R. Rauta, S. Ashe, B. Nayak, Development of highly biocompatible Gelatin & i-Carrageenan based composite hydrogels: In depth physiochemical analysis for biomedical applications, *Carbohydr. Polym.* 153 (2016) 292–301. doi:10.1016/j.carbpol.2016.07.098.
- [24] A. Pourjavadi, M. Doroudian, A. Ahadpour, S. Azari, Injectable chitosan/ κ -carrageenan hydrogel designed with au nanoparticles: A conductive scaffold for tissue engineering demands, *Int. J. Biol. Macromol.* 126 (2019) 310–317. doi:10.1016/j.ijbiomac.2018.11.256.
- [25] B. Paradela-Dobarro, B.K. Rodiño-Janeiro, J. Alonso, S. Raposeiras-Roubín, M. González-Peteiro, J.R. González-Juanatey, E. Álvarez, Key structural and functional differences between early and advanced glycation products, *J. Mol. Endocrinol.* 56 (2015) 23–37. doi:10.1530/JME-15-0031.
- [26] T.L. Riss, R.A. Moravec, A.L. Niles, S. Duellman, H.A. Benink, T.J. Worzella, L. Minor, Cell Viability Assays, Assay Guid. Man. (2004) 1–31. <http://www.ncbi.nlm.nih.gov/pubmed/23805433>.
- [27] Y. Chen, H. Jin, F. Yang, S. Jin, C. Liu, L. Zhang, J. Huang, S. Wang, Z. Yan, X. Cai, R. Zhao, F. Yu, Z. Yang, G. Ding, Y. Tang, Physicochemical, antioxidant properties of giant croaker (*Nibea japonica*) swim bladders collagen and wound healing evaluation, *Int. J. Biol. Macromol.* 138 (2019) 483–491. doi:10.1016/j.ijbiomac.2019.07.111.
- [28] V.T.N.T. Bui, B.T. Nguyen, T. Nicolai, F. Renou, Mixed iota and kappa carrageenan gels in the presence of both calcium and potassium ions, *Carbohydr. Polym.* 223 (2019) 115107. doi:10.1016/j.carbpol.2019.115107.
- [29] L. Rioux, S.L. Turgeon, Chapter 7 - Seaweed carbohydrates, Elsevier Inc., 2015. doi:10.1016/B978-0-12-418697-2/00007-6.

- [30] M. Dionísio, A. Grenha, Locust bean gum : Exploring its potential for biopharmaceutical applications, *J. Pharm. Bioallied Sci.* 4 (2012) 175–185. doi:10.4103/0975-7406.99013.
- [31] J. Liu, X. Zhan, J. Wan, Y. Wang, C. Wang, Review for carrageenan-based pharmaceutical biomaterials : Favourable physical features versus adverse biological effects, *Carbohydr. Polym.* 121 (2015) 27–36. doi:10.1016/j.carbpol.2014.11.063.
- [32] N.G. Voron'ko, S.R. Derkach, M.A. Vovk, P.M. Tolstoy, Formation of κ -carrageenan–gelatin polyelectrolyte complexes studied by ^1H NMR, UV spectroscopy and kinematic viscosity measurements, *Carbohydr. Polym.* 151 (2016) 1152–1161. doi:10.1016/j.carbpol.2016.06.060.
- [33] J.S. Varghese, N. Chellappa, N.N. Fathima, Gelatin-carrageenan hydrogels: Role of pore size distribution on drug delivery process, *Colloids Surfaces B Biointerfaces*. 113 (2014) 346–351. doi:10.1016/j.colsurfb.2013.08.049.
- [34] M. Şen, E.N. Erboz, Determination of critical gelation conditions of κ -carrageenan by viscosimetric and FT-IR analyses, *Food Res. Int.* 43 (2010) 1361–1364. doi:10.1016/j.foodres.2010.03.021.
- [35] K.M. Zepon, M.M. Martins, M.S. Marques, J.M. Heckler, F.D.P. Morisso, M.G. Moreira, A.L. Ziulkoski, L.A. Kanis, F. Dal Pont Morisso, M.G. Moreira, A.L. Ziulkoski, L.A. Kanis, Smart wound dressing based on κ -carrageenan/locust bean gum/cranberry extract for monitoring bacterial infections, *Carbohydr. Polym.* 206 (2019) 362–370. doi:S014486171831347X.
- [36] A. Rasool, S. Ata, A. Islam, R.U. Khan, Fabrication of novel carrageenan based stimuli responsive injectable hydrogels for controlled release of cephadrine, *RSC Adv.* 9 (2019) 12282–12290. doi:10.1039/c9ra02130b.
- [37] L.G. Gómez-Mascaraque, B. Llavata-Cabrero, M. Martínez-Sanz, M.J. Fabra, A. López-Rubio, Self-assembled gelatin- ι -carrageenan encapsulation structures for intestinal-targeted release applications, *J. Colloid Interface Sci.* 517 (2018) 113–123. doi:10.1016/j.jcis.2018.01.101.
- [38] S.R. Derkach, S.O. Ilyin, A.A. Maklakova, V.G. Kulichikhin, A.Y. Malkin, The rheology of gelatin hydrogels modified by κ -carrageenan, *LWT - Food Sci. Technol.* 63 (2015) 612–619. doi:10.1016/j.lwt.2015.03.024.

- [39] J. Nourmohammadi, F. Roshanfar, M. Farokhi, M.. Nazarpak, Silk fibroin / kappa - carrageenan composite scaffolds with enhanced biomimetic mineralization for bone regeneration applications, *Mater. Sci. Eng. C.* 76 (2017) 951–958. doi:10.1016/j.msec.2017.03.166.
- [40] J. Li, B. Yang, Y. Qian, Q. Wang, R. Han, T. Hao, Y. Shu, Y. Zhang, F. Yao, C. Wang, Iota-carrageenan/chitosan/gelatin scaffold for the osteogenic differentiation of adipose-derived MSCs in vitro, *J. Biomed. Mater. Res. - Part B Appl. Biomater.* 103 (2015) 1498–1510. doi:10.1002/jbm.b.33339.
- [41] U.G. Spizzirri, C. Giuseppe, *Functional Hydrogels in Drug Delivery*, Taylor & Francis, 2017. doi:10.5302/J.ICROS.2011.17.8.731.
- [42] J. Li, D.J. Mooney, Designing hydrogels for controlled drug delivery, *Nat. Rev. Mater.* 1 (2016) 16071. doi:10.1038/natrevmats.2016.71.
- [43] International Organization for Standardization, ISO 10993-5 . Biological evaluation of medical devices. Part 5: Tests for in vitro cytotoxicity. Geneva, Switzerland, 2009.
- [44] G. Graulus, A. Mignon, S. Van Vlierberghe, H. Declercq, K. Fehér, M. Cornelissen, J.C. Martins, P. Dubrule, Cross-linkable alginate-graft-gelatin copolymers for tissue engineering applications, *Eur. Polym. J.* 72 (2015) 494–506. doi:10.1016/j.eurpolymj.2015.06.033.
- [45] E. Hoch, C. Schuh, T. Hirth, E.M. Tovar, K. Borchers, Stiff gelatin hydrogels can be photochemically synthesized from low viscous gelatin solutions using molecularly functionalized gelatin with a high degree of methacrylation, (2012) 2607–2617. doi:10.1007/s10856-012-4731-2.
- [46] U. Hersel, C. Dahmen, H. Kessler, RGD modified polymers: Biomaterials for stimulated cell adhesion and beyond, *Biomaterials.* 24 (2003) 4385–4415. doi:10.1016/S0142-9612(03)00343-0.
- [47] B. V Slaughter, S.S. Khurshid, O.Z. Fisher, A. Khademhosseini, N.A. Peppas, Hydrogels in Regenerative Medicine, *Adv. Mater.* 21 (2009) 3307–3329. doi:10.1016/B978-0-323-22805-3.00012-8.
- [48] W. Götz, C. Reichert, L. Canullo, A. Jäger, F. Heinemann, Coupling of osteogenesis and angiogenesis in bone substitute healing - A brief overview, *Ann. Anat.* 194 (2012) 171–

173. doi:10.1016/j.aanat.2011.10.002.
- [49] J. O'Dwyer, R. Murphy, E.B. Dolan, L. Kovarova, M. Pravda, V. Velebny, A. Heise, G.P. Duffy, S.A. Cryan, Development of a nanomedicine-loaded hydrogel for sustained delivery of an angiogenic growth factor to the ischaemic myocardium, *Drug Deliv. Transl. Res.* (2019). doi:10.1007/s13346-019-00684-5.
- [50] C.C. Liang, A.Y. Park, J.L. Guan, In vitro scratch assay: A convenient and inexpensive method for analysis of cell migration in vitro, *Nat. Protoc.* 2 (2007) 329–333. doi:10.1038/nprot.2007.30.
- [51] N. Cormier, A. Yeo, E. Fiorentino, J. Paxson, Optimization of the wound scratch assay to detect changes in murine mesenchymal stromal cell migration after damage by soluble cigarette smoke extract, *J. Vis. Exp.* 2015 (2015) 1–9. doi:10.3791/53414.

CAPÍTULO 7: Conclusiones generales

En esta tesis nuevos hidrogeles compuestos con potencial para ser usados en diferentes aplicaciones biomédicas fueron preparados y caracterizados. Fueron diseñados hidrogeles interpenetrados y semi-interpenetrados, hidrogeles compuestos incorporando micropartículas e hidrogeles físicos híbridos. Las aplicaciones biomédicas a las que se dirigió esta tesis fueron la administración de fármacos, reparación de tejidos y curación de heridas. El desarrollo de este trabajo permitió tener una visión general de las propiedades de los hidrogeles y su utilidad en el área biomédica, lo que condujo a abrir una nueva línea de investigación en el laboratorio, en cuanto al material desarrollado y el área de aplicación.

Los resultados obtenidos en este trabajo pueden ser resumidos en las siguientes conclusiones:

1. Se obtuvieron nuevos hidrogeles compuestos de monómeros sintéticos y polisacáridos con propiedades mecánicas y de hinchamiento mejoradas. Los resultados mostraron que los hidrogeles semi -IPN con monómeros sintéticos y quitosano tuvieron una absorción de agua (WU) mayor y propiedades mecánicas más bajas que el hidrogel sintético (SH). Los hidrogeles semi-IPN con pectina presentaron la más baja WU de todos los hidrogeles y las propiedades mecánicas fueron similares a los del SH. Los hidrogeles IPN con κ -carragenina mostraron la mayor absorción de agua y pueden ser clasificados como hidrogeles superabsorbentes. Además, la adición de κ C mejoró considerablemente las propiedades mecánicas del SH. Los resultados de los ensayos MMT y de nitrito indicaron que los hidrogeles compuestos son biocompatibles, principalmente los hidrogeles con quitosano y κ -carragenina. Por lo tanto, la incorporación de κ -carragenina dentro del SH mejora tanto el hinchamiento como las propiedades mecánicas y podría considerarse como un biomaterial potencial en la ingeniería de tejidos y la administración de fármacos.
2. Se preparó un nuevo hidrogel para la administración dual de fármacos poco solubles en agua. Este hidrogel está compuesto por κ -carragenina/goma de algarrobo e incorpora

micropartículas de PHBV cargadas con ketoprofeno y mupirocina. Este sistema que combinó micropartículas e hidrogel mejoró la cinética de liberación de ambos fármacos mostrando una liberación más lenta que la obtenida desde las micropartículas y el hidrogel por separado a 37 °C. La liberación de los fármacos se observó durante 7 días a 37 °C. El comportamiento de liberación del hidrogel compuesto se ajustó al modelo cinético de Higuchi. Además, este hidrogel tiene un comportamiento de hinchamiento sensible a la temperatura, propiedades reológicas apropiadas y mostró biocompatibilidad con fibroblastos. Por lo tanto, el sistema de micropartículas de PHBV cargadas dentro de un hidrogel de κ -carragenina/goma de algarrobo, puede considerarse como un potencial portador de fármacos poco solubles en agua, principalmente para aplicaciones en la curación de heridas.

3. Se preparó un nuevo hidrogel inyectable que combina iota y kappa carrageninas, goma de algarrobo y gelatina con potencial para ser usado en la cicatrización de heridas y la reparación de tejidos. El hidrogel preparado mostró una estabilidad mecánica y fisiológica, adhesión celular y la capacidad de liberar un factor de crecimiento para promover la migración celular. Se determinó que la incorporación de goma de algarrobo al hidrogel a base de carragenina mejora las propiedades de hinchamiento y mecánicas, y también la estabilidad fisiológica. Mientras que la adición de gelatina mejora la adhesión y proliferación celular. Los fibroblastos 3T3-L1 fueron capaces de crecer, adherirse y propagarse dentro del hidrogel. Además, el hidrogel aceleró la migración de células HUVEC a través de la liberación del factor de crecimiento VEGF y por lo tanto podría ser útil para la administración de biomoléculas. En consecuencia, este hidrogel inyectable podría utilizarse potencialmente en la curación de las heridas y la reparación de los tejidos.

En conclusión, la combinación de polímeros de distinto origen y el empleo de diferentes métodos de preparación y tipos de entrecruzamiento permitió obtener hidrogeles con las

propiedades adecuadas para un potencial uso en determinadas aplicaciones, como la liberación de fármacos, reparación de tejidos y curación de heridas. Finalmente, el desarrollo del trabajo llevó a la elección de hidrogeles físicos a base de polisacáridos, ya que no requieren de un agente entrecruzante que deba ser extraído previo a su uso, mostraron biocompatibilidad y propiedades mecánicas y de hinchamiento favorables para las aplicaciones requeridas. Por lo tanto, estos resultados son de gran interés para el desarrollo de nuevos biomateriales “inteligentes” en el área biomédica y permiten seguir incursionando en el mundo de los hidrogeles, considerando que el desarrollo de matrices poliméricas con capacidades adaptables y propiedades adecuadas para una determinada aplicación continuará siendo un desafío.

ANEXO: Financiamiento

El apoyo financiero fue proporcionado por:

- Xunta de Galicia Government/FEDER: Program of Consolidation and Structuring Competitive Research Units [GRC 2014/036].
- Xunta de Galicia Government/FEDER: Program of Consolidation and Structuring Competitive Research Units [ED431C 2019/17].
- Fondef ID16I10425; REDES190181; R18F10016; CIPA, CONICYT Regional, GORE BIO BIO, R17A10003; CONICYT PIA/APOYO CCTE AFB170007.
- Parcialmente por Sociedad Española de Cardiología (Projects Call 2016/2017)